Proulx, Jessica M., The ER-mitochondrial Interface in astrocytes during methamphetamine exposure and HIV-1 infection. Doctor of Philosophy (Biomedical Sciences), October 2022, 165 pp., 4 tables, 27 illustrations, bibliography, 271 titles.

Early during infection, human immunodeficiency virus 1 (HIV-1) invades the central nervous system (CNS) and can persist for life, despite effective antiretroviral treatment. Infection and activation of residential glial cells leads to low viral replication and chronic inflammation, which damage neurons contributing to a spectrum of HIV-associated neurocognitive disorders (HAND). Notably, substance use, including methamphetamine (METH) is disproportionately elevated among people living with HIV-1 and can increase the risk and severity of HAND. Thus, the National Institutes on Drug Abuse have declared HIV-1 and substance use comorbidity as a high research priority. Astrocytes are the most numerous glial cells and provide essential support to neurons. Chronic activation of astrocytes, such as during HAND or METH use disorders, can shift astrocytes to become neurotoxic. Delineating cellular targets to regulate astrocyte function is essential to ensure neuronal fitness during a pathological challenge. Endoplasmic reticulum (ER) and mitochondria contact sites, termed mitochondria-associated ER membranes (MAMs), are key cellular platforms in neuropathology, where calcium dysregulation, unfolded protein response (UPR) sensors, and mitochondrial dysfunction are notable MAM-mediated mechanisms underlying astrocyte dysfunction. We hypothesize that the ER-mitochondria interface may serve as a therapeutic target for astrocyte dysfunction *via* calcium and non-canonical UPR signaling during HIV-1 and METH pathogenesis.

Primary human astrocytes were infected with a pseudotyped HIV-1 and/or exposed to low doses of METH for seven days. Following HIV-1 infection and/or chronic METH exposure, astrocytes had increased mitochondrial respiration, cytosolic calcium flux and protein expression of UPR/MAM mediators. Notably, inositol-requiring enzyme 1α (IRE1α) was prominently upregulated following both HIV-1 infection and chronic METH exposure. Further investigations revealed IRE1α modulates astrocyte mitochondrial respiration, glycolytic function, morphological activation, inflammation, and glutamate uptake. We then investigated a novel METH-binding receptor, trace amine-associated receptor 1 (TAAR1) as a potential upstream regulator to METH-induced UPR/MAM mediator expression. Indeed, selective antagonism of TAAR1 significantly suppressed UPR/MAM protein expression, including IRE1α. Altogether, our findings emphasize the importance and potential therapeutic intervention of UPR/MAM messengers, namely IRE1α and calcium, to combat astrocyte dysfunction, Moreover, TAAR1 may be an upstream target for METH-mediated astrocyte dysfunction.

THE ER-MITOCHONDRIAL INTERFACE IN ASTROCYTES DURING METHAMPHETAMINE EXPOSURE AND HIV-1 INFECTION

DISSERTATION

Presented to the Graduate Council of the School of Biomedical Sciences

University of North Texas Health Science Center (HSC) in Fort Worth

in Partial Fulfillment of the Requirements

for the Degree of:

DOCTOR OF PHILOSOPHY

IN

BIOMEDICAL SCIENCES

By:

Jessica M. Proulx, B.S.

Fort Worth, Texas

October 2022

ACKNOWLEDGEMENTS

A tremendous thank you to all the professors and peers who have aided in and supported my training throughout my academic and research journey. Most indispensable to my mentorship were my major professors (Drs. Kathleen Borgmann & In-Woo Park), F31 cosponsors (Drs. In-Woo Park, Shaohua Yang, & David Siderovski), committee members (Drs. Rebecca Cunningham, Raghu Krishnamoorthy, Shaohua Yang, & Scott Maddux), and graduate advisor (Dr. Rance Berg) at HSC. I especially would like to extend my appreciation to all the members of Borgmann lab, who were much more than colleagues, but rather, a lab family.

I also would like to acknowledge all my incredible friends and family members who have provided me with unwavering love and support. Specifically, I would like to thank my parents Sue and Neil Proulx. Coming from a disadvantaged background, I had to overcome many challenges. My mom passed away when I was eleven, and my dad overexerted his body to its breaking point by the time I turned eighteen. While my mom and dad had their own struggles, I never felt less fortunate or unloved. Despite our circumstances, my mom and dad did everything they could to encourage me and provide me with a life that they never could have. I would also like to thank my stepmom, Linda Daniel. She dedicated her life for the last 17 years to loving and taking care of my dad. If not for her commitment to his well-being and quality of life, I would have never had the luxury to seek greater opportunities for myself.

LIST OF PUBLICATIONS

Proulx, J., Stacy, S., Park I-W., & Borgmann K. A non-canonical role for IRE1α links ER and mitochondria as key regulators of astrocyte dysfunction: Implications in methamphetamine use and HIV-associated neurocognitive disorders. *Frontiers in Neuroscience*, 17 June 2022. https://doi.org/10.3389/fnins.2022.906651.

Proulx J., Ghaly M., Borgmann K., & Park I-W. HIV-1-mediated acceleration of oncovirus-related non-AIDS-defining cancers. *Biomedicines*, 2022. 10(4), 768; https://doi.org/10.3390/biomedicines10040768.

Proulx J., Park I-W., Borgmann K. Cal"MAM"ity at the ER-mitochondrial interface: A potential therapeutic target for neurodegeneration and HIV-associated neurocognitive disorders. *Front. Neurosci*. 2021. doi: 10.3389/fnins.2021.715945.

Proulx J., Borgmann K., & Park I-W. Role of deubiquitinating enzymes in regulation of the virus life cycle. *International Journal of Molecular Sciences*, 2021 Apr 23;22(9):4438. doi: 10.3390/ijms22094438.

Edara, V., Nooka, S., **Proulx, J**., Stacy, S., Ghorpade, A., & Borgmann K. β-catenin regulates wound healing and il-6 expression in activated human astrocytes. *Biomedicines*, 2020. 8(11), 479. doi: 10.3390/biomedicines8110479.

Proulx J., Borgmann K., & Park I-W. Post-translational modifications inducing proteasomal degradation to counter HIV-1 infection. *Virus Research*, 2020. doi: 10.1016/j.virusres.2020.198142.

Proulx J., Joshi C., Vijayaraghavalu S., Saraswathy M., Labhasetwar V., Ghorpade A., & Borgmann, K. Poly (lactide co-glycolide) (PLGA) and arginine-modified polyethylenimine (PEI) integration enhances astrocyte gene delivery. *International Journal of Nanomedicine*, 2020. 15, 3639–3647. doi: 10.2147/IJN.S250865.

IN PREPARATION

Proulx J., Park I-W, & Borgmann K. HIV-1 and methamphetamine comorbidity in primary human astrocytes: TAARgeting ER/UPR dysfunction. *Journal of Neuroimmune Pharmacology*, 2022.

Swanta, N., Stacy, S., Tang, L., **Proulx, J**., Edara, V., Ghorpade, A., & Borgmann K. Sex differences in the functional characterization of primary human astrocytes. *Biology of Sex Differences*, 2022.

TABLE OF CONTENTS

LIST OF TABLES

LIST OF ILLUSTRATIONS

Page

ABBREVIATIONS

α-syn, α-synuclein; Aβ, amyloid β; AD, Alzheimer's disease; ALS, amyotrophic lateral sclerosis; ApoE4, ε4 allele of apolipoprotein E; ANT, adenine nucleotide translocase; APP, amyloid precursor protein; ART, antiretroviral therapy; ATF6, activating transcription factor 6; AUC, area under the curve; Bap31, B cell receptor-associated protein 31; BBB, blood brain barrier; BCA, bicinchoninic acid; BECN1, beclin 1; BiP, binding immunoglobulin protein; Calcium, Ca^{2+}; CEPIA2mt, calcium-measuring organelle-entrapped protein indicator for the mitochondria; CCL2, C-C motif chemokine ligand 2; CNS, central nervous system; CXCL8, C-X-C motif chemokine ligand 8; DAPI, 4′,6-diamidino-2-phenylindole; Drp1, dynamin-related protein 1; ECAR, extracellular acidification rate; ELISA, enzyme-linked immunosorbent assays; ER, endoplasmic reticulum; ETC, electron transport chain; FCCP, carbonyl cyanide-4 (trifluoromethoxy) phenylhydrazone; Fis1, fission 1; FUS, fused in sarcoma; GCaMP6s, GFP-calmodulin calcium sensor; GFAP; glial fibrillary acid protein; gp120, glycoprotein 120; grp75, glucose-regulated protein 75 kDa; GSK-3β, glycogen synthase kinase-3β; HBMEC; human brain microvascular endothelial cells; pHEF, p-human elongation-factor; HEK, human embryonic kidney; HIV-1, human immunodeficiency virus type 1; HAND, HIV-associated neurocognitive disorders; IL-1β, interleukin-1β; IMM, inner mitochondrial membrane; IP_3R, inositol 1,4,5-triphosphate receptors; IRE1α, inositol-requiring protein 1α; LC3, microtubule-associated protein 1A/1B-light chain 3; LDH, lactate dehydrogenase; MAM, mitochondria-associated ER membrane; MAVS, mitochondrial antiviral signaling; MCU, mitochondrial calcium uniporter; MEF; mouse embryonic fibroblasts; METH, methamphetamine; MFN, mitofusin; Miro, mitochondrial Rho

GTPases; MPER, mammalian protein extraction buffer; mPTP, mitochondrial permeability transitional pore; mtDNA, mitochondrial DNA; MTT, 3-(4,5-dimethylthiazol-2-yl)-2,5-diphenyltetrazolium bromide; Nef, negative factor; NIDA, National Institute on Drug Abuse; OCR, oxygen consumption rate; Oligo, oligomycin; OMM, outer mitochondrial membrane; OPA1, optic atrophy protein 1; PACS2, phosphofurin acidic cluster sorting 2; PD, Parkinson's disease; PERK, protein kinase RNA-like endoplasmic reticulum kinase; PGC1α, proliferator-activated receptor γ coactivator 1α; PHA, primary human astrocytes; PINK1, phosphatase and tensin homolog (PTEN)-induced putative kinase; PLWH, people living with HIV; PS, presenilin; PTPIP51, protein tyrosine phosphatase-interacting protein 51; RIDD, regulated IRE1-dependent decay; ROS, reactive oxygen species; Rot/AA, rotenone/antimycin A; RT, reverse transcriptase; RyR, ryanodine receptors; SOD1, superoxide dismutase 1; σ1R or Sig1R, sigma-1 receptor; Tat, transactivator of transcription; TDP-43, transactive response DNA-binding protein 43; TFAM, transcription factor A; UPR, unfolded protein response; VAPB, vesicle-associated membrane protein-associated protein B; VDAC, voltage-dependent anion-selective channel; Vpr, viral protein R; VSVg, vesicular stomatitis virus glycoprotein; XBP1, X-box binding protein

CHAPTER 1

INTRODUCTION

AUTHOR

J. PROULX

1.1 Rationale

There are approximately 38 million people living with HIV-1 (PLWH) worldwide. Despite intervention with antiretroviral therapy (ART), these individuals have a heightened and accelerated risk for a number of age-associated pathologies including cancer, cardiovascular disease, and neurocognitive disorders (Schouten et al. 2014; Gabuzda et al. 2020). The spectra of HIV-associated neurocognitive disorders (HAND) are caused by early invasion of HIV-1 into the central nervous system (CNS) leading to persistent low-level viral replication and chronic neuroinflammation. This neuropathological environment is further characterized by glial cell dysfunction and neurotoxicity. Additional factors that can influence the development and severity of HAND include toxicity by ART itself, health comorbidities, socioeconomic status, and substance use disorders **(Figure 1.1)**. It is well established that substance use, including methamphetamine (METH), is disproportionally elevated among PLWH; thus, the National Institute on Drug Abuse (NIDA) have declared HIV-1 and substance use research as a high priority.

As glial cell dysfunction is a key etiology of HAND, the present investigations are centered around a fundamental neurosupportive glial cell, astrocytes. Astrocytes are the most numerous glial cells in the CNS. Their foot processes are critical in maintaining the blood brain barrier (BBB) integrity as well as neurosynaptic communication through the 'tripartite synapse'. Moreover, astrocytes provide essential metabolic, antioxidant, and neurotrophic support to neurons to ensure neuronal health and function. During a neuropathological challenge, such as HIV-1 infection or METH exposure, astrocytes can shift their neuroprotective functions and instead become neurotoxic **(Figure 1.2)** (Natarajaseenivasan et al. ; Salamanca et al. 2014; Borgmann and Ghorpade 2017; Nooka and Ghorpade 2018; Borgmann and Ghorpade 2015; Cisneros and

Ghorpade 2012; Edara, Ghorpade, and Borgmann 2020; Cisneros, Ghorpade, and Borgmann 2020; Proulx, Park, and Borgmann 2021; Proulx et al. 2022). Notably, at least two METH receptors have been identified in astrocytes, trace amine associated receptor 1 (TAAR1) (Cisneros and Ghorpade 2012, 2014; Cisneros, Ghorpade, and Borgmann 2020) and sigma 1 receptor (Sig1R) (Zhang et al. 2015) which have been shown to mediate some METH-associated dysregulation of astrocyte activities. Identifying underlying cellular or molecular mechanisms that regulate astrocyte dysfunction are critical to illuminate therapeutic targets that can restore a neurosupportive phenotype to protect neurons during CNS pathologies.

ER and oxidative stress, mitochondrial dysfunction, and calcium dysregulation are three key cellular disturbances that characterize neurodegenerative pathologies (Brown and Naidoo 2012; Muller et al. 2018). Cooperation between the ER and mitochondria is essential both for the maintenance and restoration of cellular homeostasis. In fact, direct contact sites between these organelles termed mitochondrial-associated ER membranes (MAMs) have been identified as critical intracellular hubs for determining cellular function and survival (Filadi, Theurey, and Pizzo 2017; Bravo et al. 2012). Modifications in MAM tethering and activity are implicated in a number of neurodegenerative diseases such as Alzheimer's, Parkinson's, and amyotrophic lateral sclerosis (Leal et al. 2018; Hedskog et al. 2013; Area-Gomez et al. 2012; Area-Gomez and Schon 2017; Erpapazoglou, Mouton-Liger, and Corti 2017; Rodriguez-Arribas et al. 2017). An extensive review of MAMs in neuropathology as well as their implications and potential therapeutic application in HAND is illustrated in Chapter 2. Briefly, prior studies of ER-mitochondrial cooperation have emphasized the ER as a regulator of mitochondrial function *via* calcium signaling and the unfolded protein response (UPR), especially under stress (Bravo et al. 2012; Lebeau et al. 2018; Rainbolt, Saunders, and Wiseman 2014; Vannuvel et al. 2013; Balsa et al. 2019). We

hypothesize that the ER-mitochondria interface is a key regulator of astrocyte dysfunction *via* calcium and non-canonical UPR signaling during HIV-1 and METH pathogenesis **(Figure 1.3)**.

1.2 Experimental Design and Aims

All experiments were performed in primary human astrocytes from a minimum of three independent biological donors that were isolated in full compliance with local, federal, and NIH ethical guidelines. Prior to use, astrocyte cultures were characterized as previously described (Borgmann and Ghorpade 2017; Gardner et al. 2006; Edara, Ghorpade, and Borgmann 2020; You et al. 2020). A pictural overview of our HIV-1/METH experimental paradigms are illustrated in **Figure 1.4** and additional descriptions of materials and methods will be found in relevant chapters. Briefly, the effects of METH exposure and HIV-1 infection are examined independently as well as in combination to decipher the independent versus synergistic consequences of METH exposure and HIV-1 infection on astrocyte function. Moreover, we investigated how chronic METH exposure or HIV-1 infection alters astrocyte homeostasis by re-challenging with acute METH.

For METH exposure paradigms, cultured astrocytes were treated with acute (0 - 24 h) and/or chronic (7 d) METH with doses ranging from 50 nM - 250 μM to assess astrocyte responses to differing intensities and durations of METH-induced stress. These doses were determined based on the physiological peak (6 μM – 2 mM) and prolonged METH ranges (60 – 600 nM) found *in vivo* and our previous investigations (Won et al. 2001; Rivière, Gentry, and Owens 2000; Cisneros and Ghorpade 2014, 2012; Borgmann and Ghorpade 2015; Shah and Kumar 2016; Borgmann and Ghorpade 2017). Thus, we will use higher doses (5 – 250 μM) for acute assessment and lower doses (50 nM – 250 nM) for chronic studies to model the low levels of residual METH present in

the brains of chronic METH users in between binges. Primary astrocyte cultures without METH treatment were compared as negative controls.

For HIV-1 studies, astrocytes do not express the key receptor (CD4) required for conventional HIV-1 entry. However, astrocytes can undergo other means of HIV-1 infection such as direct cell-cell transfer *via* infected CD4+ T cells (Luo and He 2015; Lutgen et al. 2020), whose trafficking in to the CNS has been established (Mathe et al. 1997; Spudich et al. 2019). Therefore, to investigate specifically how HIV-1 infection alters astrocyte activities, we used a pseudotyped HIV-1 that modifies the viral coat with vesicular stomatitis virus glycoprotein (VSVg) to permit entry independent of CD4 expression as previously described (Canki et al. 2001; Ojeda et al. 2018; Edara, Ghorpade, and Borgmann 2020). A T-tropic HIV-1 strain (NL4-3) was used to model astrocytes infected *in vivo* by T-cell-mediated HIV-1 transfer. As HAND is a chronic condition, astrocyte responses to HIV-1 infection were assessed up to 7 d. Confirmation of our pseudotyped model is illustrated in Chapter 3 **(Figure 3.1)**.

To investigate our hypothesis: "the ER-mitochondria interface is a key regulator of astrocyte dysfunction *via* calcium and non-canonical UPR signaling during HIV-1 and METH pathogenesis", these studies were divided into three overall aims.

Aim 1: How do METH exposure and HIV-1 infection affect astrocyte ER and mitochondrial function and dynamics? To investigate astrocyte metabolic profile, we quantified essential biological outputs of mitochondrial function using Seahorse extracellular flux assays, as previously described (Prah et al. 2019; Chaphalkar et al. 2020). Functional parameters included basal and maximal oxygen consumption rate (OCR), spare respiratory capacity, non-mitochondrial oxygen consumption rate, proton leak, and ATP production. We then used Simple Wes to characterize protein expressional changes of key ER-mitochondrial signaling and regulatory

factors. Astrocyte antioxidant capacity was determined by superoxide dismutase protein levels. Mitochondrial fission (Drp1) and fusion (MFN2) proteins were measured for insights into mitochondrial and MAM dynamics. To characterized changes in ER/UPR homeostasis, we evaluated protein expression profiles of the three UPR sensors [PERK, IRE1α, ATF6] and their negative signaling regulator [binding immunoglobulin protein/78 kDa glucose-regulated protein (BiP/grp78)]. Finally, glucose-regulated protein 75 (grp75) and sigma 1 receptor (Sig1R)] were assessed as MAM-mediated calcium signaling proteins.

Aim 2: How do ER signaling pathways and inter-organelle communication regulate HIV-1/METH-mediated changes in astrocyte dysfunction? Calcium transfer between the ER and mitochondria is essential for inter-organelle communication. Both cytosolic and mitochondrial calcium flux was assessed by transfecting astrocytes with genetically modified organelle-targeted fluorescent calcium indicators followed by time series microscopy techniques. To delineate ER/UPR-associated regulation of astrocyte mitochondrial function, we used pharmacological inhibitors of the three UPR arms. Our findings implicated IRE1α to be uniquely involved in regulating astrocyte mitochondrial function during chronic METH exposure and HIV-1 infection (Chapter 3). Thus, we further investigated IRE1α as a key regulator of astrocyte function. To mimic the increased expression of IRE1α during chronic METH exposure and HIV-1 infection, we used an ectopic IRE1α overexpression vector (Chapter 3). Backbone vector was used as control.

Aim 3: How does astrocyte TAAR1 regulate ER-mitochondrial dysfunction in the context of METH exposure and HIV-1 infection? In the final research chapter **(Chapter 4; Figure 4.6)**, we investigate astrocyte TAAR1 as a potential upstream regulator of METH-induced ER/UPR dysfunction. We first quantify TAAR1 mRNA expression following our pseudotyped HIV-1

infection. Next, we inhibit TAAR1 with a selective antagonist, EPPTB, and investigate downstream parameters, including acute METH-induced calcium flux and UPR/MAM protein expression.

1.3 Significance and Innovation

The comorbidity of HIV-1 and METH are of high priority to NIDA research. While ER and oxidative stress are known outcomes of both METH and HIV-1 cytotoxicity, their connection remains largely unknown, having been explored primarily in the context of apoptosis (Tsai, Bendriem, and Lee 2019; Shah and Kumar 2016; Shah et al. 2016). However, the resiliency of human astrocytes during chronic METH and HIV-1 exposures supports the capacity of quality control mechanisms to enable survival. Our investigations are targeted at elucidating novel signaling pathways linking ER and mitochondria during HIV-1 infection and both acute and chronic models of METH exposure. Moreover, the majority of MAM research in the brain has largely been focused on neurons or whole brain tissues (Hedskog et al. 2013; Leal et al. 2018; Erpapazoglou, Mouton-Liger, and Corti 2017; Rodriguez-Arribas et al. 2017). Therefore, exploration of astrocyte MAMs in both health and disease will provide unique insights into astrocyte biology and inter-organelle communication. Finally, identifying key regulatory mechanisms will help expose novel therapeutic targets that could be used to manipulate astrocyte function and thereby control the balance between astrocyte-mediated neurotoxicity and neuroprotection during HIV-1/METH pathogenesis.

1.4 Figures

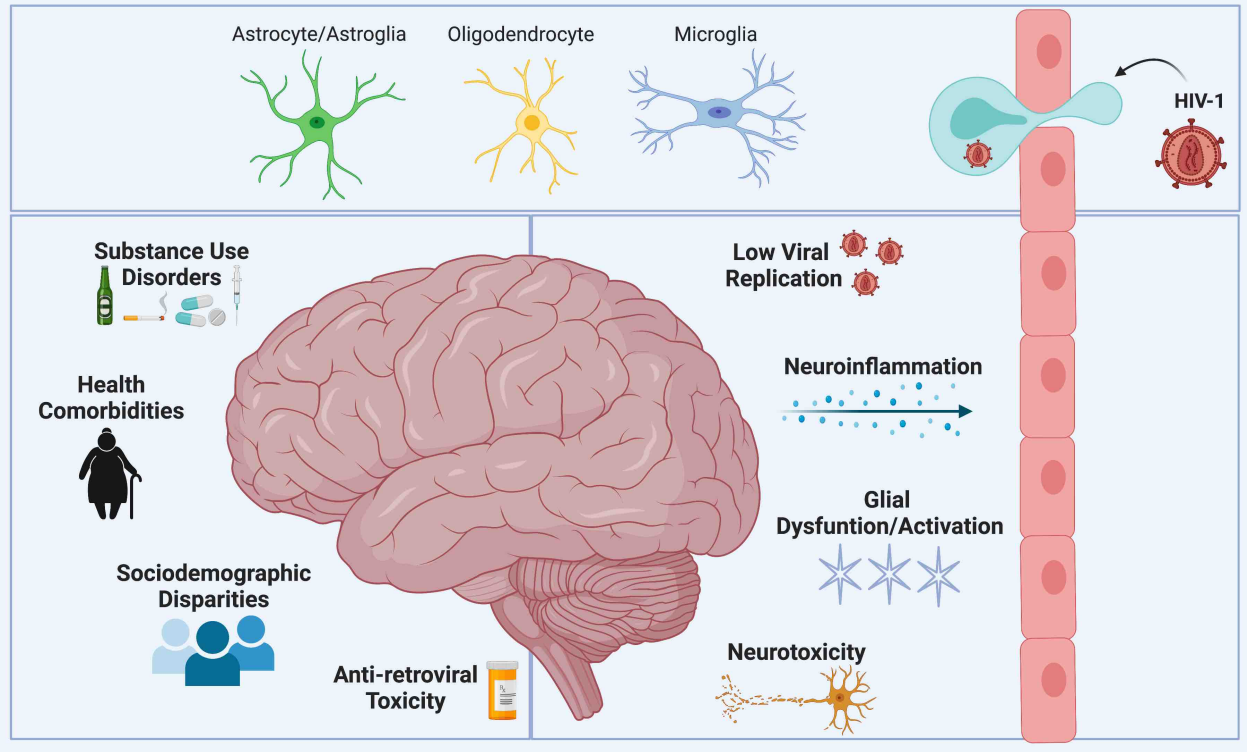

Figure 1.1 The pathology of HIV-associated neurocognitive disorders (HAND). The pathology of HAND is characterized by the early invasion of HIV-1 into the CNS mediated by infiltrating infected immune cells where it can then infect residential glial cells (including astrocytes, microglia, and oligodendrocytes) and persists in the CNS for life. Chronic levels of low viral replication, neuroinflammation, glial dysfunction/activation, and neurotoxicity are the key biological characteristics perpetuating the clinical manifestation of HAND. However, there are also additional factors that influence the both the development and severity of HAND, including ART toxicity, sociodemographic disparities, health comorbidities, substance use disorders. Made with BioRender.

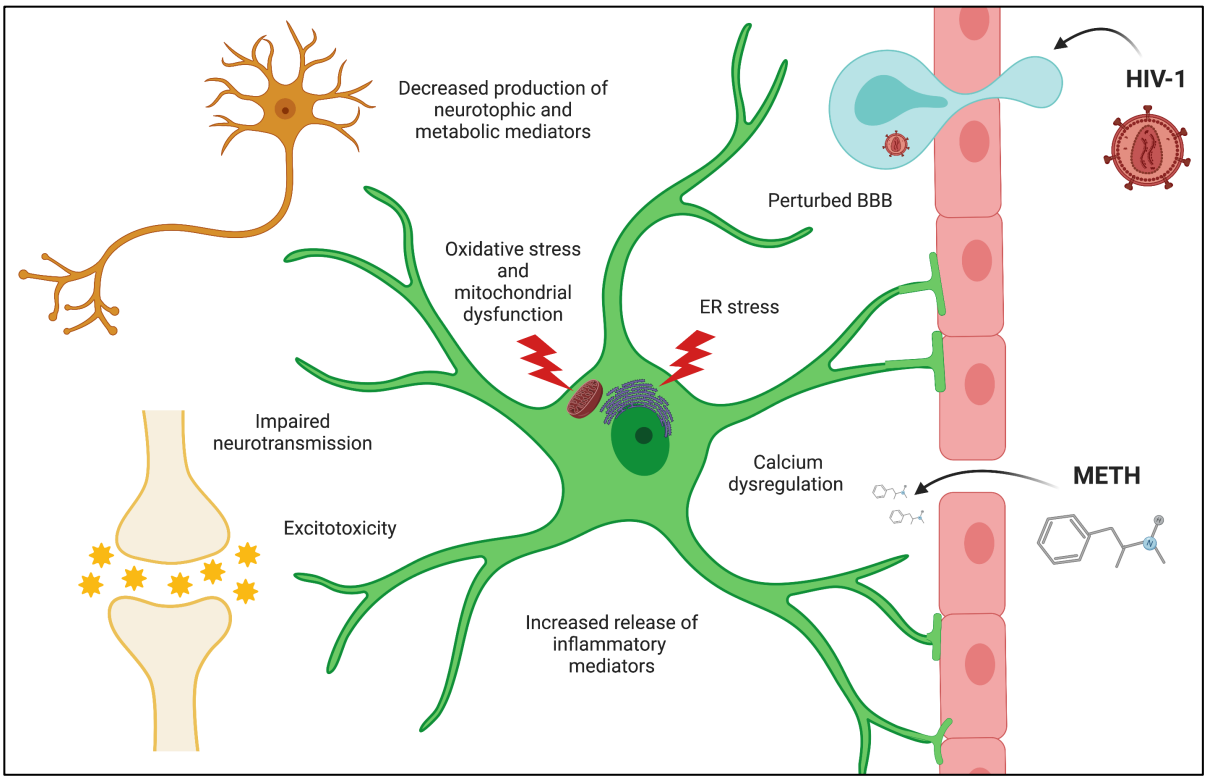

Figure 1.2 Characteristics of Astrocyte Dysfunction. During a neuropathological challenge, astrocytes become activated, shifting their primary neurosupportive functions. During acute insult or injury (such as stroke), these functional changes can be neuroprotective; however, chronic astrocyte activation during conditions like HIV-1 infection or METH use disorders leads to astrocyte dysfunction which can mediate neurotoxic consequences. These functional outcomes include ER and oxidative stress; mitochondrial dysfunction; calcium dysregulation; increased inflammatory profile; impaired neurotransmission and tripartite synaptic maintenance; glutamate excitotoxity; decreased neurotrophic, antioxidant and metabolite support, increased release of toxic ROS/RNS radical and/or extracellular ATP, and perturbed BBB integrity. Indeed, these characteristics of astrocyte dysfunction and astrocyte-mediated neurotoxicity are hallmarks of neurodegenerative pathologies. Identifying cellular and/or molecular targets to prevent astrocyte dysfunction and optimize the coupling between astrocytes and neurons is essential to promote neuronal fitness during a neuropathological challenge. Image made with BioRender.

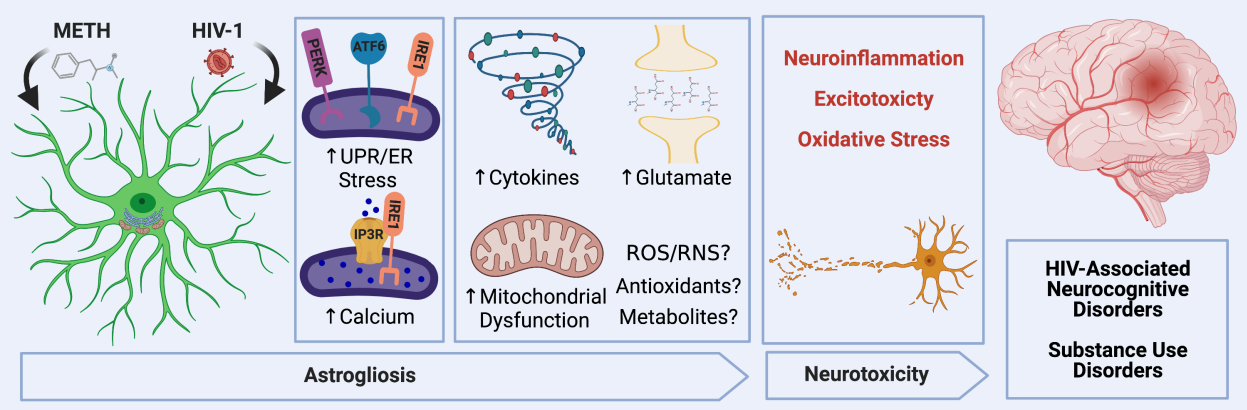

Figure 1.3 The ER-mitochondria interface may be a key regulator of astrocyte dysfunction *via* calcium and non-canonical UPR signaling during HIV-1 and METH pathogenesis. HIV-1 infection and METH exposure alter astrocyte function leading to impaired neuroprotection and increased neurotoxicity. ER-associated signaling mechanisms, such as UPR and calcium, may be potential targets to combat outcomes of astrocyte-mediated neurotoxicity, including neuroinflammation, glutamate excitotoxicity, and oxidative stress through the regulation of cytokine release, tripartite synaptic maintenance (glutamate uptake), and mitochondrial dysfunction, respectively. Abbreviations: activating transcription factor 6 (ATF6) endoplasmic reticulum (ER); inositol 1,4,5-triphosphate receptors (IP_3R); inositol-requiring protein 1α (IRE1α); protein kinase RNA-like endoplasmic reticulum kinase (PERK); reactive oxygen/nitrogen species (ROS/RNS); unfolded protein response (UPR). Image made with BioRender.

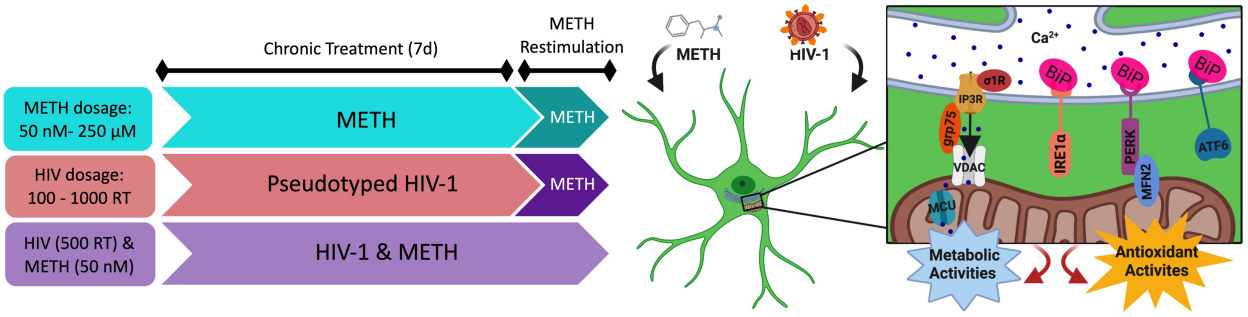

Figure 1.4 Experimental design for HIV-1/METH comorbidity in astrocytes. Primary human astrocytes were exposure to low dose METH (50 nM – 250 µM) and/or infected with pseudotyped HIV-1 for seven days. To determine how chronic METH exposure or HIV-1 infection shift astrocyte stress responses, astrocytes were restimulated with acute METH (5 – 250 µM; under 24 h). Changes in astrocyte ER-mitochondrial interface, including intracellular calcium flux, UPR/MAM protein expression, and mitochondrial metabolic and antioxidant function, were evaluated following acute or chronic METH exposure alone or in combination with HIV-1 infection. Key UPR/MAM mediators included the three UPR arms (ATF6, IRE1, & PERK) and their negative binding partner BiP, calcium transfer regulators (Sig1R & grp75), and a known mediator for MAM tethering (MFN2). Abbreviations: activating transcription factor 6 (ATF6); calcium (Ca^{2+}); endoplasmic reticulum (ER); glucose-regulated protein 75 kDa (grp75); inositol 1,4,5-triphosphate receptors (IP_3R); inositol-requiring protein 1α (IRE1α); mitochondria-associated ER membrane (MAM); mitofusin (MFN); mitochondrial calcium uniporter (MCU); protein kinase RNA-like endoplasmic reticulum kinase (PERK); sigma-1 receptor (σ1R or Sig1R); unfolded protein response (UPR); voltage-dependent anion-selective channel (VDAC). Made with BioRender.

CHAPTER 2

CAL"MAM'ITY AT THE ER-MITOCHONDRIAL INTERFACE: A POTENTIAL THERAPEUTIC TARGET FOR NEURODEGENERATION AND HIV-ASSOCIATED NEUROCOGNITIVE DISORDERS

AUTHORS

J. PROULX, I-W. PARK, & K. BORGMANN

PORTION FORMATTED AND PUBLISHED AS:

Proulx J., Park I-W., Borgmann K. Cal"MAM"ity at the ER-mitochondrial interface: A potential therapeutic target for neurodegeneration and HIV-associated neurocognitive disorders. Front. Neurosci. 2021. doi: 10.3389/fnins.2021.715945.

2.1 Abstract

The endoplasmic reticulum (ER) is a multifunctional organelle and serves as the primary site for intracellular calcium storage, lipid biogenesis, protein synthesis, and quality control. Mitochondria are responsible for producing the majority of cellular energy required for cell survival and function and are integral for many metabolic and signaling processes. Mitochondria-associated ER membranes (MAMs) are direct contact sites between the ER and mitochondria that serve as platforms to coordinate fundamental cellular processes such as mitochondrial dynamics and bioenergetics, calcium and lipid homeostasis, autophagy, apoptosis, inflammation and intracellular stress responses. Given the importance of MAM-mediated mechanisms in regulating cellular fate and function, MAMs are now known as key molecular and cellular hubs underlying disease pathology. Notably, neurons are uniquely susceptible to mitochondrial dysfunction and intracellular stress, which highlights the importance of MAMs as potential targets to manipulate MAM-associated mechanisms. However, whether altered MAM communication and connectivity are causative agents or compensatory mechanisms in disease development and progression remains elusive. Regardless, exploration is warranted to determine if MAMs are therapeutically targetable to combat neurodegeneration. Here, we review key MAM interactions and proteins both *in vitro* and *in vivo* models of Alzheimer's disease, Parkinson's disease, and amyotrophic lateral sclerosis. We further discuss implications of MAMs in HIV-associated neurocognitive disorders (HAND), as MAMs have not yet been explored in this neuropathology. These perspectives specifically focus on mitochondrial dysfunction, calcium dysregulation and ER stress as notable MAM-mediated mechanisms underlying HAND pathology. Finally, we discuss potential targets to manipulate MAM function as a therapeutic intervention against neurodegeneration. Future

investigations are warranted to better understand the interplay and therapeutic application of MAMs in glial dysfunction and neurotoxicity.

2.2 Introduction

Crosstalk amongst subcellular organelles is an intricate and essential phenomenon for coordinating intracellular communication and ultimately regulating cellular fate. In fact, organelles such as the nucleus, endoplasmic reticulum (ER), golgi apparatus, plasma membrane, mitochondria, lysosomes, peroxisomes and endosomes are now known to both functionally and physically interact with each other to carry out distinct cellular functions (Khan et al. 2019; Picca et al. 2020; Liao, Dong, and Cheng 2020). Notably, this review will focus on the direct contact sites between the ER and mitochondria. The ER has many pivotal functions that regulate cellular function and physiology, including calcium storage and release, lipid biogenesis, and protein folding, assembly, modification and sorting. Moreover, the ER is an intracellular stress sensor, which uses well-established quality control mechanisms such as the unfolded protein response (UPR) and ER-associated degradation (ERAD) signaling pathways to respond to cellular stress and maintain homeostasis (Vincenz-Donnelly and Hipp 2017). Mitochondria, having often been renowned as the 'powerhouse of the cell', are essential for ATP production, calcium buffering as well as regulating various elements of cellular fate through metabolic, apoptotic, and redox signaling (Friedman and Nunnari 2014; Brand et al. 2013). The direct contact sites between the ER and mitochondria are crucial to regulate both the dynamic structure and function of these two organelles (van Vliet, Verfaillie, and Agostinis 2014).

2.3 Mitochondria-associated ER Membranes (MAMs)

While the first indication of direct ER-mitochondria contact was described in 1956, it took nearly four decades of continued exploration before the concept of a physical ER-mitochondrial interaction gained acceptance and the term, mitochondria-associated membranes (MAMs), was coined (Herrera-Cruz and Simmen 2017). Following acceptance of this phenomenon, it was not until over 20 years later that we were able to produce the first comprehensive analysis of the MAM proteome (Herrera-Cruz and Simmen 2017; Janikiewicz et al. 2018; Moltedo, Remondelli, and Amodio 2019). Since these initial investigations, multiple mediators have been identified in regulating both the structure and function of the ER-mitochondrial interface, which are illustrated in **Figure 2.1**.

Strides have been made in our understanding of how MAMs are integral signaling platforms that regulate multiple cellular functions and maintain homeostasis. In addition to regulating the function and dynamics of both the ER and mitochondria, as discussed below, MAMs are considered central hubs for regulating key cellular processes including apoptosis, autophagy, calcium and lipid homeostasis, inflammation, and inflammasome formation (Paillusson et al. 2016; Janikiewicz et al. 2018; Moltedo, Remondelli, and Amodio 2019). Tether proteins between the ER and mitochondria serve as essential scaffolds in regulating MAM-mediated mechanisms whereas communication between these two organelles is primarily facilitated by calcium and redox signaling (Marchi et al. 2017; Yoboue, Sitia, and Simmen 2018; Moltedo, Remondelli, and Amodio 2019).

Briefly, the transfer of calcium from the ER to mitochondria is facilitated by inositol 1,4,5-triphosphate receptors (IP_3R) on the ER membrane, voltage-dependent anion-selective channel (VDAC) on the outer mitochondrial membrane (OMM), and cytosolic glucose-regulated protein

75 kDa (grp75), which stabilizes IP_3R and VDAC association within the MAM interface. Notably, cytosolic DJ-1 is newly identified as a critical component in the IP_3R -grp75-VDAC complex (Liu et al. 2019; Basso, Marchesan, and Ziviani 2020). On the inner mitochondrial membrane (IMM) mitochondrial calcium uniporter (MCU) enables the calcium transfer into the matrix, which increases the electrochemical potential and thus oxidative phosphorylation power (Rizzuto et al. 2012; van Vliet, Verfaillie, and Agostinis 2014; Giorgi, Marchi, and Pinton 2018). On the ER membrane side of the interface, the sigma-1 receptor (Sig1R) promotes of calcium transfer by associating with IP_3R (Hayashi and Su 2007).

One of the most researched proteins involved in MAM tethering is mitofusin (MFN) 2, which localizes to both the OMM and ER membrane forming a homodimer as well as a heterodimer with MFN1 (de Brito and Scorrano 2008; Leal and Martins 2021). However, whether MFN2 positively or negatively regulates MAM tethering remains controversial across differing conditions and cell types (de Brito and Scorrano 2008; Filadi et al. 2015; Janikiewicz et al. 2018; Moltedo, Remondelli, and Amodio 2019; Leal and Martins 2021); thus, functional outcomes of MFN2 manipulation can vary. Additional regulators of MAM tethering are vesicle-associated membrane protein-associated protein B (VAPB) on the ER membrane and protein tyrosine phosphatase-interacting protein 51 (PTPIP51) on the OMM (Gomez-Suaga et al. 2019; Leal and Martins 2021; De Vos et al. 2012). Interestingly, MAMs are origin sites for autophagy initiation and autophagosome formation (Yang et al. 2020), which is negatively regulated by VAPB-PTPIP51 tethering (Gomez-Suaga et al. 2017). Finally, MAM tethering *via* ER-associated B cell receptor-associated protein 31 (Bap31) and mitochondrial fission 1 (Fis1) construct a scaffold for apoptotic signaling (Iwasawa et al. 2011), where phosphofurin acidic cluster sorting 2 (PACS2) is a pivotal regulator (Simmen et al. 2005).

MAMs are indispensable for ER physiology and health and are intricately involved in cellular responses to UPR/ER stress signaling. Interestingly, many studies have revealed distinct associations between the UPR sensors and MAM regulation both in response to and in the absence of ER stress, highlighting possible non-canonical functions for these proteins (van Vliet, Verfaillie, and Agostinis 2014; van Vliet and Agostinis 2018; Saito and Imaizumi 2018; Bravo et al. 2011). Briefly, there are three arms to the UPR cascade: protein kinase RNA-like endoplasmic reticulum kinase (PERK), inositol-requiring protein 1α (IRE1α), and activating transcription factor 6 (ATF6). PERK is proposed as a key regulator of MAM tethering through direct interaction with MFN2 and is also linked to regulating mitochondrial dynamics and bioenergetics (Verfaillie et al. 2012; van Vliet and Agostinis 2016; Lebeau et al. 2018; Rainbolt, Saunders, and Wiseman 2014; Balsa et al. 2019; Munoz et al. 2013). IRE1α, which is commonly associated with cellular responses to infections or inflammation, is implicated in ER-mitochondrial calcium transfer, mitochondrial respiration and redox homeostasis through associations with IP_3R (Son et al. 2014; Carreras-Sureda et al. 2019) and/or Sig1R (Mori et al. 2013). ATF6 is shown to both interact with and be regulated by the key MAM tethering protein VAPB (Gkogkas et al. 2008). Moreover, ATF6 can regulate lipid biosynthesis and ER expansion suggesting a possible interplay in MAM-mediated lipid homeostasis and ER-mitochondrial physiology (Bommiasamy et al. 2009). Most recently, ATF6 has also been implicated in ER-mitochondrial calcium homeostasis (Burkewitz et al. 2020).

The ER and mitochondria contact sites are fundamental for regulating mitochondrial function, dynamics, and homeostasis. For example, calcium and redox signaling between the ER and mitochondria are essential for regulating mitochondrial integrity and bioenergetic activity. Moreover, mitochondrial dynamics are regulated by a balance between fission and fusion both of

which are coordinated by the ER-mitochondrial interface. In fact, fission requires the physical maneuvering of the ER membrane to constrict around the mitochondrion fission site which then recruits the primary regulator of mitochondrial fission: dynamin-related protein 1 (Drp1), along with fission adaptor proteins, mitochondrial fission factor and Fis1 (Friedman et al. 2011; Moltedo, Remondelli, and Amodio 2019). Fusion of mitochondria require the involvement of MFN1 and MFN2 which, as aforementioned, are enriched at MAMs and regulate MAM tethering (Moltedo, Remondelli, and Amodio 2019). Notably, MFN1/2 coordinated OMM fusion while optic atrophy protein 1 (OPA1) mediated IMM fusion.

Beyond fission and fusion, biogenesis and degradation are also vital for ensuring healthy mitochondria turnover. Following mitochondrial fission events, damaged mitochondria are removed *via* mitophagy, in which phosphatase and tensin homolog (PTEN)-induced putative kinase (PINK1) and beclin 1 (BECN1) at the MAM interface promote autophagosome formation (Gelmetti et al. 2017). Notably, PINK1 phosphorylates MFN2 leading to Parkin recruitment and initiation of mitophagy machinery while proteins such as p62 and microtubule-associated protein 1A/1B-light chain 3 (LC3) coordinate cargo selection and autophagosome/mitophagosome maturation (Moltedo, Remondelli, and Amodio 2019; Yang et al. 2020). Meanwhile, biogenesis is a self-renewal process in which mitochondrial machinery is 'replenished' by increased transcription and translation of mitochondrial DNA (mtDNA) as well as increased synthesis, import, and assembly of nuclear DNA-encoded mitochondrial proteins (Popov 2020). While the role of MAMs in mitochondrial biogenesis is not clear, expression of proliferator-activated receptor γ coactivator 1α (PGC1α), a master regulator of mitochondrial biogenesis, controls ER-mitochondrial contact. Notably, PGC1α knockout perturbs MAM contact while overexpression promotes increased interaction (Ciron et al. 2015). Finally, mitochondrial transport is essential to

ensure mitochondria are distributed to meet the energetic demands of a cell. Trafficking of mitochondria is facilitated by mitochondrial Rho GTPases (Miro), which directly interact with MFN1/2 and regulate ER-mitochondrial contact (Modi et al. 2019; Misko et al. 2010; Misko et al. 2012). Moreover, functional MFN2 is required for mitochondrial mobility (Misko et al. 2010; Misko et al. 2012).

2.4 MAMs in Neuropathology

Given the importance of MAM-associated mechanisms in cellular homeostasis, MAMs are gaining attention as plausible pathological platforms underlying the development and/or progression of disease (Pinton 2018). Briefly, the role of MAMs in neuropathology, which have been previously reviewed (Raeisossadati and Ferrari 2020; Wilson and Metzakopian 2020; Leal and Martins 2021), have primarily been centered on neurons, highlighting MAMs as pivotal regulators of synaptic transmission and neuronal health (Bernard-Marissal, Chrast, and Schneider 2018; Shirokova, Pchelin, and Mukhina 2020; Gomez-Suaga et al. 2019; Leal and Martins 2021). Astrocyte MAMs are largely a new exploration. Notably, enrichment of MAMs in astrocyte endfeet may be crucial for regulating the blood-brain interface and brain healing following injury (Gbel et al. 2020; Bergami and Motori 2020). Moreover, knockdown of MAM-associated proteins, PACS2 or Sig1R, induces degeneration of hippocampal neurons and astrocytes, supporting the importance of MAMs for neural cell survival (Hedskog et al. 2013). The presence and function of MAMs in other neural cells, microglia and oligodendrocytes, remain unconfirmed (Bernard-Marissal, Chrast, and Schneider 2018; Shirokova, Pchelin, and Mukhina 2020).

Many of the cellular processes that are implicated in the etiology of neurodegenerative diseases are coordinated at the ER-mitochondrial interface such as dysregulated lipid and calcium

homeostasis, mitochondrial dysfunction, ER and oxidative stress, impaired autophagy, and inflammation. Neurons are particularly susceptible to mitochondrial dysfunction given the high energetic demand of brain tissue (Grimm and Eckert 2017; Picca et al. 2020). Moreover, ER stress is induced by the aggregation of misfolded proteins, which is a physical hallmark of most neurogenerative pathologies. Formation of protein aggregates can be a consequence of increased production of misfolded proteins (ER dysfunction), the impaired removal of dysfunctional proteins (impaired autophagy), or both (Sweeney et al. 2017; Monaco and Fraldi 2020). Regardless, ER stress and mitochondrial dysfunction are increasingly being proposed as key therapeutic targets for combating neuropathology, with MAMs arising as the essential crossroad for this collaboration. It is worth considering whether these central hubs can be manipulated to reconcile cellular dysfunction and degeneration and to restore CNS homeostasis.

Beyond the classic hallmarks of neuropathology in the context of known MAM-associated functions, dysregulation of MAM tethering and activity are implicated in a number of neurodegenerative diseases such as Alzheimer's disease (AD), Parkinson's disease (PD), and amyotrophic lateral sclerosis (ALS). However, whether these MAM alterations arise as intended remedial responses or are the causative agents in these disease pathologies remains to be determined. The distinct interplay of MAMs in these neuropathological conditions are illustrated in **Figure 2.2** and discussed below.

2.4.1 Alzheimer's Disease

As one of the most common forms of dementia, Alzheimer's disease is characterized by the aggregation of extracellular amyloid β (Aβ) peptides and intracellular hyperphosphorylated tau proteins, termed plaques and tangles, respectively. Treatment with Aβ in primary hippocampal

neurons increases expression of MAM-associated PACS2 and Sig1R proteins, as well as direct ER-mitochondrial contact *via* the IP_3R-VDAC bridging complex. Expression of PACS2 and Sig1R was also increased in the hippocampus, cortex, and cerebellum brain regions of a potent amyloid precursor protein (APP) mutant AD mouse model. However, in human AD postmortem cortical tissues, PACS2 increased but Sig1R expression decreased (Hedskog et al. 2013). Interestingly, MAMs serve as a key production site for Aβ peptides (Schreiner et al. 2015). The formation of Aβ plaques occurs following the catalytic processing of APP by the γ-secretase complex. Two major components of this complex, presenilin (PS) 1 and PS2, localize to the ER-mitochondria interface and modulate MAM functions, specifically lipid and calcium homeostasis (Area-Gomez et al. 2009; Area-Gomez et al. 2012; Zampese et al. 2011; Galla et al. 2020). Notably, overexpressing PS2 increases both ER-mitochondria contact and calcium transfer from the ER to mitochondria (Zampese et al. 2011; Galla et al. 2020). This phenomenon appears to be mediated through interactions between PS2 and MFN2 (Filadi et al. 2016). Furthermore, silencing MFN2 in human embryonic kidney (HEK) 293 cells stably expressing an APP mutant to overproduce Aβ, increases MAM contact and calcium transfer, which impairs γ-secretase maturation and activity, ultimately decreasing Aβ production (Leal et al. 2016). This same group recently reported decreased expression of MFN1/2 in postmortem human AD brain tissues. They further confirmed a positive correlation between Aβ and MAM contact in multiple AD mouse models and *in vitro* neuron cultures exposed to Aβ. The increased connectivity between ER and mitochondria in response to Aβ subsequently increased mitochondrial metabolic function and autophagosome formation, likely to promote removal of Aβ aggregates (Leal et al. 2020). Of note, another recent examination of human AD cortical tissues showed a decreased expression and interaction of MAM tether proteins, VAPB and PTPIP51, in addition to decreased IP_3R expression. The decreased expression of these

proteins also correlated with increased disease stage severity (Lau et al. 2020). Thus, decreased expression of MAM-mediators in human AD tissues is reported across three separate studies (Hedskog et al., 2013; Leal et al., 2020; (Lau et al. 2020) suggesting impaired ER-mitochondrial tethering, highlighting unique differences between animal models and human tissues. Regardless, these findings strongly implicate MAMs as possible targets to combat AD/Aβ pathology.

Disease-associated tau protein alters mitochondrial transport, dynamics, bioenergetics and degradation as recently reviewed (Szabo, Eckert, and Grimm 2020). These findings further discuss the implications of MAMs in tau pathology as only two studies have so far explored this phenomenon; both of these models identify increased ER-mitochondrial contact during tau pathology (Perreault et al. 2009; Cieri et al. 2018). The ε4 allele of apolipoprotein E (ApoE4) significantly associates with an increased risk for sporadic AD. Treatment of astrocyte conditioned media cultured from ApoE4 knock-in mice, upregulates MAM activity in human fibroblasts and mice neurons, as measured by the synthesis of phospholipids and cholesteryl esters (Tambini et al. 2016). This outcome was averted when repeated in mouse embryonic fibroblasts (MEF) harboring MFN2 knockout, which in this model, decreased MAM tethering (Tambini et al. 2016; de Brito and Scorrano 2008).

2.4.2 Parkinson's Disease

Parkinson's disease is a neurodegenerative disease manifesting with primarily motor deficits due to damaged and degenerative dopaminergic neurons in the substantia nigra. A key pathophysiology underlying PD is the presence of 'Lewy bodies' comprised of α-synuclein (α-syn) aggregates. However, tau pathology is also present in some cases. PD pathology is characterized by a number of MAM-associated cellular processes including impaired autophagy,

calcium homeostasis, lipid metabolism, ER stress, and mitochondrial dynamics as previously reviewed (Rodriguez-Arribas et al. 2017; Gomez-Suaga et al. 2018). Notably, overexpression or silencing of α-syn confirms regulation on mitochondrial dynamics, ER-mitochondrial coupling and calcium transfer (Cali et al. 2012; Guardia-Laguarta et al. 2014). However, these findings are also inconsistent as one demonstrates increased organelle contact while the other reports disruption in tethering. From a more recent report, α-syn binds to VAPB on the ER membrane, disrupting interaction with PTPIP51 on the OMM and subsequently, MAM tethering, calcium transfer, and ATP production (Paillusson et al. 2017). Thus, the effects of α-syn on MAM function is linked to impaired bioenergetic activity.

Another MAM connection to the neuropathology of PD involves PINK1 and Parkin. Mutations in PINK1 and Parkin are key risk factors for the development of PD. The functions of these proteins are critical in maintaining mitochondrial health by regulating mitochondrial biogenesis, degradation, dynamics, function, and transport. PINK1 and Parkin localize to MAMs, which is not surprising given their prominent roles in mitophagy and MAM's being the site for mitochondrial fission (Gomez-Suaga et al. 2018). Moreover, Parkin is implicated as a possible regulator for MAM tethering although controverting evidence has been reported as to whether it is a positive or negative regulator (Cali et al. 2013; Gautier et al. 2016). Briefly, overexpression of Parkin in both HeLa and a neuroblastoma cell line enhanced MAM coupling and calcium transfer to increase ATP production (Cali et al. 2013). Expression of Parkin is encoded by the PARK2 gene. Increased mitochondrial-ER contact was found in fibroblasts from a PARK2 knockout mouse and PD patients with PARK2 mutation (Gautier et al. 2016). Moreover, mutations in the gene for DJ-1, which as mentioned above has been identified as a novel component in the IP_3R-grp75-VDAC complex, is causative for autosomal recessive familial PD. The DJ-1 protein has

been identified to have a protective role in oxidative stress and modulates mitochondrial morphology. Similar to a report on α-syn, overexpression of DJ-1 enhances ER-mitochondrial coupling and calcium transfer while silencing of DJ-1 impairs mitochondrial calcium flux and induces fragmentation (Ottolini et al. 2013). All these findings highlight the importance of MAMs as regulators of mitochondrial function and physiology in the context of PD pathology.

2.4.3 Amyotrophic Lateral Sclerosis

A key component of ALS pathology is deposits of transactive response (TAR) DNA-binding protein 43 (TDP-43). Like α-syn, TDP-43 alters MAM tethering and calcium homeostasis by interrupting the relationship between VAPB and PTPIP51. However, the mechanism of disruption is instead mediated through activation of glycogen synthase kinase-3β (GSK-3β) (Stoica et al. 2014). Interestingly, accumulation of fused in sarcoma (FUS), a key pathological feature characterizing ALS, also interrupts VAPB and PTPIP51 association and MAM tethering *via* GSK-3β activation (Stoica et al. 2016). This interruption was accompanied by compromised mitochondrial calcium uptake and ATP production. Thus, ALS pathology is characterized by two factors that activate GSK-3β to disentangle the MAM interface; however, the target of GSK-3β to facilitate this interference remains unknown. The significance of MAM tethering in ALS pathology is further supported as a P56S mutation in VAPB is causative of ALS (Nishimura et al. 2004). Moreover, mutation or perturbed function of another MAM protein, Sig1R, which is essential for calcium transfer from the ER to mitochondria, is a causal agent to ALS pathology and motor neuron degeneration (Al-Saif, Al-Mohanna, and Bohlega 2011; Bernard-Marissal et al. 2015). Additional implications and associations of MAMs in ALS pathology are previously reviewed (Manfredi and Kawamata 2016; Lau et al. 2018).

2.5 HIV-Associated Neurocognitive Disorders (HAND)

Human immunodeficiency virus type 1 (HIV-1) can invade the CNS early during infection and infect residential glial cells (astroglia, microglia, and oligodendrocytes) where infection can persist for life. Even with the medical advancement of antiretroviral therapy (ART), low viral replication, chronic neuroinflammation, glial dysfunction, and HIV-1 protein toxicity contribute to the development of a spectrum of HAND. In fact, HAND continue to afflict approximately 30-70% of people living with HIV, depending on cohort demographics (Simioni et al. 2010; Heaton et al. 2011). HAND are characterized by different levels of cognitive impairments and interference with one's daily functioning. At the extreme end of the spectrum, symptoms clinically manifest as dementia (Mackiewicz et al. 2019).

The pathology of HIV-1 infection often includes "accelerated aging". Thus, HIV-1 patients are more prone to developing early onset symptoms for a number of age-related diseases including the neurodegenerative pathologies discussed above (Cody and Vance 2016; Robertson et al. 2007; Wang et al. 2017; Mackiewicz et al. 2019). In fact, Aβ plaques as well as tauopathy can both associate with and be exacerbated by HAND pathology (Brown et al. 2014; Kim, Yoon, and Kim 2013; Hategan, Masliah, and Nath 2019). Of note, the primary HIV-1 proteins implicated in neurotoxicity are transactivator of transcription (Tat), glycoprotein (gp)120, viral protein R (Vpr), and negative factor (Nef). Moreover, ART drugs are now identified as key contributors to the cellular senescence and accelerated aging underlying HIV/HAND pathology as reviewed preciously, with emphasis of mitochondrial dysfunction (Schank et al. 2021).

Khan et al. recently published insights into potential inter-organelle collaborations in HIV/HAND pathogenesis (Khan et al. 2019). Despite obvious disruptions in ER and mitochondrial homeostasis in HAND pathology, as will be discussed below, there remains limited investigations

and/or considerations of MAMs (Nooka and Ghorpade 2017; Ma et al. 2016; Khan et al. 2019). Below we discuss the implications of MAMs in HAND pathology by reviewing the effects of HIV-1 on ER stress, calcium dysregulation and mitochondrial dysfunction, which is also illustrated in **Figure 2.3**. Together, these findings strongly support altered MAM signaling as a prominent contributor to HAND pathology.

2.5.1 HIV-1 and ER Stress

As aforementioned, ER stress is a key characteristic in neurodegenerative pathologies, and MAMs are intricately involved in cellular responses to ER stress. Indeed, the three UPR arms are now increasingly considered integral mediators within the MAM proteome (van Vliet and Agostinis 2016, 2018; Saito and Imaizumi 2018; Malli and Graier 2019). In the context of HAND, significant increases in ER stress markers are detected in the frontal cortex of brain tissues from HIV-1 positive individuals. In fact, the levels of ER stress positively correlate with cognitive decline, wherein the most severe cases of HAND have the highest expression of ER stress markers (Lindl et al. 2007; Akay et al. 2012). Interestingly, these studies show that while ER stress is evident in both neurons and astrocytes, astrocytes appear to have higher expression of ER stress markers. These findings do not necessarily mean neurons are less likely to endure ER stress during HIV-1 infection. Rather, astrocytes may be more resilient to prolonged ER stress, and neurons could be more susceptible to succumb to apoptosis.

It is well-known that during neurodegenerative or neuroinflammatory conditions, astrocytes become ‘activated’, shifting their function from neurotrophic to a more neurotoxic phenotype. Astrocyte-mediated neurotoxicity has arisen as a key feature in HAND pathology with UPR/ER stress as a potential regulator (Nooka and Ghorpade 2017; Fan and He 2016;

Natarajaseenivasan et al. 2018; Shah et al. 2016; Nooka and Ghorpade 2018). In fact, while HIV-1-induced ER stress has not yet been extensively investigated, most investigations are primarily centered around astrocytes. Notably, expression of HIV-1 Tat in astrocytes induces aggregation of glial fibrillary acid protein (GFAP). Both Tat expression and GFAP aggregation activate the three UPR pathways (Fan and He 2016). HIV-1 gp120 specifically activates the IRE1α branch of UPR signaling in an astrocyte cell line, primary human astrocytes, and astrocyte-restricted gp120 transgenic mice, which is linked to the initiation of apoptotic signaling (Shah et al. 2016). Inhibition of ER stress or UPR signaling in both of these studies reverses astrocyte-mediated neurotoxicity and apoptotic signaling (Fan and He 2016; Shah et al. 2016). Moreover, studies from our lab demonstrate induction of the three UPR pathways in primary human astrocytes in response to HAND-relevant stimuli (whole HIV-1, inflammation, and ART drugs), which associate with mitochondrial depolarization (Nooka and Ghorpade 2017). HIV-1 Tat-induced ER stress in a CD4+ T cell line (Campestrini, Silveira, and Pinto 2018) neurons (Norman et al.) and human brain microvascular endothelial cells (HBMEC) (Ma et al. 2016) are also accompanied by changes in mitochondrial function and apoptotic signaling supporting cooperation of the ER and mitochondria during HIV/HAND pathology. Indeed, inhibition of ER stress reversed HIV-1-induced mitochondrial dysfunction and increased cell viability in HBMEC (Ma et al. 2016). These findings not only implicate MAMs in HAND pathology but also emphasize UPR/ER stress signaling as an important regulator of mitochondrial function, cellular fate and astrocyte-mediated neurotoxicity.

2.5.2 HIV-1 and Calcium Dysregulation

As discussed above, the ER is the primary site for intracellular calcium storage, and MAMs are hubs for regulating calcium homeostasis. HIV-1 modulates calcium signaling and perturbs

calcium homeostasis. Many of these studies have been previously reviewed or discussed (Haughey and Mattson 2002; Hu 2016; Fields and Ellis 2019). Altered calcium dynamics during HIV-1 exposure is directly linked to apoptotic signaling, UPR induction, and impaired mitochondrial integrity, energetics, and/or quality control thus implicating calcium dysregulation as a key component in HIV-1-induced neurotoxicity and astrogliosis. One of the earliest studies identifying this relationship was in rat hippocampal neurons exposed to HIV-1 Tat, which induced apoptosis through the elevation of cytoplasmic calcium and increased mitochondrial calcium uptake. Chelating cytosolic calcium or pharmacological inhibiting mitochondrial calcium uptake *via* MCU protected neurons from HIV-1 Tat-mediated neurotoxicity (Kruman, Nath, and Mattson). Interestingly, a later study in rat cortical neurons linked ER and mitochondrial calcium loss *via* ryanodine receptors (RyR) as an upstream mechanism for HIV-1 Tat-mediated UPR induction and mitochondrial hyperpolarization (Norman et al.). While less prominent, calcium mobilization is also implicated in HIV-1 gp120-(Meeker et al. 2016) and Vpr-(Jones et al.) mediated neurotoxicity, which associated with impaired axonal mitochondria transport and apoptotic signaling, respectively.

In the context of astrocytes, our previous studies indicate a pivotal role of calcium signaling in regulating ER stress and mitochondrial dysfunction induced by HAND-relevant stimuli (whole HIV-1, inflammation, and ART drugs). Notably, chelation of cytoplasmic calcium was able to reverse HIV-1-induced ER stress and mitochondrial depolarization (Nooka and Ghorpade 2017). Moreover, knockdown of MCU to reduce mitochondrial calcium uptake during exposure to HIV-1 Tat and/or cocaine reverses astrocyte mitochondrial dysfunction and metabolic switching to restore a neuroprotective phenotype (Natarajaseenivasan et al. 2018). Manipulation of VDAC1 (the OMM calcium channel within the MAM interface) or “mortalin” (a.k.a. grp75, the scaffolding

protein between IP_3R on the ER membrane and VDAC on the mitochondria) are also able to rescue neurons from HIV-1 Tat-induced astrocyte-mediated neurotoxicity (Fatima et al. 2017; Priyanka et al. 2020). Specifically, HIV-1 Tat expressing primary human astrocytes trigger neuronal death by excessive ATP release, a mechanism that was counteracted by repression of VDAC1 (Fatima et al. 2017). Neuroinflammation and glutamate excitotoxicity are additional mechanisms for which astrocytes inflict neuronal damage during HAND, as previously reviewed by our research team (Cisneros and Ghorpade ; Borgmann and Ghorpade). Overexpression of mortalin/grp75 protects neurons from astrocyte-mediated neurotoxicity by reversing HIV-1 Tat-induced astrocyte mitochondrial dysfunction and fragmentation while also reducing the release of excess ATP, inflammatory cytokines, and extracellular glutamate (Priyanka et al. 2020). Altogether, these findings strongly support MAM-mediated calcium transfer as a pivotal regulator of astrocyte-mediated neurotoxicity during HAND pathogenesis.

It is also noteworthy to mention, that while research with HIV-1 Nef is less investigated in HAND pathogenesis, it is known to play a prominent role for calcium dysregulation in T cells (Manninen and Saksela 2002; Shelton et al. 2012; Silva et al. 2016). In fact, HIV-1 Nef directly interacts with both mortalin/grp75 (Shelton et al. 2012) and IP_3R (Manninen and Saksela 2002), which are key mediators in ER to mitochondria calcium transfer. Thus, there is likely an interplay between HIV-1 Nef and the MAM interface. More studies are needed to determine the role of HIV-1 Nef and calcium dysregulation in neural cells.

2.5.3 HIV-1 and Mitochondrial Dysfunction

MAMs are essential for regulating mitochondrial function and homeostasis. Defects in mitochondrial bioenergetics, biogenesis, degradation, dynamics, integrity and transport are all

present in the pathology of HAND and are discussed below. The role of mitochondrial dysfunction in HIV/HAND pathology is rapidly gaining attention with two recent reviews by Fields et al. (Fields and Ellis 2019) and Schank et al. (Schank et al. 2021); however, neither discuss the potential interplay of MAMs. It is well established that HIV-1 can induce neuronal apoptosis, in which mitochondria [and MAMs] are known upstream regulators through calcium and redox signaling (Kruman, Nath, and Mattson ; van Vliet, Verfaillie, and Agostinis 2014; Marchi et al. 2017). In addition to regulating apoptosis, calcium and redox signaling between mitochondria and ER are also essential for regulating mitochondrial integrity and bioenergetic activity, autophagy and inflammasome activation (van Vliet, Verfaillie, and Agostinis 2014), again highlighting the importance of ER-mitochondrial inter-organelle collaboration in negotiating cellular fate.

In human neurons, exposure to HIV-1 Tat and Vpr decreased VDAC (OMM calcium transporter) protein expression, dysregulated RNA expression of several genes regulating mitochondrial metabolism and decreased ATP levels (Darbinian et al. 2020). These findings were also associated with mtDNA damage, reactive oxygen species (ROS) accumulation, increased expression apoptotic proteins, and release of cytochrome C, emphasizing the relationship of mitochondrial bioenergetics and integrity. Less clear are the effects of HIV-1 on neuronal mitochondrial dynamics, which vary greatly across investigations. Two separate studies looking at the brain tissues from HIV+ donors with or without HIV encephalitis, specifically centered on neurons, report enlarged mitochondria as a unique pathological feature of HAND (Fields et al. 2016; Avdoshina et al. 2016).

Changes in mitochondrial morphology associated with increased expression of fusion proteins (MFN1 and OPA1) and decreased expression and/or activation of mitochondrial fission proteins (Fis1 and Drp1). Interestingly, as previously discussed with ER stress markers, decreased

expression of mitochondrial Drp1 also coincided with increased HIV-associated neurocognitive decline (Fields et al. 2016). Similar disruptions on mitochondrial morphology were confirmed in gp120 transgenic mice and by gp120 treatment to neuronal cell cultures (Fields et al. 2016; Avdoshina et al. 2016). These reports also found increased extracellular acidification rate indicating increased glycolysis (Fields et al. 2016) and reduced oxygen consumption rate (OCR) (Avdoshina et al. 2016) suggesting a deviation in mitochondrial bioenergetics. Noteworthy, overexpressing Drp1 reverses gp120-meditated neuronal mitochondrial dysfunction reducing both neuroinflammation and neurodegeneration (Fields et al. 2016). These findings suggest mitochondrial fission as a potential therapeutic mechanism to combat HIV-1-mediated mitochondrial dysfunction in neurons.

On the contrary, more recent studies by Teodorof-Diedrich et al. looking at the effects of both HIV-1 gp120 and Tat on mitochondrial dynamics in human neurons (Teodorof-Diedrich and Spector 2018) and Rozzi et al. looking at the effects of HIV-1 Tat in rat cortical neurons (Rozzi et al. 2018), instead identified a proclivity towards mitochondrial fission and fragmentation. In fact, increased Drp1 expression, activity, and/or translocation were critical for these outcomes. Both studies also reported impaired mitochondrial integrity as demonstrated by decreased membrane potential ($\Delta\Psi m$). Noteworthy, Teodorof-Diedrich et al. also found an increased recruitment of mitophagy proteins (Parkin, p62, and LC3) and mitophagosome formation, yet an impaired mitophagic flux leading to accumulation of damaged mitochondria due to incomplete mitophagy. The discrepancy regarding HIV-1 gp120 on neuronal mitochondrial dynamics may be attributed to different *in vitro* models as the prior two studies were in rodents (Fields et al. 2016; Avdoshina et al. 2016) and the later in primary human neurons (Teodorof-Diedrich and Spector 2018). Moreover, there may be general discrepancies between the effects of HIV-1 gp120 versus HIV-1

Tat. Regardless, the identical findings of elongated mitochondria in neurons of HIV+ brain tissues remain a significant find.

However, there is one similarity across these four studies in regard to mitochondrial distribution/localization. There appears to be an overall decrease in mitochondrial trafficking throughout the processes with increased aggregation of mitochondria near the soma. Impaired mitochondria axonal transport is also evident in neurons exposed to HIV-1 Vpr, which was further associated with decreased ATP production and increased expression of senescent markers (Wang et al. 2017). As mitochondria are essential for synaptic maintenance and to meet the energetic demands for neurotransmission, disrupted axonal mitochondria transport arises as a potential key pathological feature in HAND and age-related axonal degeneration. Interestingly, although HIV-1 Vpr is primarily known as a nuclear protein, it also directly interacts with adenine nucleotide translocase (ANT) on the OMM, which is a key regulator of mitochondrial integrity *via* formation of the mitochondrial permeability transitional pore (Cowan, Anichtchik, and Luo 2019; Wang et al. 2017; Huang et al. 2012). In fact, inhibiting the interaction between HIV-1 Vpr and ANT was able to reverse deficits in mitochondrial trafficking (Wang et al. 2017). Finally, this study also suggests HIV-1 Vpr may disrupt mitochondrial biogenesis in neurons *via* reduction of PGC1α expression. Swinton et al. confirmed decreased expression of PGC1α in HIV+ brain cortical tissues as well as decreased transcription factor A (TFAM), another regulator of mitochondrial biogenesis (Swinton et al.).

In astrocytes, both HIV-1 infection and external HIV-1 exposure perturb mitochondrial integrity (Natarajaseenivasan et al. 2018; Ojeda et al. 2018; Nooka and Ghorpade 2017; Priyanka et al. 2020). Unlike neurons, astrocytes increase their metabolic activity and ATP production (Natarajaseenivasan et al. 2018; Swinton et al.). Moreover, while neurons have decreased TFAM

expression in HIV+ brain tissues, astrocytes have increased TFAM expression (Swinton et al.). The increased metabolic and mitochondrial biosynthetic profile may be a key feature underlying astrocyte activation and astrocyte-mediated neurotoxicity during HAND. For example, HIV-1 Tat provokes astrocytes to undergo a distinct metabolic shift from glucose to fatty acid oxidation, which restricts astrocyte provision of lactate to neurons (Natarajaseenivasan et al. 2018). In addition to decreasing release of neurotrophic factors when 'activated' by HIV-1 Tat, astrocytes increase their release of neurotoxic factors including excessive ATP (Fatima et al. 2017; Priyanka et al. 2020), ROS (Natarajaseenivasan et al. 2018; Priyanka et al. 2020), and inflammatory cytokines (Natarajaseenivasan et al. 2018). As briefly discussed in the previous section, blocking ER-mitochondrial calcium transfer *via* VDAC (on the OMM) (Fatima et al. 2017), MCU (on the IMM) (Natarajaseenivasan et al. 2018), or mortalin/grp75 (scaffold between IP_3R and VDAC) (Priyanka et al. 2020) restored an astrocyte neurotrophic phenotype, highlighting a probable MAM interplay in astrocyte-mediated neurotoxicity during HAND. Moreover, HIV-1 infection (Ojeda et al. 2018) or HIV-1 Tat expression (Priyanka et al. 2020) in astrocytes induced mitochondrial fragmentation, which may be followed by defective mitophagy, similar to what was seen by Teodorof-Diedrich et al. in neurons. Notably, accumulation of damaged mitochondria promoted inflammasome activation, which was subsequently followed by cell death (Ojeda et al. 2018). However, astrocytes that had successful mitophagy, were able to attenuate mitochondrial dysfunction and resist cell death. The divergence between these fates appeared dependent on the mode of infection, where productively infected astrocytes favored survival, and non-productive infection succumbed to inflammasome-mediated cell death.

Mitochondrial dysfunction in microglia has been less studied; however, there is a recent review discussing the important role of microglia in HAND (Borrajo et al. 2021). Similar to

astrocytes, there appears to be a delicate balance between mitophagy and inflammasome formation underlying microglia activation during HAND (Thangaraj et al. 2018; Rawat, Teodorof-Diedrich, and Spector 2019). In response to HIV-1 Tat (Thangaraj et al. 2018) or ssRNA (Rawat, Teodorof-Diedrich, and Spector 2019), there is increased expression of autophagy/mitophagy proteins (PINK1, Parkin, p62, LC3, and BECN1) with a subsequent blockade of mitophagy flux, leading to the accumulation of mitophagosomes and damaged mitochondria. These changes are associated with increased ROS generation and impaired mitochondrial integrity (Rawat, Teodorof-Diedrich, and Spector 2019). However, unlike astrocytes, there is a significant decrease in mitochondrial bioenergetic activity (Thangaraj et al. 2018). Importantly, defects in mitophagy appear to be central to microglial activation and inflammasome formation (Thangaraj et al. 2018; Rawat, Teodorof-Diedrich, and Spector 2019). Indeed, HIV-1 gp120 induces inflammasome activation in microglia *in vitro* and *in vivo*, whereas inhibiting inflammasome activation, alleviates microglia-mediated neurotoxicity, promotes neuronal regeneration, and improves cognitive function (He et al. 2020).

In summary, HIV-1-induced changes in mitochondrial bioenergetics, dynamics, degradation, integrity, and transport are MAM-regulated processes, implicating MAMs in HIV/HAND pathology. Noteworthy, mitochondrial fission events are key consequences of Tat-mediated toxicity in neurons (Teodorof-Diedrich and Spector 2018; Rozzi et al. 2018), astrocytes (Ojeda et al. 2018; Priyanka et al. 2020), and microglia (Thangaraj et al. 2018; Rawat, Teodorof-Diedrich, and Spector 2019). Further, defective mitophagy is a crucial mechanism underlying HAND pathology. The accumulation of damaged mitochondria promotes inflammasome activation in astrocytes and microglia. Thus, the balance between mitophagy and inflammasome activation is a critical determinant of glial fate during HIV-1 toxicity (Ojeda et al. 2018; Rawat,

Teodorof-Diedrich, and Spector 2019). As MAMs are the site for both mitophagy and inflammasome initiation, ER-mitochondrial cooperation is likely essential for negotiating these cellular outcomes. Finally, evidence of MAMs in HAND is further supported by a previous study in T cells showing that HIV-1 Vpr localizes to both the ER and mitochondria, and MAMs serve as a possible route for intracellular trafficking of Vpr (Huang et al. 2012). Notably, exposure to HIV-1 Vpr decreased MFN2 and Drp1 expression, impaired ER-mitochondrial interaction and morphology, and induced mitochondrial depolarization and deformation. Overexpressing MFN2 or Drp1 was able to prevent T cell mitochondrial depolarization and deformation. Additional studies in neural cells are needed to determine the role of MAMs in HAND. Moreover, HIV-1 Tat and Vpr are historically considered as nuclear proteins; however, Tat and Vpr toxicity on ER and mitochondrial homeostasis emphasizes the need to expand our classical understanding of host-viral interactions during HIV-1 infection.

2.6 Potential Therapeutic Targets

Dysfunctional MAM-mediated mechanisms are hallmarks of neurodegenerative pathologies including AD, PD, ALS, and HAND. Notably, ER-mitochondrial contact and communication are critical in regulating mitochondrial function and health. Throughout this review, we have specifically highlighted calcium, UPR/ER stress, mitochondrial fission/fusion, mitophagy and inflammasome signaling pathways as potential targets to combat mitochondrial dysfunction in neural cells during HIV/HAND, whereas MAMs serve as the central therapeutic platform. **Table 2.1** summarizes the potential therapeutic targets discussed throughout this manuscript.

Coupling between the ER and mitochondria can increase in response to stress to tailor to the functional demands of the cell (Bravo-Sagua et al. 2016). However, whether increased/decreased contact contributes to cellular dysfunction or improves cell outcomes, remains largely unknown. Notably, forcing increased ER-mitochondrial contact in Drosophila was able to extend lifespan and improve overall motor function (Garrido-Maraver, Loh, and Martins 2020). As a MAM tether protein, MFN2 may serve as a potential target to manipulate ER-mitochondria contact and communication. Overexpression of MFN2 in CD4+ T cells restored mitochondrial integrity and increased cell viability against HIV-1 Vpr toxicity (Huang et al. 2012). However, the effects of MFN2 manipulation vary across cell types. For example, knockdown of MFN2 decreases MAM contact and communication in MEF (de Brito and Scorrano 2008) but increases MAM contact and communication in an APP mutant in HEK 293 cells (Leal et al. 2016). It should be noted that increased MAM tethering following MFN2 knockdown decreased Aβ production and improved cellular outcome.

Manipulating MAM tethering can subsequently affect MAM-mediated mechanisms, such as ER to mitochondrial calcium transfer. However, with these studies, it becomes difficult to delineate the primary therapeutic mechanism, tethering versus calcium transfer. Conversely, studies that directly target MAM-mediated calcium transfer provide a clear demonstration of the therapeutic potential of targeting these pathways. For example, in astrocytes exposed to HIV-1, blocking mitochondrial calcium uptake by targeting MCU (Natarajaseenivasan et al. 2018), VDAC (Fatima et al. 2017), or cytosolic calcium (Nooka and Ghorpade 2017) can prevent astrocyte mitochondrial dysfunction and reverse astrocyte-mediated neurotoxicity. The same outcome is achieved by overexpression of mortalin/grp75 (Priyanka et al. 2020); however, this outcome was due to a direct interaction of mortalin/grp75 with HIV-1 Tat leading to Tat degradation rather than

modulating ER-mitochondrial calcium transfer. This is an important discrepancy as mortalin/grp75 manipulation in neurons can protect neurons from oxidative cell death when repressed or increase susceptibility when overexpressed (Honrath et al. 2017). Similarly, blocking MCU or cytosolic calcium in neurons improved neuronal survival against HIV-1 Tat toxicity (Kruman et al., 1998), while blocking ER calcium release *via* RyR can also attenuate Tat-induced UPR induction and mitochondrial dysfunction (Norman et al.). The potential therapeutic applications of targeting MCU and Sig1R to regulate ER-mitochondrial calcium transfer to combat neurodegenerative pathologies have also been previously reviewed (Liao, Dong, and Cheng 2017; Weng, Tsai, and Su 2017).

Other potential upstream regulators of mitochondrial dysfunction underlying neuropathology are the three UPR/ER stress pathways. In fact, targeting UPR pathways as potential neurodegenerative therapies are previously reviewed (Halliday and Mallucci 2014; Remondelli and Renna 2017; Martinez et al. 2019); however, these reports do not focus on UPR/ER stress in the context of mitochondrial dysfunction, regardless of the obvious crosstalk between these two organelles. In the context of HIV/HAND, blocking UPR/ER stress in astrocytes reverses astrocyte-mediated neurotoxicity and apoptotic signaling (Fan and He 2016; Shah et al. 2016). Similarly, inhibiting UPR/ER stress in HBMECs restored mitochondrial integrity and increased cell viability during HIV-1 Tat toxicity (Ma et al.). It is important to note that there are unique signaling pathways amongst the three arms in addition to their 'non-canonical' functions that remain ill-defined. However, given the potential regulation of the UPR/ER stress arms on MAM tethering [PERK/MFN2 (Munoz et al. 2013) and ATF6/VAPB (Gkogkas et al. 2008)], mitochondrial dynamics [PERK (Lebeau et al. 2018) and ATF6 (Bommiasamy et al. 2009)], ER-mitochondrial calcium transfer [IRE1α (Carreras-Sureda et al. 2019) and ATF6 (Burkewitz et al.

2020)], and mitochondrial bioenergetics [IRE1α (Carreras-Sureda et al. 2019) and PERK (Balsa et al. 2019)], more research is needed to delineate their therapeutic applications for regulating MAM/mitochondrial dysfunction in neurodegenerative pathologies. Moreover, IRE1α may also regulate mitochondrial dysfunction through inflammasome activation to promote inflammation (Bronner et al. 2015). Indeed, blocking inflammasome signaling in astrocyte-restricted HIV-1 gp120 transgenic mice not only reduced neuroinflammation and neurodegeneration, but also promoted neuronal regeneration and restored neurocognitive function (He et al. 2020).

The therapeutic potential of targeting inflammasome signaling gains support when considering the delicate balance between inflammasome activation and mitophagy that is evident in astrocytes and microglia during HIV/HAND. Proceeding mitophagy, mitochondrial fission *via* Drp1 is required for removal of damaged mitochondria, which is essential for cellular survival. Overexpression of Drp1 in astrocyte-restricted HIV-1 gp120 transgenic mice was able to reverse HIV-1 gp120-induced mitochondrial elongation in neurons and reduce neuroinflammation (astrogliosis) and neurodegeneration (Fields et al. 2016). Similarly, Drp1 overexpression in CD4+ T cells expressing HIV-1 Vpr protected mitochondrial integrity and increased cell survival (Huang et al. 2012). Interestingly, cells exposed to HIV-1 Tat increase Drp1 expression and activity favoring mitochondrial fragmentation. Rozzi et al. was able to prevent fragmentation by indirectly inhibiting Drp1 activation (Rozzi et al. 2018). Thus, while altered mitochondrial dynamics is a notable characteristic of HIV/HAND pathology, the therapeutic application may largely depend on the model/stimuli.

2.7 Concluding Remarks

Cooperation and communication between the ER and mitochondria are essential to ensure maintenance of cellular and organelle homeostasis. The significance of MAMs in different pathologies is indisputable; however, whether MAM dysfunction is a cause or consequence in these pathologies is not yet known. This review presents MAMs as pivotal platforms in neuropathology highlighting specific interplay of MAMs in AD, PD, and ALS. We then discuss the implications of MAMs in HAND for the first time. These reports emphasize calcium, UPR and inflammasome signaling as potential targets to regulate MAM/mitochondrial dysfunction during neuropathological challenges.

The presence and function of MAMs can differ across cell types and pathological conditions. A better understanding of the mechanisms regulating changes in MAMs in a respective cell type and/or pathology is critical to illuminate possible targets for therapeutic manipulation. For example, neurons are not directly infected by HIV-1; thus, indirect HIV-1-induced toxicity *via* infected glia are key mechanisms in HAND pathology. Glial cells (astrocytes, microglia, and oligodendrocytes) are essential for neural and CNS homeostasis yet, studies focusing on the presence and function of MAMs in glia are either severely deficient (astroglia) or non-existent (microglia and oligodendrocytes) highlighting the need to investigate ER-mitochondria contact and communication beyond the scope of neurons. Particularly, astrocytes provide essential metabolic and antioxidant support to neurons. Aberrant astrocyte mitochondrial function is a prominent threat to neuronal health and function. Targeting MAMs to manipulate astrocyte mitochondrial function could be a promising avenue to optimize the metabolic and antioxidant coupling between astrocytes and neurons and promote neuronal fitness against CNS pathologies.

Moreover, microglia and astrocytes are the residential immune cells participating in neuroinflammation, and MAMs may serve as key hinges for their activated/inflammatory status.

2.8 Figures and Tables

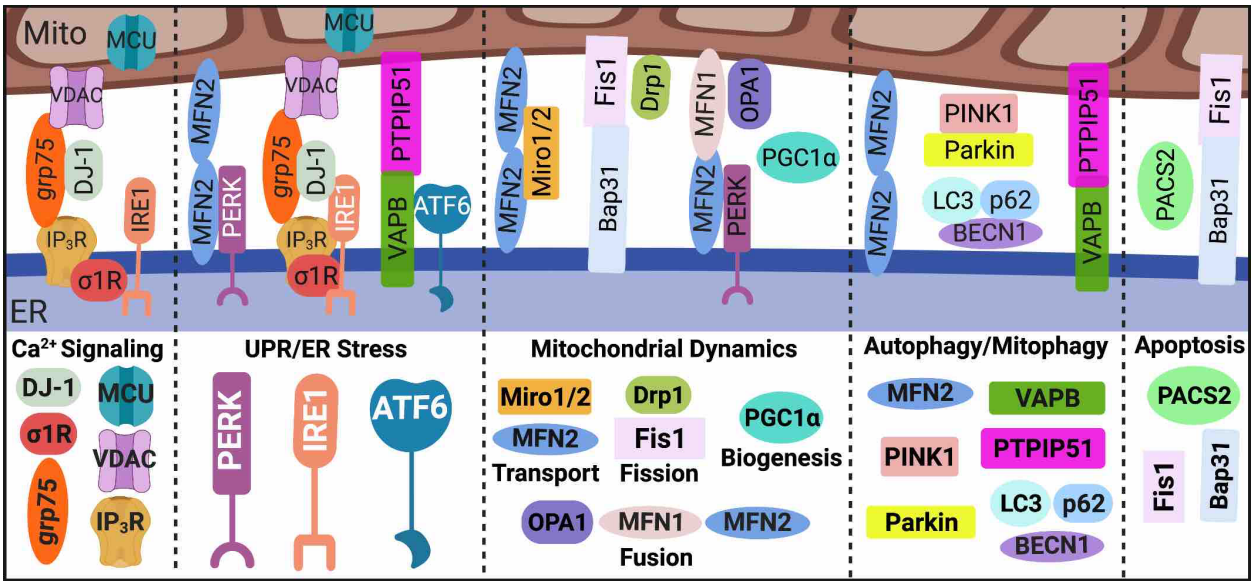

Figure 2.1 MAM proteome. Direct contact sites between the ER and mitochondria, MAMs, are tightly regulated by key tethering factors: MFN2, VAPB-PTPIP51, IP_3R -grp75-DJ1-VDAC, and Bap31-Fis1. Mediators within the ER-mitochondrial interface regulate distinct MAM-mediated mechanisms such as calcium signaling, UPR/ER stress, mitochondrial dynamics, autophagy/mitophagy, and apoptosis. Abbreviations: mitochondria-associated ER membrane (MAM); mitochondria (Mito); endoplasmic reticulum (ER); calcium; inositol 1,4,5-triphosphate receptors (IP_3R); voltage-dependent anion-selective channel (VDAC); glucose-regulated protein 75 kDa (grp75); mitochondrial calcium uniporter (MCU); sigma-1 receptor (σ1R); unfolded protein response (UPR); protein kinase RNA-like endoplasmic reticulum kinase (PERK); inositol-requiring protein 1α (IRE1α); activating transcription factor 6 (ATF6); mitofusin (MFN); mitochondrial Rho GTPases (Miro); dynamin-related protein 1 (Drp1); fission 1 (Fis1); optic

atrophy protein 1 (OPA1); proliferator-activated receptor γ coactivator 1α (PGC1α); phosphatase and tensin homolog (PTEN)-induced putative kinase (PINK1); beclin 1 (BECN1); microtubule-associated protein 1A/1B-light chain 3 (LC3); membrane protein-associated protein B (VAPB); protein tyrosine phosphatase-interacting protein 51 (PTPIP51); phosphofurin acidic cluster sorting 2 (PACS2); and B cell receptor-associated protein 31 (Bap31). Image created with BioRender.com.

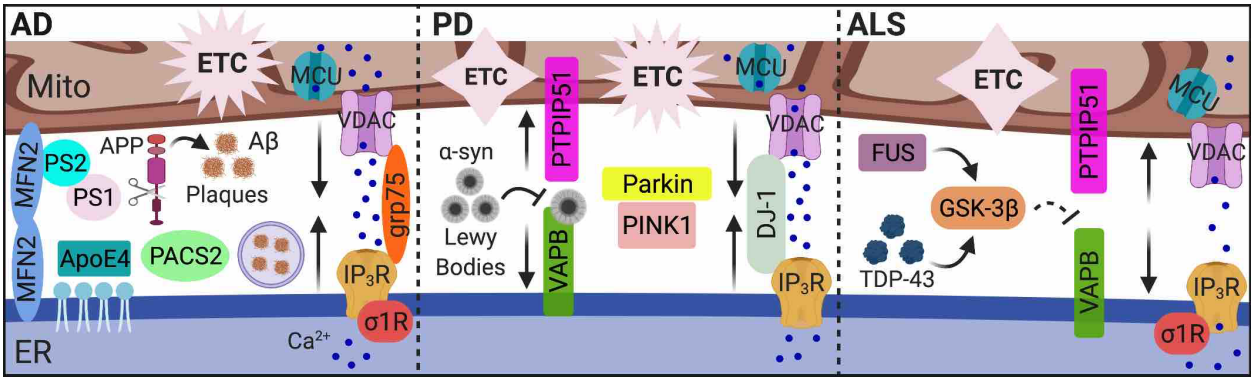

Figure 2.2 MAMs in AD, PD, and ALS. While dysregulated MAM-associated mechanisms are hallmarks of neurodegenerative pathology, the unique pathological features of AD, PD, and ALS alter MAM contact and communication emphasizing MAMs as pivotal players in neuropathology. In AD, MAM contact, calcium transfer, and MAM-mediated mechanisms (i.e. autophagy) are increased among *in vitro* and mouse models, yet deceased MAM-mediator expression and interaction was found in human AD cortical tissues. In PD, both increased and decreased MAM contact and communication are reported. In ALS, MAM tethering and calcium transfer are significantly impaired. Abbreviations: mitochondria-associated ER membranes (MAMs); mitochondria (Mito); endoplasmic reticulum (ER); Alzheimer's disease (AD); amyloid β (Aβ); amyloid precursor protein (APP); ε4 allele of apolipoprotein E (ApoE4); presenilin (PS); mitofusin (MFN); phosphofurin acidic cluster sorting 2 (PACS2); calcium (Ca^{2+}); inositol 1,4,5-triphosphate

receptors (IP_3R); voltage-dependent anion-selective channel (VDAC); glucose-regulated protein 75 kDa (grp75); mitochondrial calcium uniporter (MCU); sigma-1 receptor (σ1R); electron transport chain (ETC); Parkinson's disease (PD); α-synuclein (α-syn); vesicle-associated membrane protein-associated protein B (VAPB); protein tyrosine phosphatase-interacting protein 51 (PTPIP51); phosphatase and tensin homolog (PTEN)-induced putative kinase (PINK1); amyotrophic lateral sclerosis (ALS); transactive response (TAR) DNA-binding protein 43 (TDP-43); glycogen synthase kinase-3β (GSK-3β); and fused in sarcoma (FUS). Image created with BioRender.com.

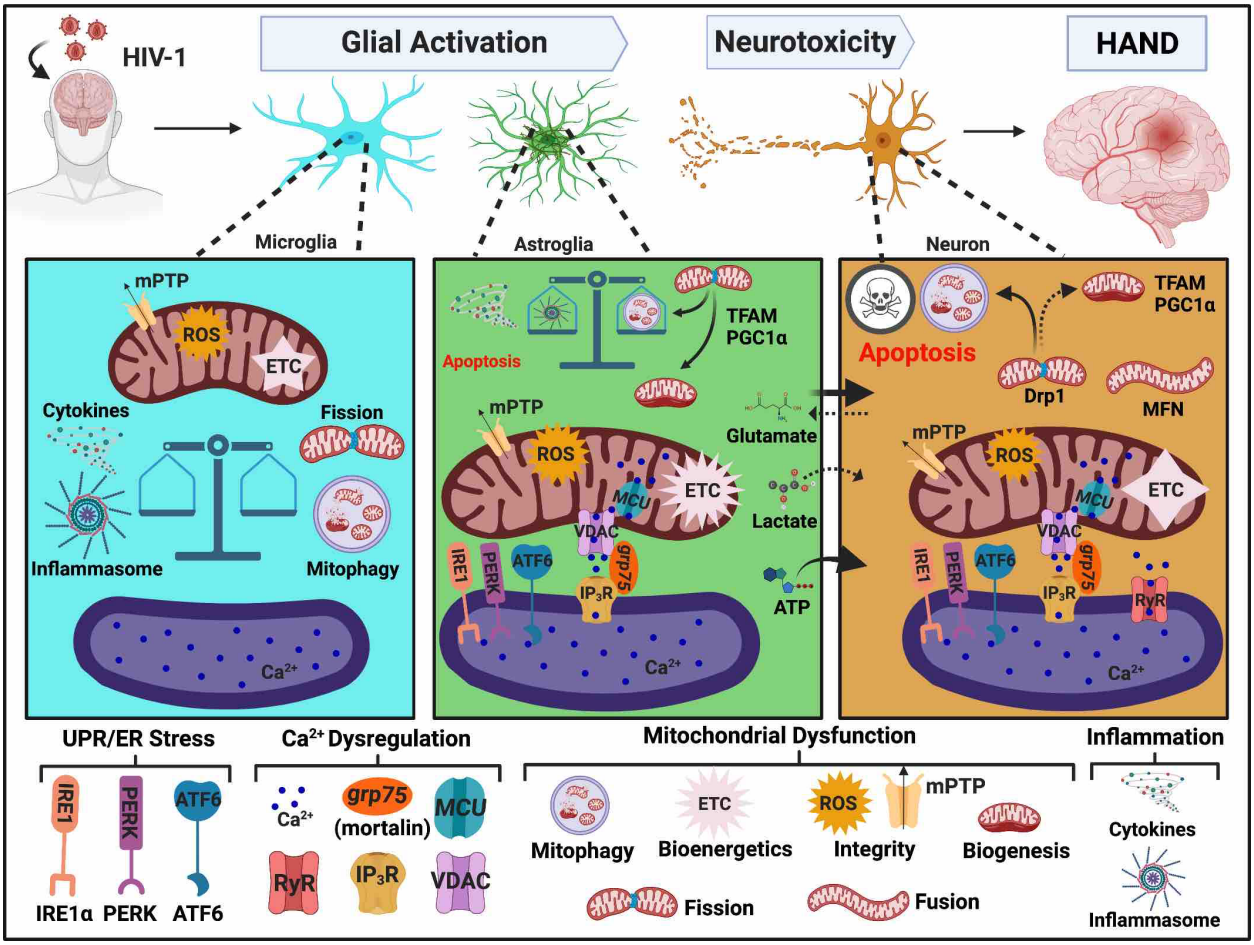

Figure 2.3 MAMs in HAND. HIV-1 in the CNS leads to glial activation and neurotoxicity, which are key mechanisms mediating HAND pathology. HIV-1-induced UPR/ER stress, calcium dysregulation, and mitochondrial dysfunction strongly implicate MAMs as potential regulators of glial activation and neurotoxicity. In microglia, the initiation of mitophagy is essential to buffer HIV-1-induced mitochondrial dysfunction but accumulation of damaged mitochondria induces a heightened inflammatory response which is associated with impaired mitochondrial integrity and a significant decrease in bioenergetic capacity. Conversely, astrocytes increase their calcium signaling and metabolic capacity. Astrocyte shift in function leads to increased release of neurotoxic factors and well as impaired provision of essential nutrients to neurons. Similar to microglia, a balance between mitophagy and inflammasome activation appears to be a critical determinate to astrocyte fate. Notably, ER-mitochondrial calcium transfer and UPR/ER stress also arise as potential pivotal players in astrocyte-mediated neurotoxicity. While astrocytes and microglia teeter between toxic and tropic, neurons are highly vulnerable to HIV-1-induced mitochondrial dysfunction caused by both direct and indirect insults. Targeting MAMs to combat mitochondrial dysfunction is of heightened importance to enhance CNS fitness against neuropathologic challenges, including HIV/HAND. Abbreviations: mitochondria-associated ER membranes (MAMs); human immunodeficiency virus type 1 (HIV-1); HIV-associated neurocognitive disorders (HAND); endoplasmic reticulum (ER); unfolded protein response (UPR); protein kinase RNA-like endoplasmic reticulum kinase (PERK); inositol-requiring protein 1α (IRE1α); activating transcription factor 6 (ATF6); calcium (Ca^{2+}); inositol 1,4,5-triphosphate receptors (IP_3R); voltage-dependent anion-selective channel (VDAC); glucose-regulated protein 75 kDa (grp75); mitochondrial calcium uniporter (MCU); ryanodine receptors (RyR); mitofusin (MFN); dynamin-related protein 1 (Drp1); mitochondrial permeability transitional pore (mPTP);

reactive oxygen species (ROS); electron transport chain (ETC); proliferator-activated receptor γ coactivator 1α (PGC1α); transcription factor A (TFAM). Image created with BioRender.com.

Table 2.1 Potential Therapeutic Targets.

Manuscript	Model	Cell type	Target	Outcome
(Garrido-Maraver, Loh, and Martins 2020)	Drosophila	Drosophila	ⓣ ER-mitochondrial contact	Extended Drosophila lifespan and improved overall motor function
(Leal et al. 2016)	APP mutant	HEK 293 cells	⊗ MFN2	Increased MAM contact and calcium transfer and decreased Aβ production
(Huang et al. 2012)	HIV Vpr expression	T cells	ⓣ MFN2 and Drp1	Restored mitochondria integrity and morphology and increased cell viability
(Kruman, Nath, and Mattson)	HIV Tat exposure	Neurons	⊗ Cytosolic calcium & MCU	Protected neurons for HIV-1 Tat-mediated neurotoxicity
(Norman et al.)	HIV Tat exposure	Neurons	⊗ RyR	Attenuated UPR induction and mitochondrial dysfunction
(Fields et al. 2016)	HIV+ brain tissues, Tg-gp120 mice, gp120 exposure	Neurons	ⓣ Drp1	Restored mitochondrial dynamics and reduced neuroinflammation (astrogliosis) and neurodegeneration
(Rozzi et al. 2018)	HIV Tat exposure	Neurons	⊗ Drp1 (Indirect inhibition)	Prevented Tat-mediated effects on mitochondrial dynamics
(He et al. 2020)	HIV gp120 exposure; Tg-gp120 mice	Microglia	⊗ Inflammasome	Reduced neuroinflammation and neurodegeneration. Promoted neuronal regeneration and restored neurocognitive function
(Nooka and Ghorpade 2017)	HIV, ART, & IL-1β exposure	Astrocytes	⊗ Cytosolic calcium	Restored mitochondria integrity
(Natarajaseenivasan et al. 2018)	HIV Tat exposure	Astrocytes	⊗ MCU	Reversed metabolic switch and astrocyte-mediated neurotoxicity
(Fatima et al. 2017)	HIV Tat expression	Astrocytes	⊗ VDAC1	Reversed astrocyte-mediated neurotoxicity
(Priyanka et al. 2020)	HIV Tat expression	Astrocytes	ⓣ Mortalin/grp75	Reversed astrocyte mitochondrial dysfunction and astrocyte-mediated neurotoxicity
(Fan and He 2016)	HIV Tat exposure	Astrocytes	⊗ UPR/ER stress	Reversed astrocyte-mediated neurotoxicity and apoptotic signaling
(Shah et al. 2016)	HIV gp120 exposure; Tg-gp120 mice	Astrocytes	⊗ UPR/ER stress	Reversed astrocyte-mediated neurotoxicity and apoptotic signaling
(Ma et al. 2016)	HIV Tat exposure	HBMECs	⊗ UPR/ER stress	Restored mitochondria integrity and cell viability

⊗inhibition/knockdown; ⊕overexpression/upregulation. Abbreviations: amyloid β (Aβ); amyloid precursor protein (APP); antiretroviral therapy (ART); calcium (Ca^{2+}); dynamin-related protein 1 (Drp1); endoplasmic reticulum (ER); glycoprotein (gp)120; glucose-regulated protein 75 kDa (grp75); human brain microvascular endothelial cells (HBMEC); human embryonic kidney (HEK); human immunodeficiency virus type 1 (HIV-1); interleukin-1β (IL-1β); mitofusin (MFN); mitochondrial calcium uniporter (MCU); ryanodine receptors (RyR); transactivator of transcription (Tat); transgenic (Tg); unfolded protein response (UPR); voltage-dependent anion-selective channel (VDAC); viral protein R (Vpr)

CHAPTER 3

A NON-CANONICAL ROLE FOR IRE1α LINKS ER AND MITOCHONDRIA AS KEY REGULATORS OF ASTROCYTE DYSFUNCTION: IMPLICATIONS IN METHAMPHETAMINE USE AND HIV-ASSOCIATED NEUROCOGNITIVE DISORDERS

AUTHORS

J. PROULX, I-W. PARK, & K. BORGMANN

PORTION FORMATTED AND PUBLISHED AS:

Proulx, J., Stacy, S., Park I-W., & Borgmann K. A non-canonical role for IRE1α links ER and mitochondria as key regulators of astrocyte dysfunction: Implications in methamphetamine use and HIV-associated neurocognitive disorders. Frontiers in Neuroscience, 17 June 2022. https://doi.org/10.3389/fnins.2022.906651.

3.1 Abstract

Astrocytes are one of the most numerous glial cells in the central nervous system (CNS) and provide essential support to neurons to ensure CNS health and function. During a neuropathological challenge, such as during human immunodeficiency virus (HIV)-1 infection or methamphetamine (METH) exposure, astrocytes shift their neuroprotective functions and can become neurotoxic. Identifying cellular and molecular mechanisms underlying astrocyte dysfunction is of heightened importance to optimize the coupling between astrocytes and neurons and ensure neuronal fitness against CNS pathology, including HIV-associated neurocognitive disorders (HAND) and METH use disorder. Mitochondria are essential organelles for regulating metabolic, antioxidant, and inflammatory profiles. Moreover, endoplasmic reticulum (ER)-associated signaling pathways, such as calcium and the unfolded protein response (UPR), are important messengers for cellular fate and function, including inflammation and mitochondrial homeostasis. Increasing evidence supports that the three arms of the UPR are involved in the direct contact and communication between ER and mitochondria through mitochondria-associated ER membranes (MAMs). The current study investigated the effects of HIV-1 infection and chronic METH exposure on astrocyte ER and mitochondrial homeostasis and then examined the three UPR messengers as potential regulators of astrocyte mitochondrial dysfunction. Using primary human astrocytes infected with pseudotyped HIV-1 or exposed to low doses of METH for seven days, astrocytes had increased mitochondrial oxygen consumption rate (OCR), cytosolic calcium flux and protein expression of UPR mediators. Notably, inositol-requiring protein 1α (IRE1α) was most prominently upregulated following both HIV-1 infection and chronic METH exposure. Moreover, pharmacological inhibition of the three UPR arms highlighted IRE1α as a key regulator of astrocyte metabolic function. To further explore the regulatory role of astrocyte IRE1α, astrocytes

were transfected with an IRE1α overexpression vector followed by stimulation with proinflammatory cytokine, interleukin 1β. Overall, our findings confirm IRE1α modulates astrocyte mitochondrial respiration, glycolytic function, morphological activation, inflammation, and glutamate uptake, highlighting a novel potential target for regulating astrocyte dysfunction. Finally, these findings suggest both canonical and non-canonical UPR mechanisms of astrocyte IRE1α. Thus, additional studies are needed to determine how to best balance astrocyte IRE1α functions to both promote astrocyte neuroprotective properties while preventing neurotoxic properties during CNS pathologies.

3.2 Introduction

According to the World Health Organization and the Joint United Nations Programme on HIV/AIDS, there are nearly 38 million individuals living with HIV/AIDS worldwide with an estimated 1.5 million newly infected individuals annually. Thanks to the development of the antiretroviral therapy (ART), HIV-1 diagnosis is no longer a death sentence; however, this increases the global burden of people living with HIV-1 (PLWH). Moreover, poor ART penetration to the central nervous system (CNS) allows persistent low levels of HIV-1 replication and chronic neuroinflammation, which lead to the manifestation of HIV-associated neurocognitive disorders (HAND). These individuals are afflicted by different spectra of cognitive impairments and inference with daily functioning often referred to as “accelerated aging”. Even in the post ART era, approximately 30 – 70% of PLWH suffer from HAND depending on various combinational factors, including toxicity of ART itself, various sociodemographic disparities, comorbid health complications, and substance use disorders, which are disproportionately elevated among HIV-1-1-infected individuals (Parikh et al. 2012; Blackard and Sherman 2021). As a common comorbidity

among HIV-1 infected individuals, methamphetamine (METH) use can leave patients vulnerable to impaired immune function, insufficient adherence and resistance to treatment, and enhanced viral replication and infectivity (Salamanca et al. 2014; Toussi et al. 2009; Liang et al. 2008; Basova et al. 2018; Passaro et al. 2015; Ellis et al. 2003; Colfax et al. 2007; Skowronska et al. 2018). The use of METH can have long-lasting consequences on CNS homeostasis (Jablonski, Williams, and Vorhees 2016; Hoefer et al. 2015; Volkow et al. 2001). The combined neurological complications of HIV-1/METH comorbidity include increased excitotoxicity, oxidative damage, neuroinflammation, blood brain barrier (BBB) and neuronal injury, and neurocognitive impairment, which in turn impact the development and severity of HAND (Soontornniyomkij et al. 2016; Kesby et al. 2015; Rippeth et al. 2004; Fattakhov et al. 2021).

Astrocytes are one of the most abundant glial cells in the brain and are critical for CNS homeostasis. Paramount astrocyte functions include maintaining the integrity of BBB and participating in tripartite communication for proper neurotransmission. Moreover, astrocytes provide essential metabolic, antioxidant, and neurotrophic support to neurons to promote neuronal function and survival (Ricci et al. 2009; Chen et al. 2020). The consensus of the scientific community is that at least some human astrocytes are infected by HIV-1. An infection rate of even 1% would correlate to 0.4 – 1.3 billion HIV-1+ astrocytes in a human brain, which could have widespread consequences on neuronal survival, BBB permeability, and neuroinflammation. Astrocytes can not only serve as reservoirs for infection, but can also undergo activation, or "reactive astrogliosis" leading to phenotypic shifts in function (Edara, Ghorpade, and Borgmann 2020; Li et al. 2020). In the context of METH, astrocytes can become activated and remain reactive for extended periods of time even after withdrawal (Friend and Keefe 2013; Narita et al. 2008; Bortell et al. 2017). The functional changes of astrogliosis are often associated with a more

inflammatory and/or neurotoxic phenotype that can disrupt their ability to maintain CNS homeostasis and provide essential neuroprotective support to neurons. Indeed, reactive astrocytes are a central hallmark of many forms of neuropathology (Matias, Morgado, and Gomes 2019; Li et al. 2019). Identifying the underlying mechanisms that regulate astrocyte dysfunction during both HIV-1 infection and chronic METH exposure will illuminate therapeutic targets that can promote a disease preventative or neuroprotective phenotype during CNS pathology.

Cooperation between the endoplasmic reticulum (ER) and mitochondria is essential for the maintenance and restoration of cellular homeostasis. In fact, direct contact sites between these organelles termed mitochondria-associated ER membranes (MAMs) have been identified as critical intracellular hubs for determining cellular function and survival, especially during stress (Filadi, Theurey, and Pizzo 2017; Bravo et al. 2012). Notably, the ER-mitochondria interface is a key regulator of mitochondrial physiology during both basal and stress-induced conditions (Bravo et al. 2012; Lebeau et al. 2018; Rainbolt, Saunders, and Wiseman 2014; Vannuvel et al. 2013). For example, calcium ion transfer from the ER to mitochondria is vital for mitochondrial respiration and ATP synthesis (Filadi, Theurey, and Pizzo 2017; Bravo et al. 2012). Commonly accepted MAM-associated calcium transporters include inositol 1,4,5-trisphosphate receptor (IP_3R) on the ER membrane, voltage-dependent anion channel 1 (VDAC1) on the outer mitochondrial membrane, and mitochondrial calcium uniporter (MCU) on the inner mitochondrial membrane. However, recent studies focusing on the kinetics of astrocyte mitochondrial calcium influx confirmed a strong dependency on ER calcium stores but illuminated a minimal contribution of MCU (Huntington and Srinivasan 2021). In addition, the three unfolded protein response (UPR) arms that are classically activated during ER stress demonstrate distinct contributions to both MAM regulation and mitochondrial homeostasis, beyond their classical UPR/ER stress functions.

Briefly, protein kinase RNA-like endoplasmic reticulum kinase (PERK) is a key regulator of MAM formation as well as mitochondrial dynamics and bioenergetics (Verfaillie et al. 2012; van Vliet and Agostinis 2016; Lebeau et al. 2018; Rainbolt, Saunders, and Wiseman 2014; Balsa et al. 2019). Inositol-requiring protein 1α (IRE1α), commonly associated with cellular responses to infections or inflammation, is also implicated in ER-mitochondrial calcium transfer and regulation of mitochondrial respiration through association with IP_3R on the ER membrane (Son et al. 2014; Carreras-Sureda et al. 2019) or sigma 1 receptor (Sig1R) in the ER lumen (Mori et al.). Activating transcription factor 6 (ATF6) is known to both interact with and be regulated by the key MAM tethering protein vesicle-associated membrane protein-associated protein B (VAPB) (Gkogkas et al. 2008). Moreover, ATF6 regulates lipid biosynthesis and ER expansion, suggesting a possible interplay in MAM-mediated lipid homeostasis and ER-mitochondrial physiology (Bommiasamy et al. 2009).

The complete composition and function of MAMs remain unclear and can vary across cell types (Herrera-Cruz and Simmen 2017; Janikiewicz et al. 2018; Moltedo, Remondelli, and Amodio 2019). Modifications in MAM tethering and activity are implicated in a number of neurodegenerative diseases such as Alzheimer's disease, Parkinson's disease, and amyotrophic lateral sclerosis (Leal et al. 2018; Hedskog et al. 2013; Area-Gomez et al. 2012; Area-Gomez and Schon 2017; Erpapazoglou, Mouton-Liger, and Corti 2017; Rodriguez-Arribas et al. 2017) but have not yet been investigated in HAND or substance use disorders. Indeed, ER and oxidative stress, mitochondrial dysfunction, and calcium dysregulation are three MAM-associated disturbances that characterize neurodegenerative pathologies (Brown and Naidoo 2012; Muller et al. 2018), including HAND, which our group recently reviewed (Proulx, Park, and Borgmann 2021). The forefront of MAM research in the brain has largely been focused on neurons or whole

brain tissues (Hedskog et al. 2013; Leal et al. 2018; Erpapazoglou, Mouton-Liger, and Corti 2017; Rodriguez-Arribas et al. 2017). However, recent studies have demonstrated that astrocyte ER-mitochondrial contact and communication are critical regulators and potential therapeutic targets for astrocyte-mediated vascular remodeling (Gbel et al. 2020) and synaptic homeostasis (Serrat et al. 2021). Further exploration of astrocyte MAMs in health and disease will provide unique insights into astrocyte biology and inter-organelle communication to better understand how to regulate reactive astrocyte dysfunction. Moreover, METH- and HIV-1-relevant stimuli can induce ER stress and alter mitochondrial function, health, and/or morphology in astrocytes (Nooka and Ghorpade 2017; Fan and He 2016; Shah and Kumar 2016; Shah et al. 2016; Borgmann and Ghorpade 2017; Nooka and Ghorpade 2018; Borgmann and Ghorpade 2015), suggesting an important role of the astrocyte ER-mitochondrial interface during HIV-1 infection and METH exposure. However, these findings have varied substantially across difference models.

Indeed, defects in mitochondrial bioenergetics, biogenesis, dynamics, degradation, integrity and transport are all hallmarks of HAND pathology (Haughey and Mattson 2002; Nooka and Ghorpade 2017; Area-Gomez and Schon 2017; Fields and Ellis 2019; Avdoshina et al. 2016; Swinton et al. 2019; Thangaraj et al. 2018; Huang et al. 2012; Teodorof-Diedrich and Spector 2018; Natarajaseenivasan et al. 2018; Rozzi et al. 2018; Ojeda et al. 2018; Rawat, Teodorof-Diedrich, and Spector 2019; Khan et al. 2019). However, prior research into mitochondrial dysfunction in HAND has primarily concentrated on neurons or whole brain tissues, and results have varied substantially across different models(Fields and Ellis 2019; Rozzi et al. 2017; Wang et al. 2017; Avdoshina et al. 2016; Teodorof-Diedrich and Spector 2018; Fields et al. 2016). Specific investigations in astrocytes have suggested that HAND-relevant stimuli can induce mitochondrial depolarization and oxidative stress (Fields and Ellis 2019; Nooka and Ghorpade

2017, 2018; Ton and Xiong 2013; Natarajaseenivasan et al. 2018; Ojeda et al. 2018). Among these findings, it was reported that astrocytes undergo a distinct metabolic shift in the presence of HIV-1 protein transactivator of transcription (Tat) alone and in combination with cocaine – a shift that impaired their capacity to provide essential metabolites to neurons and promoted neuroinflammation (Natarajaseenivasan et al. 2018). The use of several different HIV-1 models (including restrictive and active infection, exposure to infectious HIV-1 or HIV-1 proteins and proinflammatory cytokine treatment) reinforce these findings; however, the mechanisms or pathways mediating HIV-1-induced astrocyte dysfunction remain unknown.

In the context of METH exposure, it is well-known that METH can impair electron transport chain (ETC) function (Brown, Quinton, and Yamamoto 2005; Burrows, Nixdorf, and Yamamoto 2000; Feier et al. 2012; Burrows, Gudelsky, and Yamamoto 2000). In astrocytes, acute METH exposure with HIV-1 glycoprotein 120 exposure increased oxidative stress (Shah et al. 2013). Moreover, our lab has reported disproportionately augmented astrocyte mitochondrial oxygen consumption rate (OCR) compared to ATP levels following chronic METH exposure; in parallel, METH increased astrocyte antioxidant capacity and oxidative burden (Borgmann and Ghorpade 2017). At least two METH receptors in astrocytes have been identified, trace amine associated receptor 1 and Sig1R (Zhang et al. 2015; Cisneros and Ghorpade 2012, 2014), which could regulate some METH-associated dysregulation of astrocyte function. However, the METH experimental models have focused primarily on acute high doses.

Both UPR and calcium signaling have been recognized as potential perpetrators of astrocyte dysfunction during HAND pathology (Nooka and Ghorpade 2017; Fan and He 2016; Natarajaseenivasan et al. 2018; Shah and Kumar 2016; Nooka and Ghorpade 2018). In fact, inhibition of ER/UPR signaling is seen to reverse astrocyte-mediated neurotoxicity, apoptotic

signaling, and mitochondrial dysfunction provoked by HIV-1 (Fan and He 2016; Shah and Kumar 2016; Ma et al. 2016). Moreover, manipulation of astrocyte intracellular calcium signaling provides resistance to HIV-1-induced ER stress and/or mitochondrial dysfunction (Nooka and Ghorpade 2017; Natarajaseenivasan et al. 2018). Specifically, targeting MCU on the inner mitochondrial membrane to prevent mitochondrial calcium uptake when human astrocytes are challenged by HIV-1 Tat and/or cocaine restores neurotrophic mitochondrial function and replenishes astrocyte provision of essential metabolites to neurons (Natarajaseenivasan et al. 2018). However, as stated above, MCU may have a minimal contribution on astrocyte ER-mitochondrial calcium transfer, thus alternative targets need to be explored for therapeutic application (Huntington and Srinivasan 2021). For example, suppression of astrocyte VDAC1 on the outer mitochondrial membrane was able to reverse HIV-1 Tat-induced release of ATP, subsequently rescuing neurons from astrocyte-mediated neurotoxicity (Fatima et al. 2017). Mortalin [a.k.a. glucose-regulated protein 75 kDa (grp75)] is a cytosolic scaffold protein between IP_3R and VDAC1 to regulate ER-mitochondrial calcium transfer. Overexpression of mortalin/grp75 in astrocytes expressing HIV-1 Tat was able to prevent astrocyte mitochondrial dysfunction and fragmentation and protect neurons from astrocyte-mediated neurotoxicity by reducing the release of excess ATP, inflammatory cytokines, and extracellular glutamate (Priyanka et al. 2020). Altogether, these findings strongly support UPR signaling and/or ER-mitochondrial calcium transfer as potential regulators for astrocyte dysfunction and astrocyte-associated neuronal damage. Furthermore, a study in neurons exploring a mutated MAM tethering protein, mitofusion 2 (MFN2), reported a restoration of MAM tethering and mitochondrial dynamics, thereby providing resistance to neurite degeneration. Specific mechanisms involved in neuronal protection

were preventing ER stress or activating Sig1R, a key regulator of the calcium transfer from the ER to the mitochondria (Bernard-Marissal et al. 2019).

While ER and oxidative stress are known outcomes of both METH and HIV-1 cytotoxicity, the connection between these outcomes has primarily been explored in the context of apoptosis. Interestingly, the resiliency of human astrocytes during METH- and HIV-1- relevant exposures supports the capacity of quality control mechanisms to enable survival under stressed conditions. However, as HAND and METH use disorders are chronic conditions, prolonged astrocyte activation may become neuropathic. Our investigations are specifically targeted toward elucidating novel signaling pathways linking ER and mitochondria during chronic METH exposure and HIV-1 infection in astrocytes. We then wanted to evaluate ER/MAM-associated molecules as potential regulators of astrocyte dysfunction during HIV-1/METH neuropathology. These findings demonstrate a dysregulated ER and mitochondrial homeostasis following HIV-1 infection and METH exposure in primary human astrocytes. We then further highlight UPR messenger, IRE1α, as a key signaling molecule for astrocyte mitochondrial respiration, glycolytic function, morphological activation, inflammation, and glutamate uptake. We propose further exploration into the therapeutic application of IRE1α as a central regulator of astrocyte dysfunction to help optimize the coupling between astrocytes and neurons and ensure neuronal fitness during a neuropathic challenge.

3.3 Materials and Methods

Primary human astrocyte cultures: Primary human astrocytes were obtained from first or second trimester brain tissues from a biorepository at the University of Washington and in full compliance with local, federal, and National Institutes of Health (NIH) ethical guidelines. Written

informed consent was obtained from all donors. Isolation and characterization of astrocyte cultures are previously described (Borgmann and Ghorpade 2017; Gardner et al. 2006; You et al. 2020). Fresh and cryopreserved astrocyte cultures were used experimentally between passages two and seven. All experiments were replicated in three or more astrocyte cultures isolated from biologically distinct biospecimens.

METH treatment: Astrocytes were treated with METH (cat # M8750, Sigma-Aldrich, St. Louis, MO, USA) for acute calcium signaling (250 μM; 5 min), acute protein expression (5 μM; 8 h), or chronic assessments (50 – 250 nM; 7 d). Dose and time kinetics were determined based on the physiological peak (6 μM – 2 mM) and prolonged METH ranges (60 – 600 nM) found *in vivo* and our previous investigations (Won et al. 2001; Rivière, Gentry, and Owens 2000; Cisneros and Ghorpade 2014, 2012; Borgmann and Ghorpade 2015; Shah and Kumar 2016; Borgmann and Ghorpade 2017).

Pseudotyped HIV-1: Human embryonic kidney (HEK) 293 T cells were obtained from the American Type Culture Collection (Manassas, VA, USA) and frozen at P4 according to their cryopreservation procedures. HEK 293 cells were plated in T75 flasks at 50% confluency and incubated at 37°C and 5% CO2 overnight. Cells were co-transfected with HIV-1 infectious molecular clone (pNL4-3; cat # ARP-114, NIH HIV Reagent Program, Manassas, VA, USA, contributed by Dr. M. Martin) and p-human elongation-factor (pHEF)-vesicular stomatitis virus glycoprotein (VSVg; plasmid # 22501, Addgene, Watertown, MA, USA, a gift from Dr. Sergey Kasparov) by calcium phosphate precipitation per CalPhos Mammalian Transfection kit instructions (Clontech Laboratories, Inc., Mountain View, CA, USA) (Canki et al. 2001; Ojeda et al. 2018; Edara, Ghorpade, and Borgmann 2020). A total of 5 μg of plasmid DNA (pDNA) at a ratio of 1:1.5 (pHIV-1:VSVg) was added dropwise to each flask in a 2 mL precipitate of solution

A (2 M calcium solution + pDNA diluted in sterile water) and solution B (2x HEPES solution, 1:1). Cells were incubated overnight, washed three times with PBS, and fresh culture media was added. Supernatants were collected 48 h post-wash, and pseudotyped HIV-1 was quantified by reverse transcriptase (RT) activity *via* radiometric RT assay (Edara, Ghorpade, and Borgmann 2020). Pseudotyped HIV-1 doses ranging from 100 to 1,000 units RT were tested. The optimal dose of pseudotyped HIV-1 for the present study (500 RT) was selected based on confirmed integration, detectable levels of viral protein expression, and minimal cytotoxicity to best mimic chronic *in vivo* HIV-1 astrocyte infection.

HIV-1 DNA integration assay: Astrocytes were plated in six-well plates at 1 million cells per well and treated with or without pseudotyped HIV-1 (500 RT). Cells were incubated overnight, washed three times with PBS, and fresh media was added. Astrocytes were collected using 0.05% Trypsin-EDTA (cat # T3924; Sigma-Aldrich) 7 d post infection and washed with PBS prior to DNA isolation using QIAamp DNA Micro Kit per manufacturer's instructions (Qiagen, Germany). Successful integration of HIV-1 was determined by a nested, two-step PCR integration assay as previously described (Edara, Ghorpade, and Borgmann 2020). HIV-1 lymphadenopathy-associated virus-infected 8E5 cells (8E5, cat # ARP-95, NIH HIV Reagent Program, contributed by Dr. Thomas Folks) were used as a positive control. Briefly, DNA was amplified with sequence-specific primers for Alu (5′-TCC CAG CTA CTC GGG AGG CTG AGG-3′) - gag (5′-CCT GCG TCG AGA GAG CTC CTC TGG-3′) using Phusion high-fidelity PCR kit (cat # F553S; Thermo Fisher Scientific, Waltham, MA, USA). The first PCR product was diluted 10-fold and measured in a second PCR specific for R/U5 DNA with sense primer M667 (5′-GGC TAA CTA GGG AAC CCA CTG C-3′) and antisense primer AA55 (5′-CTG CTA GAG ATT TTC CAC ACT GAC-3′).

The final PCR product was visualized with a FluorochemQ gel imaging station (ProteinSimple, San Jose, CA, USA) following electrophoresis on a 1% agarose gel with ethidium bromide.

Treatment with pharmacological inhibitors: Astrocytes were treated with inhibitors [ATF6 (AEBSF; cat # A8456, Sigma-Aldrich; 100μM), PERK (GSK2606414; cat # 516535, MilliporeSigma, Burlington, MA, USA; 1μM), IRE1α (STF-083010; cat # 412510, MilliporeSigma, 60μM; 4μ8c; cat # 50-136-4583, Thermo Fisher Scientific, 60μM)] 3 h prior to Seahorse assessment. Dose and time kinetics were selected for the inhibitors based on previous studies (Bravo et al. 2011; Nooka and Ghorpade 2017; Jiang et al. 2017; Liu et al. 2018; Liu et al. 2013; Cisneros and Ghorpade 2014).

Transfection: Transfections were performed using the Amaxa P3 primary cell 96-well kit, nucleofector and shuttle attachment (cat # V4SP-3960, Lonza, Walkersville, MD, USA) per manufacturer's instructions with modification as previously published (Nooka and Ghorpade 2017). Briefly, 250 – 500 ng of plasmid DNA was transfected per 1.6 million astrocytes in 20 μL of nucleofection reagent. A circularly permutated green fluorescent protein (GFP) with a calmodulin tag was constructed as an ultrasensitive calcium sensor (GCaMP6s) and gifted from Dr. Douglas Kim (pGP-CMV-GCaMP6s, plasmid # 40753, Addgene) (Chen et al. 2013). The same protocol was used for IRE1α overexpression (cat # SC309043, OriGene, Rockville, MD, USA) and the backbone plasmid (cat # PCMV6XL5, OriGene). Astrocytes were plated and allowed to recover for 24 – 48 h before treatment or downstream assessments.

Interleukin-1β (IL-1β) treatment: After recovery from IRE1α overexpression or backbone transfection, astrocytes were then treated with IL-1β (20 ng/mL; 24 h; cat # 201-LB, R&D Systems, Minneapolis, MN, USA) for functional analyses based on a decade-long protocol that has been optimized for astrocyte characterization (You et al. 2020).

Calcium signaling: Following transfection with GCaMP6s, astrocytes were plated at 100,000 cells per well in tissue culture treated, six channel µ-slides (0.4 VI, cat # 80606, ibidi, Madison, WI, USA). Each condition was performed in duplicate wells for each biological donor with a minimum of 20 cells imaged per donor. Changes in calcium flux were imaged with a 20x objective at excitation of 450 – 490 nm and emission of 593 – 668 nm, using time series confocal microscopy *via* Carl Zeiss LSM 510 (Jena, Germany) (Nooka and Ghorpade 2017). Time-lapse micrographs were acquired every 500 msec for 5 min. Astrocytes were treated with control media or METH (250 µg/ml) at 10 s (20 cycles) then ionomycin (10 µM) at 225 s (450 cycles). Analysis was performed using Fiji ImageJ software (Version: 2.0.0-rc-69/1.52i; National Institutes of Health, Bethesda, MD, USA). Individual cells were outlined, and the change in fluorescence was calculated by: $\Delta F=(F-F0)/(Fmax-F0)$, where F is the fluorescence intensity at any given time; F0 is the baseline (1 – 20 cycles) fluorescence intensity, and Fmax is the maximum fluorescence intensity when exposed to ionomycin (450 – 600 cycles). Calcium flux line tracings illustrate the ΔF at any given time point. Area under the curve (AUC) was calculated by the sum of ΔF between METH/media and ionomycin treatment (cycles 20 – 450).

Protein expression via Simple Wes: Astrocytes were plated 48 h prior to collection in 6-well plates at 2 million cells per well. Lysates were collected using mammalian protein extraction buffer (MPER, cat # PI78505, Thermo Fisher Scientific) with protease and phosphatase inhibitors (cat # P8340, cat # P0044 and cat # P2850, Sigma-Aldrich). Protein concentrations were quantified *via* bicinchoninic acid (BCA) assay per manufacturer's instructions (cat # 23225, Thermo Fisher Scientific). Lysates were then diluted in 0.1X Wes Sample Buffer to 2 µg/µL for HIV-1 protein assessment or 0.5 µg/µL for all other targets. Protein expression was determined using Simple Wes

in 12 – 230 kDa Separation Modules (cat # SM-W004, ProteinSimple) per manufacturer's instructions. Briefly, sample buffer, loading dye, ladder, primary antibody dilution buffer, secondary antibodies, and all other necessary reagents for separation module set-up were provided by manufacturer with instructions for reconstitution and use. Primary antibody dilutions were standardized for each target. An automated capillary system performs all sample separation, wash, and immunolabeling steps to provide quantitative, size-based data based on changes in chemiluminescence. Compass for SW software (Version 4.0.0) was used to collect digitalized data and blot images. Targets included: HIV-1 negative factor protein (Nef; cat # ARP-3689, HIV Reagent Program, contributed by Dr. James Hoxie; 1:25, ~30 kDa), HIV-1 capsid protein (p24; cat # ab43037, Abcam, Cambridge, UK; 1:25, ~32 kDa), binding immunoglobulin protein (BiP; clone C50B12, cat # 3177, Cell Signaling Technology, Danvers, MA, USA; 1:250, ~71 kDa), ATF6 (clone D4Z8V, cat # 65880, Cell Signaling Technology; 1:50, ~117 kDa), PERK (clone D11A8, cat # 5683, Cell Signaling Technology; 1:50, 170 kDa), IRE1α (clone 14C10, cat # 3294, Cell Signaling Technology; 1:50, ~130 kDa), and vinculin (clone E1E9V, cat # 13901, Cell Signaling Technology; 1:20,000, ~117 kDa). Note: molecular weights can shift in Simple Wes compared to classical western blot.

Mitochondria bioenergetics: Metabolic profiles were performed using Seahorse XFe96 analyzer technology per Seahorse XF Cell Mito Stress Test Kit User Guide instructions and as previously described (cat # 103015-100, Agilent Technologies, Santa Clara, CA, USA) (Prah et al. 2019; Chaphalkar et al. 2020). Briefly, astrocytes were plated 48 h prior to Mito Stress Test in Seahorse 96-well plates at 25,000 – 30,000 cells per well. There was a minimum of 6 wells per condition for each biological donor. On the day of experiment, astrocyte media was exchanged with assay media 1 h before testing. During assay, consecutive injections of oligomycin (Oligo; 2

μM), carbonyl cyanide-4 (trifluoromethoxy) phenylhydrazone (FCCP; 2 μM), and rotenone/antimycin A (Rot/AA; 0.5 μM) were used to modulate components of the ETC allowing assessment of key parameters of mitochondrial function. Data were collected using Wave V2.6.1.56 software and exported with Seahorse XF Cell Mito Stress Test Report Generator.

Cytotoxicity: Toxicity of the three UPR inhibitors was measured *via* extracellular lactate dehydrogenase (LDH) assay using Cytotoxicity Detection Kit (cat # 11644793001, Sigma-Aldrich). Astrocytes were plated in 48-well plates at 150,000 cells per well overnight. The next day, astrocytes were treated in triplicates with the UPR inhibitors for 3 h to model Seahorse timepoints. Duplicate supernatant collections (50 μL) per well (six total samples per experiment) were incubated 1:1 with LDH reaction buffer for 25 min in the dark per manufactures instructions. Absorbance was read at 490 nm with background correction at 650 nm.

Immunocytochemical staining: Astrocytes were plated in 48-well plates at 100,000 cells per well for 48 h prior to fixation with 1:1 acetone: methanol (24 h post IL-1β treatment). Fixed cells were then blocked and immunolabeled in 1× PBS containing 2% BSA and 0.1% Triton X-100 (PBS, cat # BP3994; BSA, cat # BP1600-1, Thermo Fisher Scientific; Triton X-100, cat # X-100, Sigma-Aldrich). Primary antibodies specific to glial fibrillary acidic protein (GFAP; chicken, cat # 829401, BioLegend, San Diego, CA, USA, 1:700) and HIV-1 structural protein p24 (mouse, cat # ab9044, Abcam, 1:100) or IRE1α (clone 14C10, rabbit, cat # 3294, Cell Signaling Technology, 1:100) were incubated overnight at 4 °C. Alexa Fluor secondary antibodies (488 nm, chicken, cat # A11042; 594 nm, mouse, cat # A11032; 594 nm, rabbit, cat # A11037; 1:400; Thermo Fisher Scientific) were incubated for 2 h at room temperature. Cells were washed between incubation steps. Nuclei were labeled with 4′,6-diamidino-2-phenylindole (DAPI; cat # D1306, 1:1000, 3 min, Thermo Fisher Scientific) prior to mounting and imaging. Fluorescent microscopy

images were obtained on ECLIPSE Ti-4 using the NIS-Elements BR. 3.2 software (Nikon, Minato, Tokyo, Japan) to visualize the proteins and cellular morphology.

Morphology activation: Glial fibrillary acidic protein (GFAP) fluorescence intensity was measured using SoftMax Pro plate reader following immunocytochemical staining. Excitation was set at 488 nm, emissions at 525 nm and auto fluorescence cutoff at 525 nm. DAPI fluorescence intensity was used to normalize GFAP per cell. Duplicate full well scans were quantified for each condition per biological donor. Astrocyte process length was measured using Fiji ImageJ software. Astrocytes were selected based on distinction of processes. For percent (%) morphological activation, astrocytes with constricted bodies and distinct processes were divided by the total number of astrocytes per image. Process length and percent morphological activation were quantified across three images per condition for each biological donor.

Chemokine expression: Astrocytes were plated in triplicates in 48-well plates at 150,000 cells per well. Supernatants were collected 48 h post plating (24 h post IL-1β treatment). Colorimetric enzyme-linked immunosorbent assays (ELISA) were performed according to the manufacturer's instructions to quantify C-C motif chemokine ligand 2 (CCL2) and C-X-C motif chemokine ligand 8 (CXCL8) secretion levels in culture supernatants (CCL2, cat # DCP00; CXCL8, cat # D8000C, R&D Systems). Cells metabolize 3-(4,5-dimethylthiazol-2-yl)-2,5-diphenyltetrazolium bromide (MTT) into formazan crystals, which was used to assess metabolic activity as an indicator for cell number. MTT activity was used to normalize ELISA results (Edara, Ghorpade, and Borgmann 2020; You et al. 2020).

Glutamate clearance: Glutamate clearance assays in primary human astrocytes were performed as previously described and published as a bio-protocol (Edara, Ghorpade, and Borgmann 2020; You et al. 2020). Briefly, astrocytes were plated in triplicates in 48-well plates at

150,000 cells per well. After 24 h, astrocytes were treated with or without IL-1β (20 ng/mL). After an additional 24 h, media was exchanged (collected for ELISA) and glutamate (400 μM; cat # G8415, Sigma-Aldrich) in phenol red-free astrocyte medium was added to cultures. Wells without astrocytes were used as controls so that uptake/clearance could be assessed overtime by quantifying remaining glutamate per manufacturer's instructions (Amplex Red glutamic acid/glutamate oxidase assay kit; Thermo Fisher Scientific). Supernatants for glutamate clearance were assessed 24 h post glutamate treatment (72 h post plating).

Data analysis and interpretation: All experiments were performed in at least three separate biological donors. Data in graphs were analyzed and presented using GraphPad Prism (version 8.1.1, GraphPad Software, San Diego, CA, USA) as mean +/- standard error of the mean with replicates from each donor compiled and represented as a single dot on graphs. For protein expression analysis following chronic conditions, each target was individually graphed and analyzed using paired t-tests. All other statistics were determined *via* one-way ANOVA followed by Fisher's LSD test (calcium signaling) or Tukey's post-test for multiple comparisons with $p \leq 0.05$. Note: Fisher's LSD test was used to account for ultra-sensitivity and variability of sensor across different biological donors.

3.4 Results

As HAND is a chronic condition, changes in astrocyte phenotype were assessed seven days following low dose METH exposure (50 or 250 nM) or post-infection to model the lingering low levels of METH in the CNS between binges of a regular user. Restimulation with acute high doses of METH (5 or 250 μM) was used to model the physiological peak of METH in the CNS during a binge to evaluate how chronic stress following METH exposure or HIV-1 infection shifts astrocyte

responses to new stimuli. Subsequent phenotype studies evaluated changes in metabolic function, calcium signaling, and UPR protein expression **(Figure 3.1A)**.

Astrocytes do not express the key receptor (CD4) required for conventional HIV-1 entry. However, astrocytes can undergo other means of HIV-1 infection such as direct cell-cell transfer of the virus *via* infected CD4+ T cells (Luo and He 2015; Lutgen et al. 2020), whose trafficking into the CNS has been established (Mathe et al. 1997; Spudich et al. 2019). To investigate specifically how HIV-1 infection alters astrocyte phenotype, a pseudotyped HIV-1 was constructed by co-transfecting an HIV-1 plasmid (pHIV-1) with pVSVg in HEK 293 cells **(Figure 3.1B)**. In VSV particles, VSVg is the predominant coat responsible for virus entry *via* membrane fusion. Thus, progeny pseudotyped HIV-1 virions will incorporate VSVg in their viral coat and permit entry independent of CD4 expression as previously described (Canki et al. 2001; Ojeda et al. 2018; Edara, Ghorpade, and Borgmann 2020). Notably, a T-tropic pHIV-1 strain (NL4-3) was used to model astrocytes infected *in vivo* by T-cell-mediated HIV-1 transfer.

HIV-1 infection of primary human astrocytes (PHA) was confirmed five days post-infection using a nested HIV-1 DNA integration assay **(Figure 3.1C)**. As a positive control for integration, 8E5 cells were used as they are a T cell generated subclone that contains a single integrated copy of proviral DNA per cell (Desire et al. 2001; Wilburn et al. 2016). Expression of the HIV-1 structural protein p24 and the regulatory protein Nef was evident only in HIV-1 treated astrocytes and was illustrated in two astrocyte donors by Simple Wes **(Figure 3.1D)**. Vinculin was used as a protein loading control. Expression of p24 (red) was visualized using immunocytochemistry in astrocytes stained with astrocyte marker, GFAP (green) following seven days infection with pseudotyped HIV-1 (1000 RT) **(Figure 3.1E)**. Notably, astrocyte staining also revealed morphological activation following infection as evident by more distinctive processes

and cell body constriction. Moreover, pseudotyped HIV-1-infected astrocyte cultures had an elevated intensity in GFAP, which is a known indicator of astrogliosis and associates with increased neuropathology (Eng and Ghirnikar 1994; Bettcher et al. 2021).

To evaluate how chronic METH exposure or HIV-1 infection alters astrocyte metabolic phenotype, astrocytes were treated with METH (50 or 250 nM) (blue bars) or infected with pseudotyped HIV-1 (100 – 1000 RT) (red bars) for seven days prior to assessing mitochondrial function *via* Seahorse XF Cell Mito Stress Test **(Figure 3.2)**. Agilent Seahorse XF Analyzers measure real-time OCR and extracellular acidification rate (ECAR) to characterize mitochondrial respiration and glycolysis, respectively. The Cell Mito Stress Test is widely regarded as a "gold standard" for quantifying key parameters of mitochondrial function in cells. Using an injection sequence of three ETC modulators, the assay determines basal respiration, ATP-linked respiration, maximal respiration, spare respiratory capacity, non-mitochondrial respiration, and proton leak from calculated OCR readouts.

Primary human astrocytes exposed to METH (50 nM) for seven days had elevated OCR overall compared to untreated controls as illustrated in an OCR line tracing from a representative astrocyte donor graphed over time **(Figure 3.2A)**. Moreover, analysis of subsequent mitochondrial parameters demonstrated dose-dependent consequences following chronic METH (50 or 250 nM) exposure **(Figure 3.2B–G)**. The basal energetic demand between conditions is reflected by baseline readouts prior to stress test modulator injections. The first injection of oligomycin (Oligo) inhibits ATP synthase (complex V) allowing quantification of ATP-linked respiration. While elevated, both basal respiration **(Figure 3.2B)** and ATP production **(Figure 3.2C)** were not statistically significant for the lower dose of METH at 50 nM but had approximately 1.75-fold increases at the higher METH dose at 250 nM ($p < 0.05$). The second injection of FCCP is an

uncoupler allowing uninhibited (maximal) electron transport and respiratory capacity. The difference between basal and maximal respiration is used to calculate spare respiratory capacity and is an indicator of "cell fitness or flexibility". Both maximal respiration **(Figure 3.2D)** and spare respiratory capacity **(Figure 3.2E)** were significantly elevated by chronic METH (50 or 250 nM) exposure ($p < 0.05$). Finally, the last injection is a combination of rotenone and antimycin A (Rot/AA), which inhibits complexes I and III, respectively and effectively shuts down ETC function allowing assessment of non-mitochondrial respiration. Non-mitochondrial respiration provides insight to oxygen-consuming enzymes outside that of the ETC, which may be contributing to metabolic demand (glycolysis, fatty acid oxidation, etc.). The difference between non-mitochondrial respiration and respiration remaining after ATP synthase inhibition indicates the proportion of proton leak between conditions and can be an indicator of mitochondrial damage. Like mitochondrial respiration, non-mitochondrial respiration **(Figure 3.2F)** was dose-dependently increased following chronic METH (50 or 250 nM) exposure ($p < 0.05$). Interestingly, proton leak **(Figure 3.2G)** was higher at the lower dose of METH (50 nM; 1.75-fold increase compared to control; $p < 0.01$) compared to 250 nM (1.5-fold increase compared to control; $p < 0.05$).

Like chronic METH exposure, HIV-1-infected astrocytes had an elevated OCR overall compared to untreated controls as illustrated in an OCR line tracing from a representative astrocyte donor graphed over time **(Figure 3.2H)**. However, there was a reverse dose trend evident in HIV-1-infected astrocytes wherein the lower concentration of HIV-1 (100 RT) had a consistently higher increased OCR in key metabolic parameters compared to the higher HIV-1 doses (500 or 1000 RT) **(Figure 3.2I–N)**. Indeed, 100 RT of pseudotyped HIV-1 induced 1.75-fold increases in basal respiration **(Figure 3.2I)**, maximal respiration **(Figure 3.2K)**, and spare respiratory capacity

(Figure 3.2L; $p < 0.01$**)**, while 500 RT doses induced 1.5-fold increases in the same parameters ($p < 0.05$). The highest HIV-1 dose (1000 RT) had similar effects as 500 RT on maximal respiration and spare respiratory capacity ($p < 0.05$) but did not significantly elevate basal respiration. All HIV-1 doses also significantly increased non-mitochondrial respiration **(Figure 3.2M**; ~1.25–1.5-fold; $p < 0.05$**)**, although less robustly than the effects on mitochondrial respiration. Notably, increased metabolic activity was not accompanied with changes in ATP production **(Figure 3.2J)** following infection at any dose tested suggesting increased respiratory demand without the energetic reward. It should also be noted that proton leak can be used as a mechanism to regulate the mitochondrial ATP production. While proton leak **(Figure 3.2N)** followed similar increased overall trends following HIV-1 infection, variable effects across separate biological donors translated to only the low HIV-1 dose (100 RT) to be statistically significant ($p < 0.05$).

Altogether, these findings demonstrate that low levels of METH or HIV-1 infection increase astrocyte metabolic activity. Increased basal respiration **(Figure 3.2B, I)**, maximal respiration **(Figure 3.2D, K)** and spare respiratory capacity **(Figure 3.2E, L)** suggest that astrocyte mitochondria may need to overcompensate during conditions of chronic stress. Increased proton leak **(Figure 3.2G, N)** and lack of significant increases in ATP production **(Figure 3.2C, J)** suggest impaired mitochondrial integrity. Meanwhile, increased non-mitochondrial oxygen consumption **(Figure 3.2F, M)** supports a potential astrocyte metabolic shift. Regardless, the cause, purpose and outcome of these increased metabolic states are not fully understood.

Mitochondrial bioenergetics is regulated by the transfer of calcium from ER, which is the primary calcium source for astrocyte mitochondrial calcium fluxes (Huntington and Srinivasan 2021). To measure changes in intracellular calcium flux following METH exposure or HIV-1 infection, astrocytes were transfected with a genetically modified GFP cytosolic calcium sensor

(GCaMP6s) **(Figure 3.3A-D)** (Chen et al. 2013; Nooka and Ghorpade 2017). Time series confocal microscopy allowed fluorescent visualization of a single cell's calcium flux post treatment **(Figure 3.3A)**, and changes in fluorescence were graphed over time **(Figure 3.3B; Supp. Figure 3.1)**. To demonstrate variability across biological donors and conditions, ten individual cellular responses were graphed per condition in at least two separate donors **(Supp. Figure 3.1)**. The AUC, following stimulation with either media or METH, was then graphed for statistical comparisons **(Figure 3.3C-D)**. In astrocytes, acute METH (250 μM, striped bars) increased astrocyte intracellular calcium flux by 2-fold versus untreated controls ($p < 0.05$). Interestingly, there was slightly increased basal calcium flux (stimulated with media) of astrocytes pretreated with chronic METH (50 nM; blue bars) **(Figure 3.3C)** or infected with pseudotyped HIV-1 (500 RT; red bars) **(Figure 3.3D)** for seven days. Restimulation of acute METH (250 μM) following chronic METH exposure or HIV-1 infection further elevated METH-induced intracellular calcium flux (~3-fold vs control, $p < 0.01$; $p < 0.05$ compared to respective media-stimulated controls). However, there were no statistically significant differences comparing chronic conditions to non-pretreated controls (white bars versus colored bars). Together, these data indicate that both prolonged METH exposure and HIV-1 infection may alter ER physiology by increasing both basal and METH-induced calcium flux, which could be contributing to the elevated levels of mitochondrial respiration following these conditions **(Figure 3.2)**.

To further examine altered ER physiology and ER-associated signaling pathways in response to METH exposure and HIV-1 infection, protein expression of the three UPR arms (ATF6, IRE1α, and PERK), along with their classical ER stress negative regulating binding partner, BiP, was determined using Simple Wes **(Figure 3.3E-H)**. To demonstrate variability across biological donors and conditions, representative Wes blots for two separate biological

donors per condition are illustrated **(Figure 3.3E-F)**. Notably, chronic METH (50 nM; blue bars) exposure significantly increased expression of UPR arm IRE1α by 50% ($p < 0.05$) without increasing BiP, ATF6, or PERK **(Figure 3.3G)**, and HIV-1 infection (500 RT; red bars) induced significant increases in all arms and their binding partner ($p < 0.05$) **(Figure 3.3H)**. Of note, most prominently elevated following HIV-1 infection was IRE1α with a two-fold increase ($p < 0.01$). Contrary to chronic METH (50 nM) exposure, astrocytes stimulated with acute METH (5 μM; striped bars) for 8 hours did not significantly increase IRE1α but instead increased expression of the other two arms, ATF6 and PERK ($p < 0.01$) **(Supp. Figure 3.2A)**. However, acute METH (5 μM) restimulation following chronic METH (50 nM) demonstrated altered responses in UPR arm protein induction **(Supp. Figure 3.2B-D)**. Indeed, acute METH-induced increases in ATF6 **(Supp. Figure 3.2B)** and PERK **(Supp. Figure 3.2C)** protein levels were significantly suppressed after chronic METH exposure ($p < 0.05$). Meanwhile, chronic METH-induced IRE1α **(Supp. Figure 3.2D)** protein levels were also reduced back to control levels when restimulated with acute METH. These altered responses support a possible phenotypic shift in astrocyte UPR/ER stress responses following chronic METH exposure.

Next, the three UPR arms were evaluated for their influence on astrocyte respiration to determine if they could be regulating astrocyte metabolic phenotypes. Astrocytes were treated with pharmacological inhibitors of the three UPR arms three hours prior to assessment of metabolic function **(Figure 3.4)**. Line tracings from representative experiments for OCR **(Figure 3.4A)** and ECAR **(Figure 3.4B)** readouts over time demonstrate decreased overall astrocyte metabolic function when any UPR arm was inhibited as compared to control rates. Subsequent parameter calculation from grouped OCR data in five separate astrocyte donors highlighted that IRE1α inhibition significantly impairs basal respiration **(Figure 3.4C**; $p < 0.01$**)**, ATP production **(Figure**

3.4D; $p < 0.001$**)**, maximal respiration **(Figure 3.4E**; $p < 0.001$**)**, spare respiratory capacity **(Figure 3.4F**; $p < 0.001$**)**, and non-mitochondrial OCR **(Figure 3.4G**; $p < 0.05$**)**. Inhibition of PERK significantly inhibited spare respiratory capacity **(Figure 3.4F**; $p < 0.05$**)**. Proton leak **(Figure 3.4H)** was not significantly altered from inhibiting any of the three UPR arms, suggesting that there were no direct effects of inhibitors on mitochondrial integrity. Instead, the effects on mitochondrial respiration were likely indirectly regulated though ER to mitochondrial signaling.

To gain further insight into the effects of the three arms on non-mitochondrial respiration, additional analysis using ECAR data allowed interpretation of basal and maximal glycolytic rates by calculating changes before and after injection of oligomycin **(Figure 3.4I-J)**. Interestingly, both basal ECAR **(Figure 3.4I)** and maximal ECAR **(Figure 3.4J)** were impaired by IRE1α inhibition. Importantly, the effects of IRE1α inhibition on downregulating mitochondrial respiration and glycolysis were not due to changes in cytotoxicity as determined by an extracellular lactate dehydrogenase (LDH) assay **(Figure 3.4K)**. Moreover, two different pharmacological inhibitors for IRE1α were tested confirming specificity of IRE1α inhibition on astrocyte metabolic function **(Supp. Figure 3.3)**. Altogether, the data demonstrate IRE1α as a potential regulator of astrocyte metabolic function, both mitochondrial respiration and glycolysis. However, it remains to be determined if IRE1α may be regulating these two metabolic pathways through distinct mechanisms.

To determine if IRE1α inhibition could rescue the increased metabolic phenotypes that followed chronic METH exposure and HIV-1 infection, astrocytes were treated with chronic METH (blue bars) or infected with HIV-1 (red bars) prior to IRE1α inhibition (triangles and pattern bars) and subsequent metabolic analysis **(Figure 3.5)**. Similar to above, OCR line tracings demonstrate that chronic treatments with METH exposure or HIV-1 infection increased astrocyte

OCR, while IRE1α inhibition decreased respiratory activity **(Figure 3.5A)**. Overall, inhibition of IRE1α significantly decreased ($p < 0.001$) METH- and HIV-1-induced increases in basal respiration **(Figure 3.5B)**, ATP production **(Figure 3.5C)**, maximal respiration **(Figure 3.5D)**, and spare respiratory capacity **(Figure 3.5E)**, indicating a potential restoration in respiratory phenotype. Indeed, HIV-1 infection with IRE1α inhibition was not significantly different from healthy controls (white bars) in basal, maximal, or spare respiration. Similarly, chronic METH with IRE1α inhibition was not significantly changed from healthy controls in both basal and spare respiration. However, IRE1α inhibition, independent of chronic treatment, significantly decreased ATP production ($p < 0.05$), suggesting an inability of IRE1α inhibition to completely rebalance astrocyte respiration following chronic METH exposure or HIV-1 infection.

To isolate IRE1α regulatory function in astrocytes and model IRE1α upregulation following chronic METH exposure or HIV-1 infection, astrocytes were transfected with an IRE1α overexpression vector (gray bars) or backbone as a control (white bars) **(Figure 3.6B, C)**. After recovery, astrocytes were treated with proinflammatory cytokine, IL-1β (20 ng/mL; checkered bars) for 24 hours followed by various functional assessments **(Figure 3.6A)**. In HAND, IL-1β is a prominent cytokine involved in astrocyte activation and has been extensively used to study the role of astrogliosis in HAND pathology (Roux-Lombard et al. 1989; Kou et al. 2009; Mamik et al. 2011; Nooka and Ghorpade 2017; Edara et al. 2020). Moreover, IL-1β is a potent inducer of ER stress in astrocytes (Nooka and Ghorpade 2017). Thus, these studies can help illuminate the functional role of both IRE1α expression and activation in astrocytes. Increased protein expression of IRE1α following both overexpression transfection and IL-1β treatment was confirmed using Simple Wes **(Figure 3.6B)**. Of the three separate biological donors tested, IL-1β treatment alone induced a ~2 – 6-fold increase in IRE1α, while overexpression varied more substantially across

biological donors with a ~2 – 40-fold increase in expression. Moreover, overexpression with IL-1β treatment further increased expression in all donors with a ~6 – 60-fold increase in IRE1α protein expression. As expected, BiP protein expression, which is classically used as an indicator for ER stress activation, was significantly increased following IL-1β treatment ($p < 0.05$) **(Figure 3.6C)**. However, overexpression of IRE1α had no effect on BiP expression.

The effects of IRE1α overexpression on astrocyte metabolic phenotype in IL-1β-stimulated and unstimulated conditions were assessed by Cell Mito Stress Test **(Figure 3.6D-I)**. Line tracings of OCR **(Figure 3.6D)** and ECAR **(Figure 3.6E)** readouts from representative astrocyte donors emphasize a unique discrepancy of the regulatory effects or IRE1α expression on astrocyte metabolic function in IL-1β-stimulated versus unstimulated conditions. Basal and maximal mitochondrial respiration, calculated from OCR, were significantly increased (~25%; $p < 0.05$) in astrocytes when IRE1α was overexpressed compared to backbone controls, independent of IL-1β treatment **(Figure 3.6F-G)**. However, basal and maximal glycolytic activities, calculated from ECAR, were only significantly increased (~25%; $p < 0.05$) by IRE1α overexpression in astrocytes when stimulated by IL-1β **(Figure 3.6H-I)**. Additional parameters calculated from OCR data, including spare respiratory capacity **(Supp. Figure 3.4A)** ATP production **(Supp. Figure 3.4B)**, non-mitochondrial respiration **(Supp. Figure 3.4C)**, and proton leak **(Supp. Figure 3.4D)**, followed similar increased trends when IRE1α was overexpressed in astrocytes. However, only proton leak in IL-1β-unstimulated astrocytes was significantly elevated (~25%; $p < 0.05$). Altogether, these findings confirm IRE1α as a regulator of astrocyte metabolic phenotype and support distinct mechanistic differences between IRE1α-mediated regulation on mitochondrial respiration versus glycolytic activity.

Previous studies linking IRE1α to metabolic regulation correlate these changes to cellular activation/inflammation suggesting IRE1α-mediated induction of mitochondrial respiration is essential for immune activation (Dong et al. 2019; Abuaita et al. 2021; Lara-Reyna et al. 2019). In fact, IRE1α has commonly been highlighted as a regulator of inflammation and immune responses to infections (Abuaita et al. 2021; Abuaita et al. 2015; Abuaita, Schultz, and O'Riordan 2018; Dong et al. 2019; Lara-Reyna et al. 2019; Wheeler et al. 2019). However, this functional linkage between metabolism and inflammation has yet to be established using an IRE1α overexpression model or in astrocytes. As astrocyte-mediated neuroinflammation is a hallmark of HAND pathology, we wanted to evaluate the potential of IRE1α in regulating astrocyte inflammatory phenotype. Thus, using our established overexpression model, we merged our lab's decade-long optimized protocol for characterizing the activation of human astrocytes (You et al. 2020; Edara, Ghorpade, and Borgmann 2020). Immunocytochemistry staining revealed an activated astrocyte morphology post treatment with IL-1β, as indicated by an increased prominence in processes and cell body constriction and increased appearance in GFAP intensity. Moreover, comparing astrocytes overexpressing IRE1α to respective untreated and IL-1β treated backbone groups demonstrated IRE1α may be contributing to astrogliosis morphology **(Figure 3.7A-D)**. Quantification of astrocyte reactivity demonstrated IL-1β stimulation did not significantly affect GFAP expression **(Figure 3.7E)**, but significantly increased astrocyte process length **(Fig. 7F**; $p < 0.001$; statistics not shown on graph**)** and overall percent of astrocytes demonstrating morphological activation **(Figure 3.7G**; $p < 0.01$; statistics not shown on graph**)**. Furthermore, IRE1α overexpression in the absence of IL-1β stimulation significantly increased GFAP intensity and astrocyte process length ($p < 0.05$) as compared to backbone controls. Similarly, IRE1α overexpression with IL-1β stimulation also increased process length and morphological activation ($p < 0.05$) as compared to

activated backbone controls. Delving into astrocyte inflammatory functions, our lab has well-established that astrocyte CCL2 **(Figure 3.7H)** and CXCL8 **(Figure 3.7I)** cytokine release is strongly upregulated in response to IL-1β ($p < 0.01$; statistics not shown on graph); however, these responses were significantly augmented when IRE1α was overexpressed ($p < 0.05$). Finally, a key functional impairment of astrocytes in neuropathology is a decrease in glutamate clearance efficacy, which can contribute to excitotoxicity in neurons. When activated by IL-1β, astrocytes were unable to clear glutamate as efficiently in comparison to untreated cultures ($p < 0.01$; statistics not shown on graph) **(Figure 3.7J)**. Interestingly, overexpression of IRE1α significantly enhanced astrocyte glutamate uptake in IL-1β unstimulated cultures ($p < 0.05$). While IL-1β-stimulated astrocytes had a slight increase when IRE1α was overexpressed, these results were not statistically significant.

3.5 Discussion

In the context of METH exposure and HIV-1-relevant stimuli, astrocytes become activated, which can lead to neurotoxic consequences and contribute to METH use and HAND pathology **(Figure 3.8)**. Major mechanisms for which astrocytes can inflict neuronal damage following METH and/or HIV-1-relevant stimuli include astrocyte-associated neuroinflammation and glutamate excitotoxicity, which our team and others have also previously characterized (Cisneros and Ghorpade 2012, 2014; Borgmann and Ghorpade 2015; Edara, Ghorpade, and Borgmann 2020; Cisneros, Ghorpade, and Borgmann 2020). Moreover, astrocyte mitochondrial dysfunction may threaten the ability of astrocytes to provide essential metabolic and antioxidant support to neurons and could also contribute to the release of toxic reactive oxygen and nitrogen species (ROS/RNS) to propagate oxidative stress.

Identifying a cellular or molecular regulator of astrocyte dysfunction will be essential to ensure neuronal fitness and restore CNS homeostasis when facing a neuropathological challenge, such as METH use and HAND. The current study was centered on evaluating the effects of chronic low-dose METH exposure and HIV-1 infection on astrocyte ER and mitochondrial homeostasis and then examining ER-associated mechanisms as potential therapeutic targets for astrocyte dysfunction. These findings illustrate that astrocytes have increased basal and maximal respiration, spare respiratory capacity and non-mitochondrial OCR following HIV-1 infection or chronic low-dose METH exposure. Increased metabolic activity suggests that astrocytes may need to compensate during HIV/METH-associated stress to meet the increased energic and antioxidant demands. However, increased metabolic respiration did not translate to increased energy output (ATP production). Coupled with an increase in proton leak, these results suggest that astrocyte mitochondrial function was impaired by chronic METH exposure or HIV-1 infection.

Importantly, increased mitochondrial respiratory activity was associated with increased calcium flux and UPR protein expression following HIV-1 infection and METH exposure in primary human astrocytes. Briefly, HIV-1 infection increased expression of all three UPR arms and a key protein-folding chaperone, highlighting profound implications on the long-term restructuring of ER and MAMs during HIV-1/HAND pathology. Acute METH exposure also induced expression of all three UPR messengers, but chronic METH only significantly increased protein expression of IRE1α. Moreover, chronic METH exposure dysregulated both calcium flux and UPR induction when astrocytes were rechallenged with acute METH, supporting altered ER and MAM function and physiology as key regulators in astrocyte dysfunction.

Unique in both HIV-1 and METH paradigms, IRE1α was prominently upregulated. Distinct from the other UPR arms, IRE1α has previously been shown to regulate mitochondrial

respiratory activity and ROS production as a mechanism to control cellular immune and inflammatory responses in a variety of different cell types (Abuaita et al. 2015; Abuaita, Schultz, and O'Riordan 2018; Dong et al. 2019; Abuaita et al. 2021). Moreover, some studies have also highlighted a novel role of IRE1α in the ER-mitochondrial interface as a key regulator of ER-mitochondrial calcium transfer as the potential mechanism for IRE1α regulation of mitochondrial function. Interestingly, these reports differ in the identified interaction in which IRE1α regulates ER-mitochondrial calcium transfer. For example, IRE1α has been shown to both directly (Carreras-Sureda et al. 2019) and indirectly (Son et al. 2014; Son et al. 2021) regulate IP_3R stability in the ER membrane as well as with Sig1R (Mori et al. 2013) in the ER lumen. Indeed, Sig1R is a known astrocyte binding receptor of METH and is implicated as a regulator of METH-mediated astrocyte dysfunction (Zhang et al. 2015). Could these regulatory mechanisms be in association with IRE1α? Notably, recent studies have illuminated IRE1α/Sig1R signaling as potential therapeutic targets for dysfunctional immune and inflammatory pathologies (Rosen et al. 2019).

Our findings suggest IRE1α activity can regulate multiple aspects of astrocyte function including ER stress, mitochondrial respiration, glycolysis, inflammation, and glutamate clearance. A summary of IRE1α-associated regulation of astrocyte function is illustrated in **Table 3.1**. The canonical model for UPR/ER stress activation occurs in response to accumulated unfolded or misfolded proteins, where each UPR arm can orchestrate unique cellular mechanisms to reprogram transcriptional profiles and restore proteostasis. These same messengers can also function to initiate apoptosis if stress is unable to be resolved (Ghemrawi and Khair 2020). However, as astrocytes are resilient to HIV-1/METH-induced stress, chronic upregulation of IRE1α may instead present as key regulator of astrogliosis beyond its classical UPR/ER stress function. The molecular mechanisms and functional diversity of IRE1α have been previously reviewed (Bashir

et al. 2021). Briefly, IRE1α has both kinase and endoribonuclease enzyme activity. There are two divergent classical pathways associated with IRE1α's UPR functions: X-box binding protein 1 (XBP1) and regulated IRE1-dependent decay (RIDD). Notably the IRE-1α/XBP1 pathway is primarily associated with upregulation of UPR gene transcription but is also implicated in metabolic disorders and cancer pathology. The IRE-1α/RIDD signaling branch primarily regulates IRE-1α-mediated mRNA degradation but is also implicated in inflammatory and apoptotic signaling. Importantly, IRE1α can also transmit information independent of its enzymatic activity. A new concept defined as a "UPRsome" has now been introduced, highlighting IRE1α as a potential signaling scaffold for a series of protein interactions to regulate cellular fate (Urra, Pihan, and Hetz 2020; Bashir et al. 2021; Riaz et al. 2020).

In our studies, inhibition of IRE1α impaired astrocyte metabolic function, both mitochondrial respiration and glycolysis. Activation of IRE1α *via* IL-1β stimulation (without IRE1α overexpression) increased astrocyte ER stress and inflammation while perturbing astrocyte glutamate uptake yet did not appear to significantly influence astrocyte metabolic function. Interestingly, overexpression alone led to increased mitochondrial OCR and increased glutamate uptake. As astrocytes convert glutamate into glutamine, which can be then used as a source for metabolic activities (Schousboe et al. 2014), it is possible IRE1a-mediated increased glutamate uptake may be related to the increased OCR. As stated above, IRE1α/XBP1 signaling has been implicated in metabolic homeostasis. In accordance, it has previously been shown that IRE1α /XBP1 signaling can regulate glutamate receptor trafficking in neurons of C. *elegans* (Shim et al. 2004). Of Note, these observations specifically proposed that partial activation of IRE1α /XBP1 signaling for glutamate receptor trafficking occur in the absence of classical ER stress. Also of note, the effects of IRE1α overexpression on astrocyte glutamate uptake were contrary to expected

outcomes; as glutamate clearance is classically impaired when astrocytes have an increased inflammatory phenotype (such as IL-1β stimulation). These findings suggest that different IRE1α-mediated mechanisms or pathways may be at play in regulating astrocyte inflammatory versus tripartite synaptic functions. Finally, combination of IRE1α overexpression with IL-1β stimulation amplified all functional outcomes except glutamate uptake, which instead may have had neutralizing effects.

The function of astrocyte IRE1α on mitochondrial and glycolytic activities may also follow similar signaling discrepancies. For example, IRE1α inhibition regulated both mitochondrial and glycolytic activity; however, overexpression alone only regulated mitochondrial respiration. While IRE1α overexpression with IL-1β stimulation increased both mitochondrial and glycolytic activity, the effects of overexpression and IL-1β activation were compounded for glycolysis, but not mitochondrial respiration. These findings suggest that astrocyte glycolysis and astrocyte mitochondrial respiration may be differentially regulated by IRE1α. Thus, while our studies highlight astrocyte IRE1α as a key regulator of ER stress, mitochondrial respiration, glycolysis, inflammation, and glutamate clearance, distinct signaling pathways and/or mechanisms may be involved in regulating these IRE1α-mediated functional outcomes. For example, some outcomes may be regulated by IRE1α classical UPR/ER stress signaling cascades; some may be through direct protein interactions in the UPRsome, while others may be regulated by IRE1α non-conical mechanisms within the ER-mitochondrial interface. Further studies are needed to delineate the mechanisms of how IRE1α regulates these astrocyte phenotypes.

Regardless, the biological relevance and potential therapeutic targeting of astrocyte IRE1α to combat HAND, METH use disorders and other neurodegenerative pathologies remain unclear. Targeting IRE1α must be balanced to diminish neurotoxic outcomes, while also preserving its

neurosupportive functions is critical to restore astrocyte cellular homeostasis. Since decreased glutamate clearance is critical mechanism of astrocyte-associated neurotoxicity, targeting IRE1α expression may be a novel therapeutic strategy. However, beneficial functional changes in one astrocyte function, could be detrimental to other critical functions. For instance, it is unknown if increased mitochondrial respiration would be associated with neuroprotective (i.e., production and release of metabolites, antioxidants) or neurotoxic consequences (i.e., release of toxic radicals and insufficient neuronal support). If IRE1α-mediated increases in astrocyte metabolic function can enhance essential metabolite and antioxidant provision to neurons without provoking oxidative stress, targeting astrocyte IRE1α may help optimize the coupling between astrocytes and neurons to promote neuronal fitness during a neuropathic challenge. Another caveat, however, are the effects of IRE1α on inflammation. Indeed, inflammation is an immunological response intended to protect a host against injury or infection. However, chronic inflammation can often be the unintended culprit causing pathological tissue damage in many different diseases, like that in HAND.

In summary, the prospect of targeting ER stress and the three UPR arms to combat neurodegeneration has been widely explored as previously reviewed (Ghemrawi and Khair 2020). It is now known that the three arms have unique non-canonical functions within the MAM interface. Moreover, the IRE1α arm has additional stress-associated and non-canonical complexity within the UPRsome. Our group recently published a review highlighting the potential of targeting MAMs in neurodegeneration with specific attention to ER stress, calcium dysregulation, and mitochondrial dysfunction in the context of HAND (Proulx, Park, and Borgmann 2021). These MAM-mediated mechanisms are prominent perpetrators underlying neuropathology among others including autophagy, inflammation, and apoptosis. Here, we highlight the importance of astrocyte

IRE1α as a key regulator of ER stress, mitochondrial respiration, glycolysis, inflammatory responses, and glutamate clearance during chronic HIV-1 infection, METH exposure and neuroinflammation. Moreover, these findings suggest that both canonical and non-canonical UPR mechanisms of astrocyte IRE1α. For IRE1α to be a targetable entity in astrocytes, additional studies will need to delineate the mechanistic properties of how IRE1α regulates these different aspects of astrocyte function. Based on our findings, among other, targeting IRE1α will likely require manipulations that target specific interactions, activities, and/or pathways that best promote neuroprotective properties while preventing neurotoxic properties. Alternatively, exploration into upstream or downstream factors could provide additional therapeutic application.

3.6 Figures and Tables

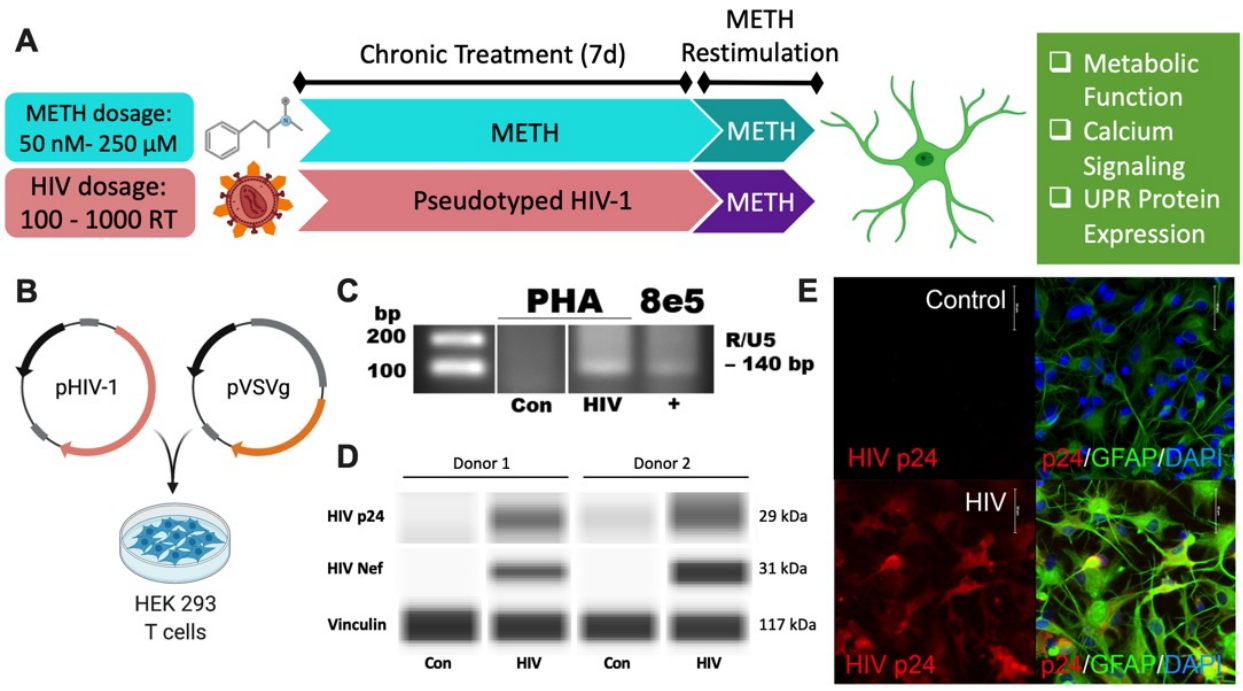

Figure 3.1 Pseudotyped HIV-1 infection in astrocytes is characterized by HIV-1 DNA integration and productive protein expression. (A) Schematic of the proposed experimental design to assess the effects of METH exposure and HIV-1 infection on astrocyte ER-mitochondrial

homeostasis. (B) Pseudotyped HIV-1 was constructed by co-transfecting an HIV-1 plasmid (pHIV-1) with vesicular stomatitis virus glycoprotein plasmid (pVSVg) in HEK 293 T cells. (C-E) Primary human astrocyte (PHA) cultures were infected with (C-D) 500 RT pseudotyped HIV-1 for 5 d or (E) 1000 RT pseudotyped HIV-1 for 7 d followed by (C) HIV-1 DNA integration assay or (D) Simple Wes to detect expression of HIV-1 proteins p24 or Nef. Vinculin was used as an internal control. (E) Immunocytochemistry staining of HIV-1 protein p24 (red), astrocyte marker glial fibrillary acidic protein (GFAP, green) with nuclear DNA labeled with DAPI (blue). Experimental illustrations were made with BioRender.

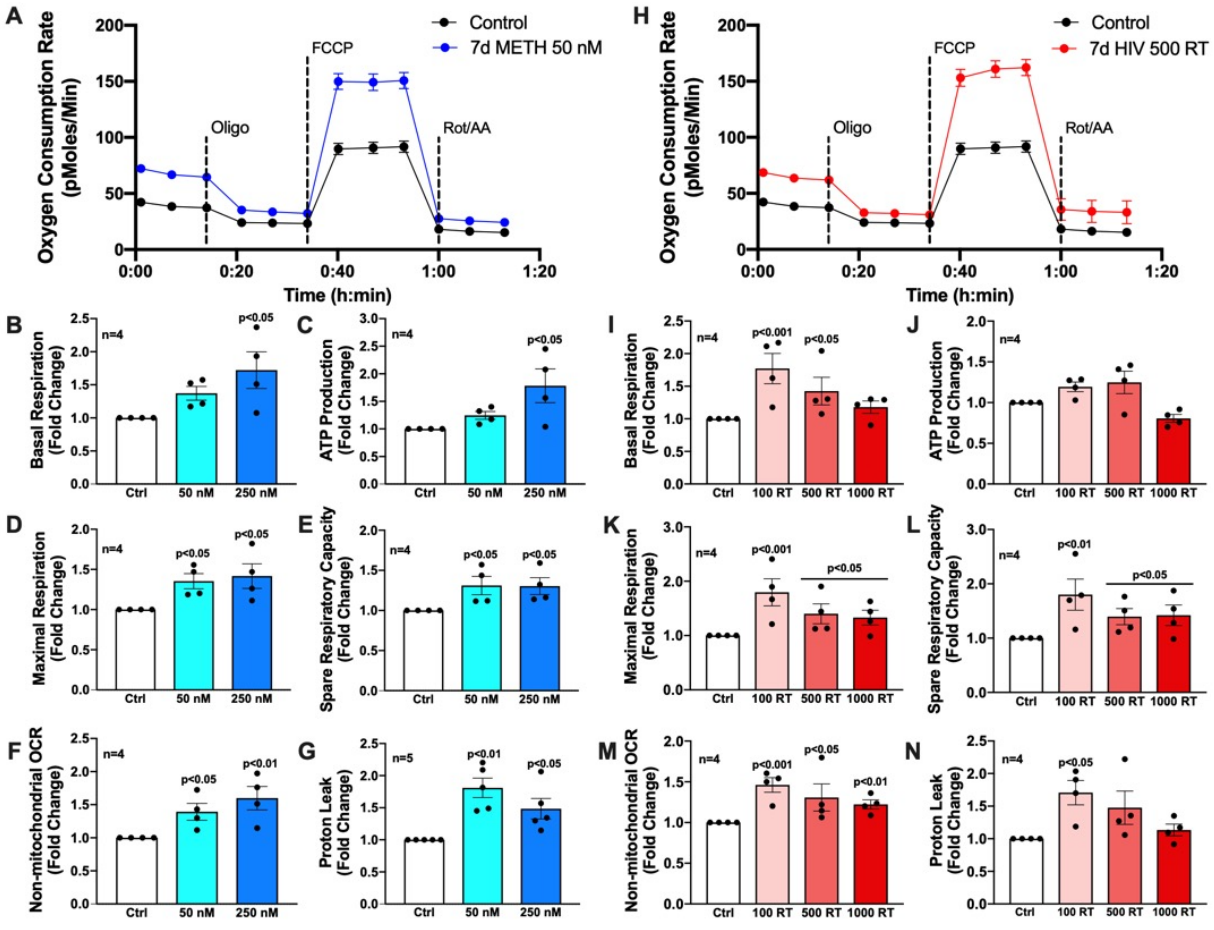

Figure 3.2 Chronic METH exposure and HIV-1 infection increase astrocyte metabolic

activity. Astrocytes were treated with (A-G) METH (50 or 250 nM) or (H-N) infected with pseudotyped HIV-1 (100 – 1000 RT) for 7 d prior to Seahorse XF Cell Mito Stress Test. (A, H) Representative metabolic profile tracings from a single astrocyte donor are graphed over time. Fold changes in oxygen consumption rates (OCR) quantifying (B, I) basal respiration, (C, J) ATP production, (D, K) maximal respiration, (E, L) spare respiratory capacity, (F, M) non-mitochondrial OCR, and (G, N) proton leak were graphed for statistical comparisons. Individual dots on graphs represent the averaged data from a minimum of 6 replicates per biological donor. Statistical significance was determined by one-way ANOVA followed by Tukey's post-hoc for multiple comparisons.

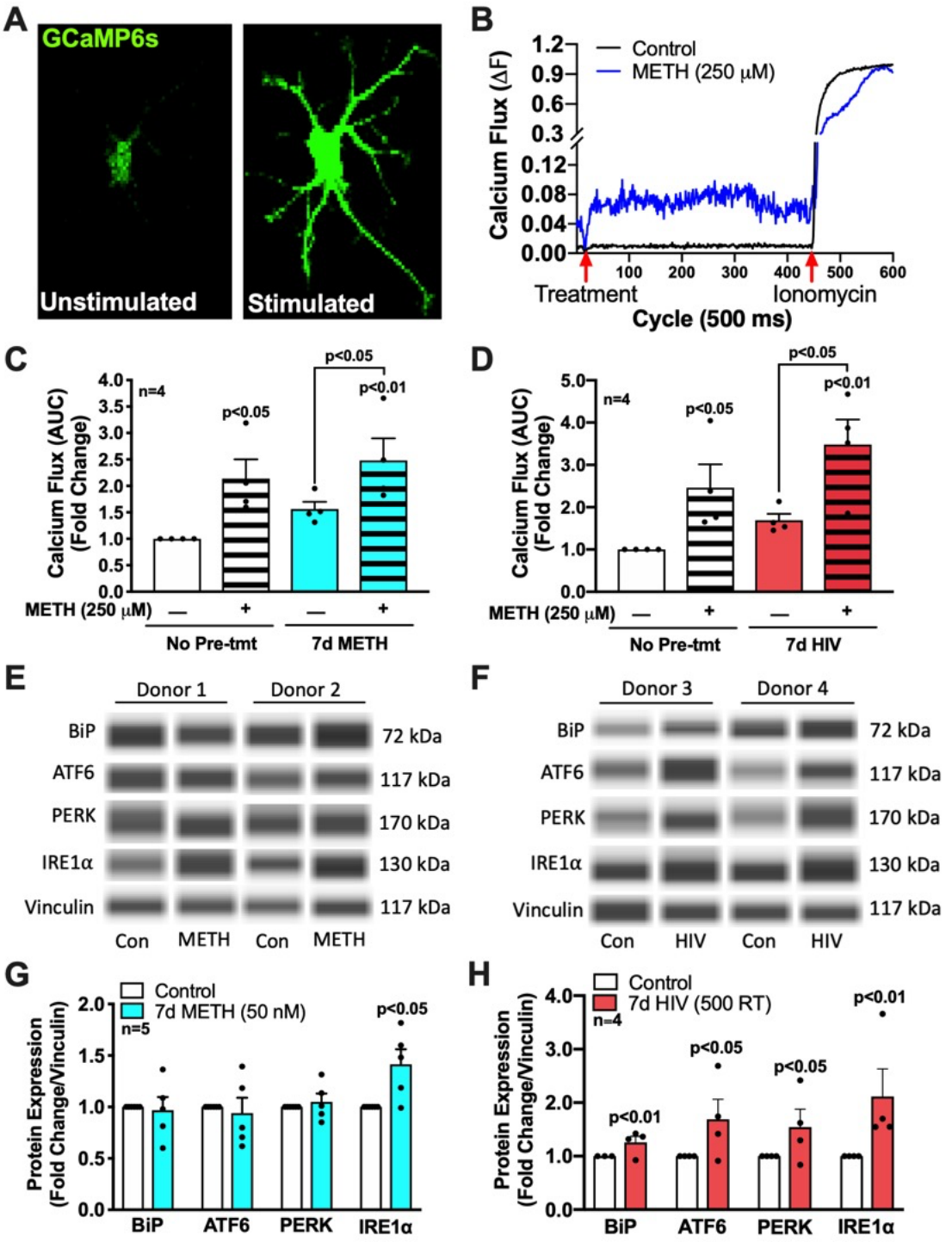

Figure 3.3 METH and HIV-1 upregulate ER/UPR signaling mediators. Astrocytes were treated with (C, E) METH (50 nM) for 7 d (blue bars) or (D, F) pseudotyped HIV-1 (500 RT) for 7 d (red bars) before (A-D) calcium imaging or (E-F) protein analysis *via* Simple Wes. (A-D)

Astrocytes were transfected with a GFP-calmodulin calcium sensor (GCaMP6s) for 48 h prior to calcium flux analysis. (A-B) Time series confocal imaging was used to measure changes in fluorescence every 500 ms for a total of 5 min (600 cycles). (B) Representative calcium flux line tracings illustrate the change in astrocyte calcium flux (ΔF) at any given time point, with control media or METH (250 μM) at 20 cycles (10 sec) and ionomycin (10 μM) at 450 cycles (225 sec). Calcium flux was calculated by: $\Delta F=(F-F0)/(Fmax-F0)$, where F is the fluorescence intensity at any given time; F0 is the baseline (1 – 20 cycles) fluorescence intensity, and Fmax is the maximum fluorescence intensity when exposed to ionomycin (450 – 600 cycles). (C-D) Area under the curve (AUC) was calculated by the sum of ΔF following treatment with control media or METH (250 μM) at 20 cycles (10 sec) and before ionomycin (10 μM) at 450 cycles (225 sec). Individual dots represent the average AUC from a minimum of 20 cells per biological donor and are graphed as fold changes. One-way ANOVA was performed for statistical analysis followed by Fisher's LSD test for stand-alone comparisons to account for sensitivity of calcium flux variation across different biological donors. (E-H) Protein expression of BiP, ATF6, PERK, and IRE1α was measured *via* Simple Wes post-treatment of (E, G) chronic (7 d) METH (50 nM) or (F, H) HIV-1 infection (7 d; 500 RT). (E-F) Representative blot images are illustrated from two separate biological donors per post-treatment paradigm. (G, H) Data from a minimum of 4 donors are compiled for graphical representation. Individual dots on graphs represent fold changes to vinculin for separate biological donors. Statistics were performed using ratio-paired t-tests for individual targets per condition.

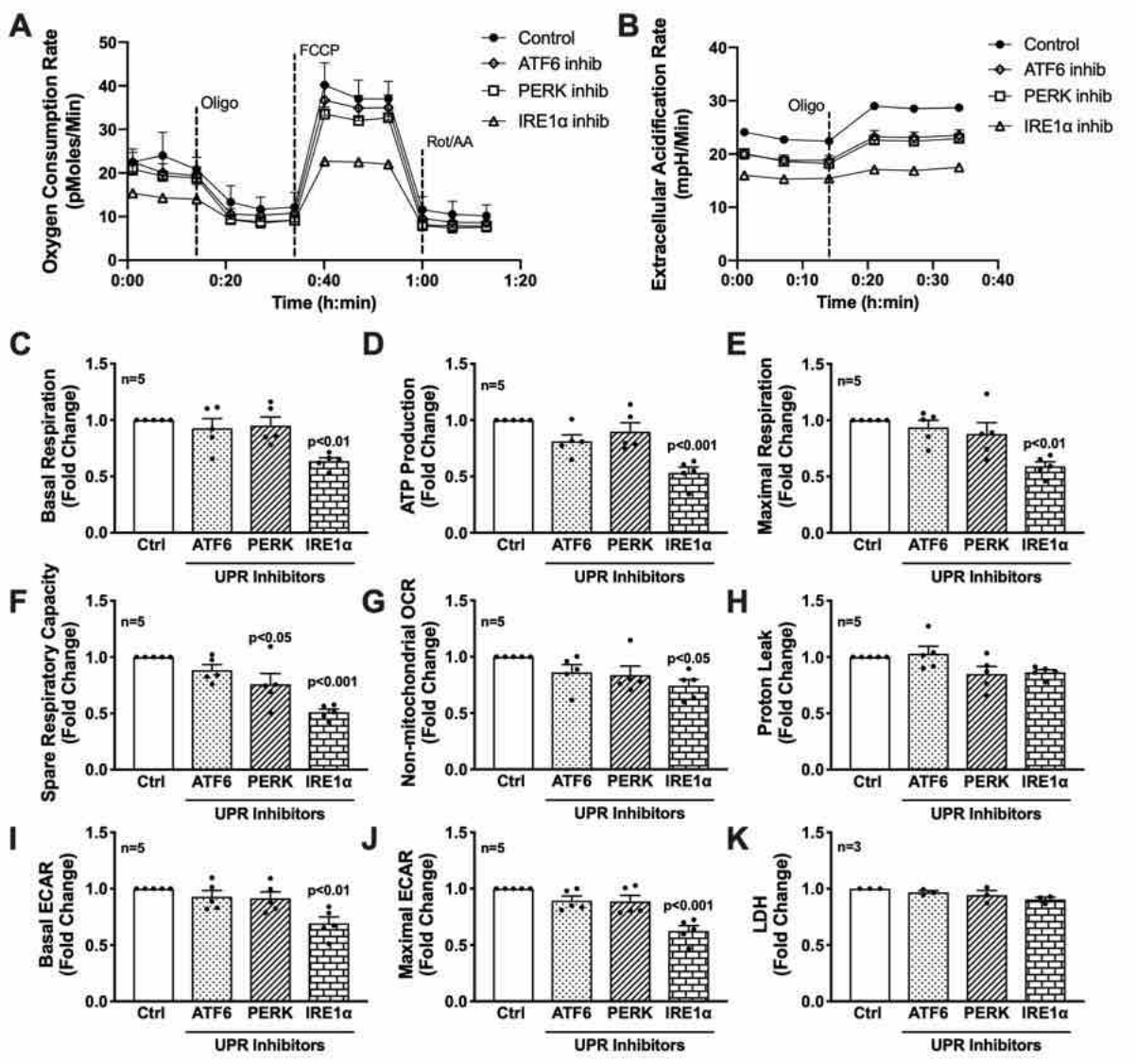

Figure 3.4 Inhibition of IRE1α decreases astrocyte metabolic function. (A-K) Astrocytes were treated with pharmacological inhibitors for the three UPR arms [ATF6 (AEBSF; 100 μM), PERK (GSK2606414; 1 μM), IRE1α (STF-083010; 60 μM)] for 3 h prior to (A-J) Seahorse Mito Stress Test for metabolic assessment or (K) extracellular lactate dehydrogenase (LDH) assay for cytotoxicity. Representative (A) OCR and (B) ECAR profile tracings from a single astrocyte donor were graphed over time. Compiled data from five separate biological donors quantifying fold changes in (C) basal respiration, (D) ATP production, (E) maximal respiration, (F) spare respiratory capacity, (G) non-mitochondrial OCR, (H) proton leak, (I) basal ECAR, and (J)

maximal ECAR were graphed for statistical comparisons. Statistical significance was determined *via* one-way ANOVA followed by Tukey's post-hoc for multiple comparisons. Each dot on graphs represents the averaged data from a minimum of 6 replicates per biological donor.

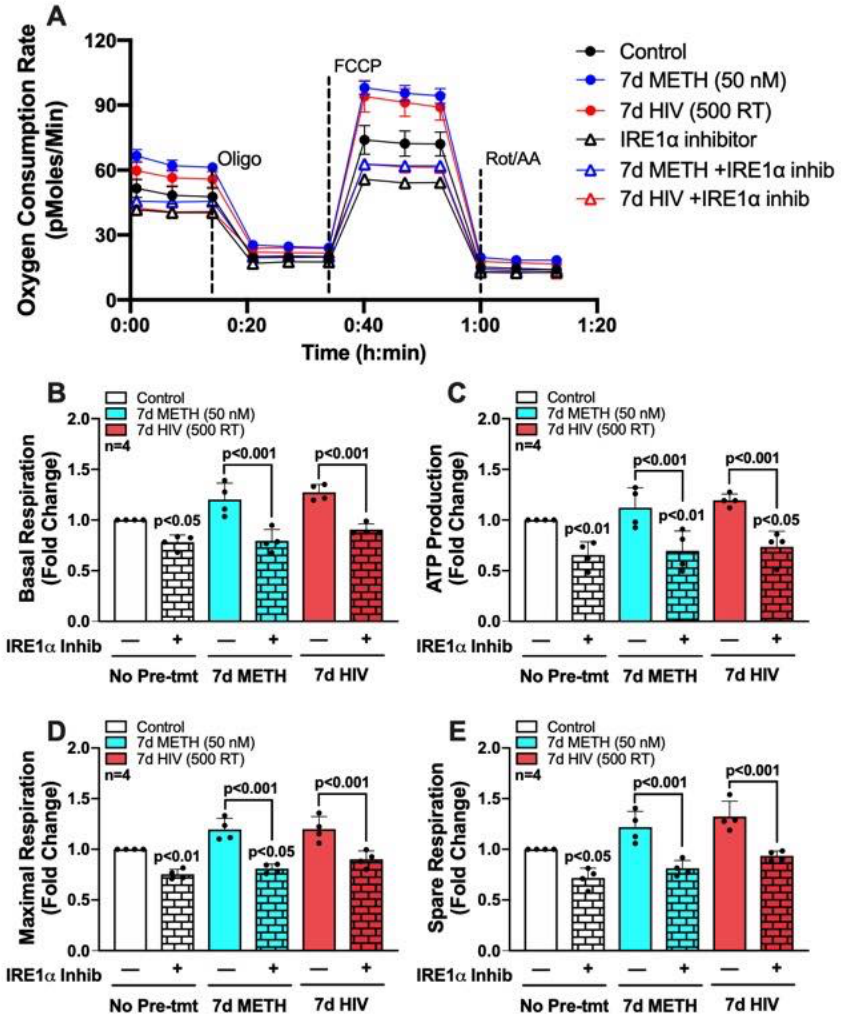

Figure 3.5 IRE1α inhibition can partially restore astrocyte metabolic function following HIV-1 infection and chronic METH exposure. (A-E) Astrocytes were treated with METH (50 nM; blue bars) or infected with pseudotyped HIV-1 (500 RT; red bars) for 7 d followed by IRE1α pharmacological inhibition (STF-083010, 60 μM) for 3 h prior to Seahorse Mito Stress Test. (A) Representative metabolic OCR profile tracing is illustrated from a single astrocyte donor.

Compiled data quantifying fold changes in (B) basal respiration, (C) ATP production, (D) maximal respiration, and (E) spare respiratory capacity were graphed for statistical comparisons. Rescue experiments were performed twice in two separate biological donors to acquire four separate data sets. A minimum of six replicates were performed per experiment. Statistical significance was determined by one-way ANOVA followed by Tukey's post-hoc for multiple comparisons.

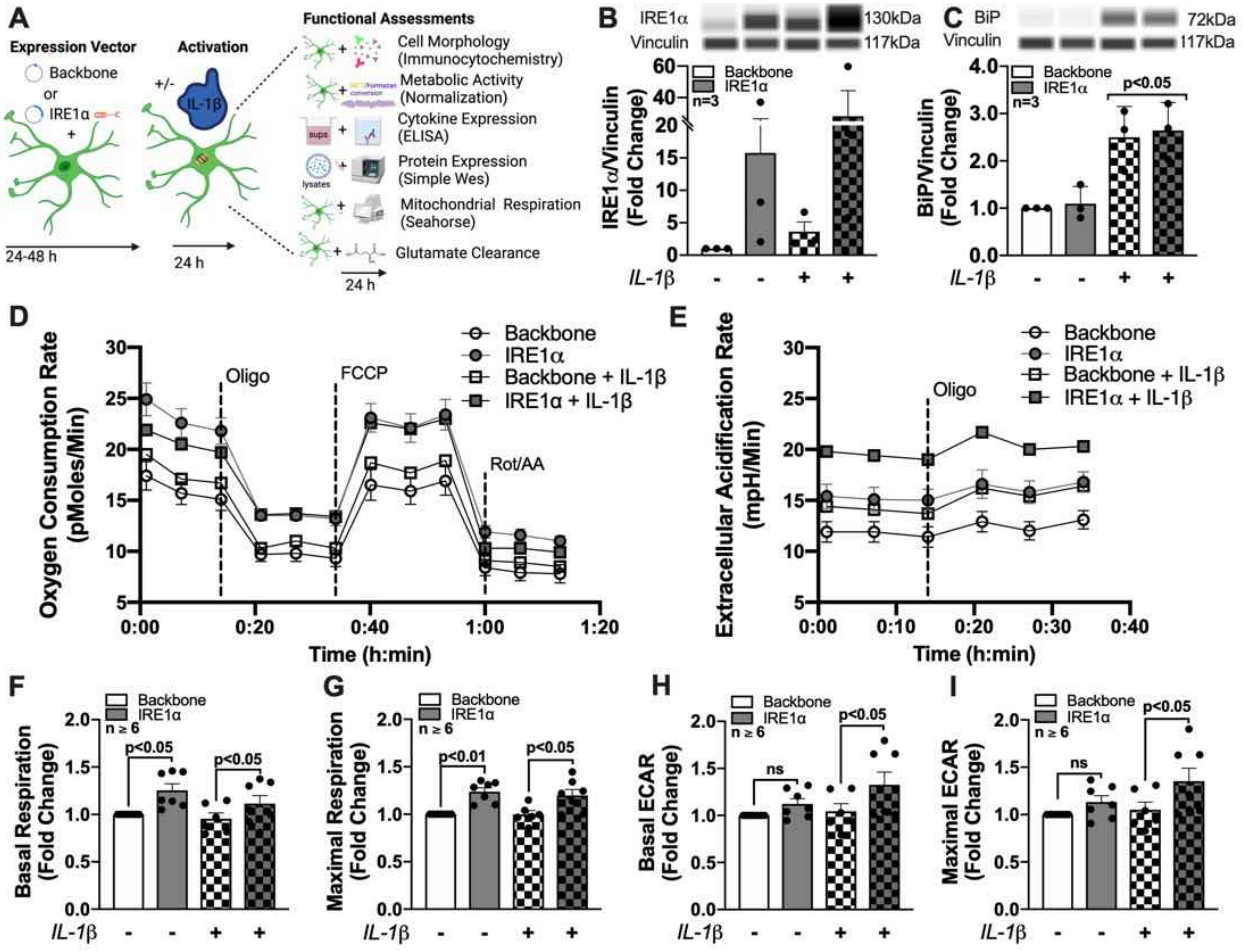

Figure 3.6 Astrocyte IRE1α regulates both mitochondrial respiration and glycolytic activity through distinct mechanisms. (A-I) Astrocytes were transfected with an IRE1α overexpression vector (gray bars) or backbone (white bars) and then treated with IL-1β for 24 h (checkered bars) prior to functional assessments. (B, C) Cellular lysates were collected and assayed by Simple Wes

to quantify (B) IRE1α and (C) BiP expression levels. Vinculin was used as an internal control. (D, F-G) Mitochondrial respiration and (E, H-I) glycolytic activity were assessed by Seahorse metabolic assay. (D) OCR and (E) ECAR profile tracings from a representative astrocyte donor were graphed over time. Fold changes in (F) basal respiration, (G) maximal respiration, (H) basal ECAR, and (I) maximal ECAR were graphed for statistical comparisons. Individual dots on graphs represent the averaged data from a minimum of 6 replicates per biological donor. Significance was determined by one-way ANOVA and Tukey's post-hoc for multiple comparisons. Experimental Illustration was made with BioRender.

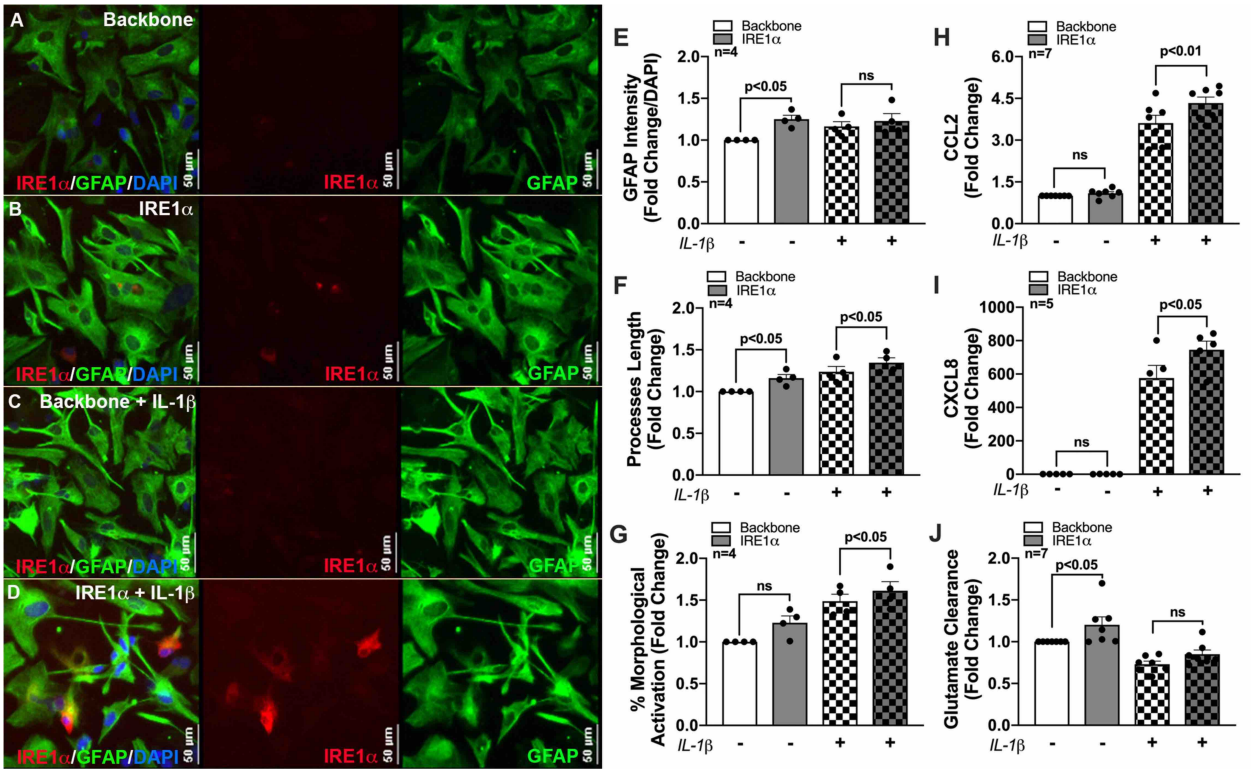

Figure 3.7 IRE1α overexpression augments cytokine expression and increases glutamate clearance in human astrocytes. Backbone and IRE1α transfected astrocytes were treated with IL-1β for 24 h. (A-D) Cells were immunolabeled with antibodies specific for IRE1α (red) and the astrocyte marker glial fibrillary acidic protein (GFAP, green). Nuclear DNA was labeled with

DAPI (blue). (E-G) Experiments in four separate biological donors were analyzed to quantify morphological activation. Individual dots on graphs represent compiled fold-changes calculated from duplicate wells and/or triplicate images per condition for each biological astrocyte donor. (E) GFAP intensity was measured across full-well scans using SoftMax Pro and normalized to DAPI. (F) Process length of individual astrocytes was manually traced and measured using ImageJ Software. (G) Percent morphological activation was calculated based on the number of astrocytes presenting with 'reactive' morphology divided by the total number of astrocytes imaged. (H) CCL2 and (I) CXCL8 levels were assessed by an ELISA, and expression was normalized to metabolic activity prior to calculating fold changes to backbone. (J) Astrocytes were treated with 400 nM glutamate for 24 h. Remaining glutamate levels were quantified by fluorescent assay to calculate % glutamate clearance followed by fold change for each individual donor. Individual dots on graphs represent compiled data from triplicate experiments per biological astrocyte donor. Significance was determined by one-way ANOVA and Tukey's post-hoc for multiple comparisons.

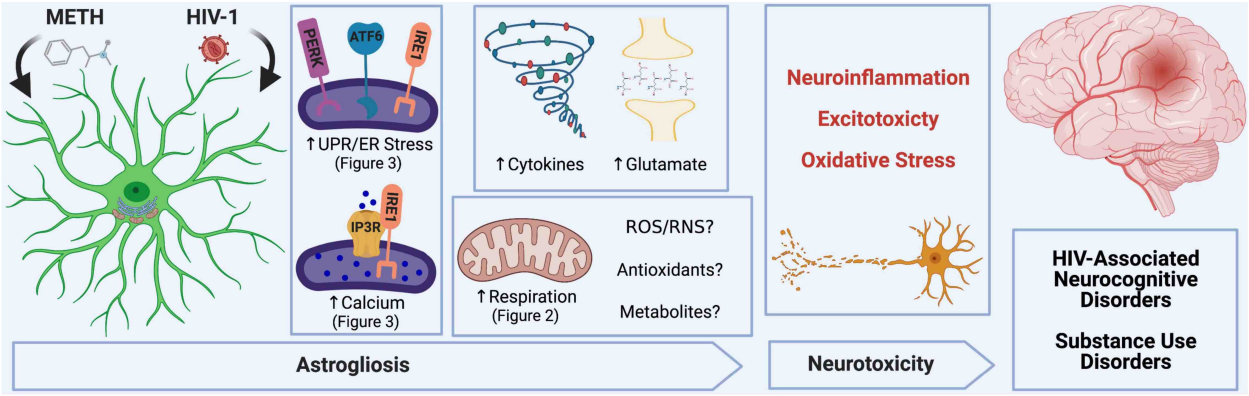

Figure 3.8 METH and HIV-1 alter astrocyte function to induce neurotoxicity, which determines the pathology of HAND and METH use disorders. Neuroinflammation, oxidative stress and glutamate excitotoxicity are hallmarks of neurodegenerative pathology and are all

propagated by astrocyte dysfunction. During a pathological challenge, such as METH exposure and HIV-1 infection, astrocytes became reactive leading to a shift in their neurotrophic functions to become neurotoxic. This reactive state, often termed as astrogliosis, is characterized by an increased inflammatory phenotype which promotes neuroinflammation. Moreover, decreased provision of essential metabolic and antioxidant support to neurons and increased release of toxic radicals such as reactive oxygen and nitrogen species (ROS/RNS) are triggers for oxidative stress. Finally, excitotoxicity arises from an impaired uptake of excess glutamate between synaptic junctions. Our studies emphasize the role of astrocyte ER-associated mechanisms and mitochondrial dysfunction following METH exposure and HIV-1 infection as potential underlying mechanics controlling astrocyte dysfunction and astrocyte-associated neurodegeneration. Experimental Illustration was made with BioRender.

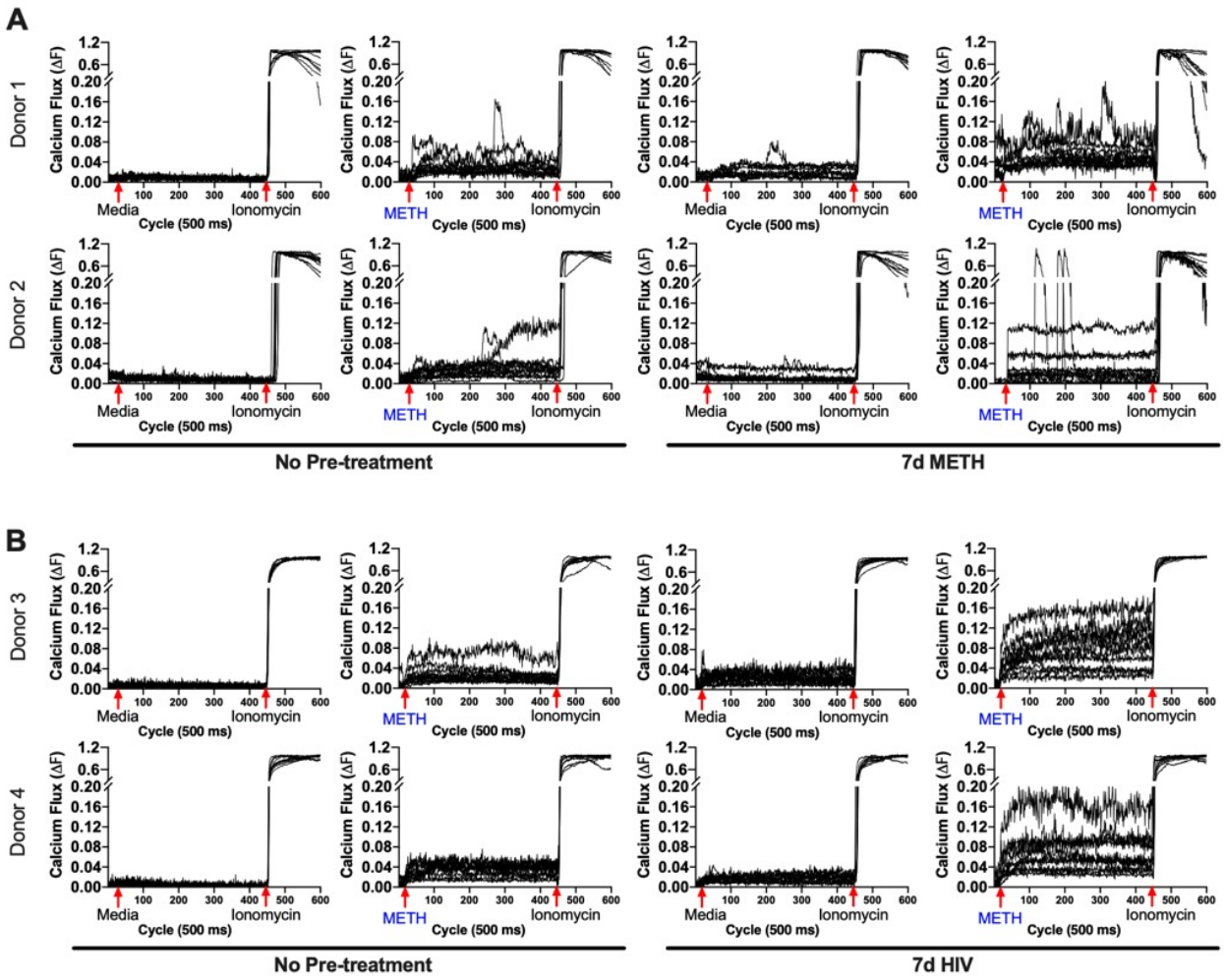

Supplementary Figure 3.1 Chronic METH or HIV-1 infection increase basal and METH-induced astrocyte calcium flux. Astrocytes were untreated (No Pre-treatment) or treated with (A) METH (50 nM) or (B) infected with pseudotyped HIV-1 (500 RT) for 7 d and transfected with a GFP/calmodulin calcium sensor (GCaMP6s) for 48 h prior to calcium flux analysis. Time series confocal imaging was used to measure changes in fluorescence every 500 ms for a total of 5 min (600 cycles). Astrocyte were stimulated with control media or METH (250 μM) at 20 cycles (10 sec) and ionomycin (10 μM) at 450 cycles (225 sec) as positive control for maximum fluorescence. Changes in astrocyte calcium flux (ΔF) was calculated by: $\Delta F=(F-F0)/(Fmax-F0)$, where F is the fluorescence intensity at any given time; F0 is the baseline (1 – 20 cycles) fluorescence intensity,

and Fmax is the maximum fluorescence intensity when exposed to ionomycin (450 – 600 cycles). (A-B) Calcium flux line tracings illustrate the ΔF at any given time point. A total of 10 cells per condition are graphed from two separate donors per chronic treatment paradigm.

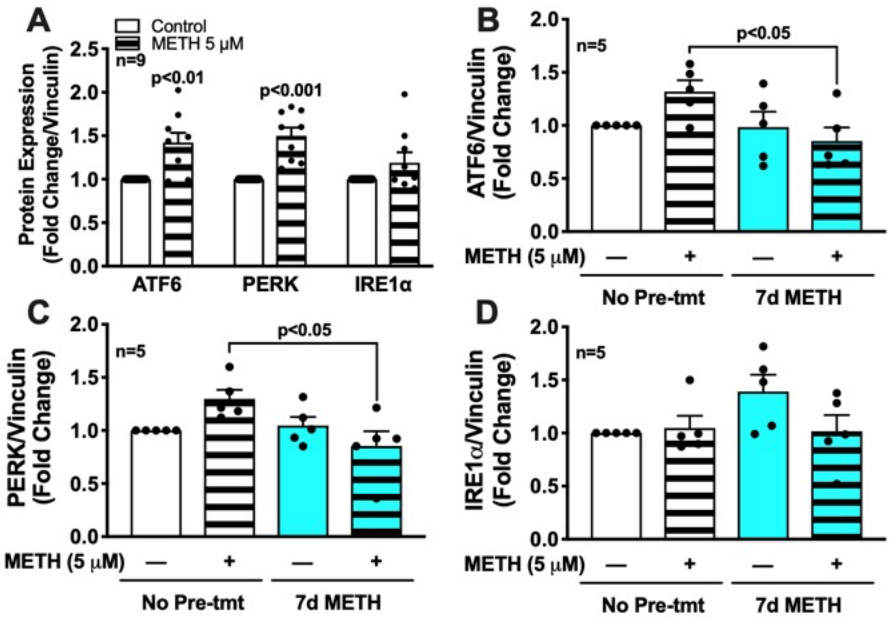

Supplementary Figure 3.2 Astrocyte UPR expression is altered by acute and chronic METH exposure. Astrocytes were treated with acute METH (5 μM) for 8 h (striped bars) and/or chronic METH (50 nM) for 7 d (blue bars) prior to protein lysate collection. Protein expression of (A, B) ATF6, (A, C) PERK, (A, D) IRE1α was measured *via* Simple Wes. Each dot represents separate biological donors. Statistics was performed using (A) ratio-paired t-tests for individual targets per condition or (B-D) one-way ANOVA followed by Tukey's post-hoc for multiple comparisons.

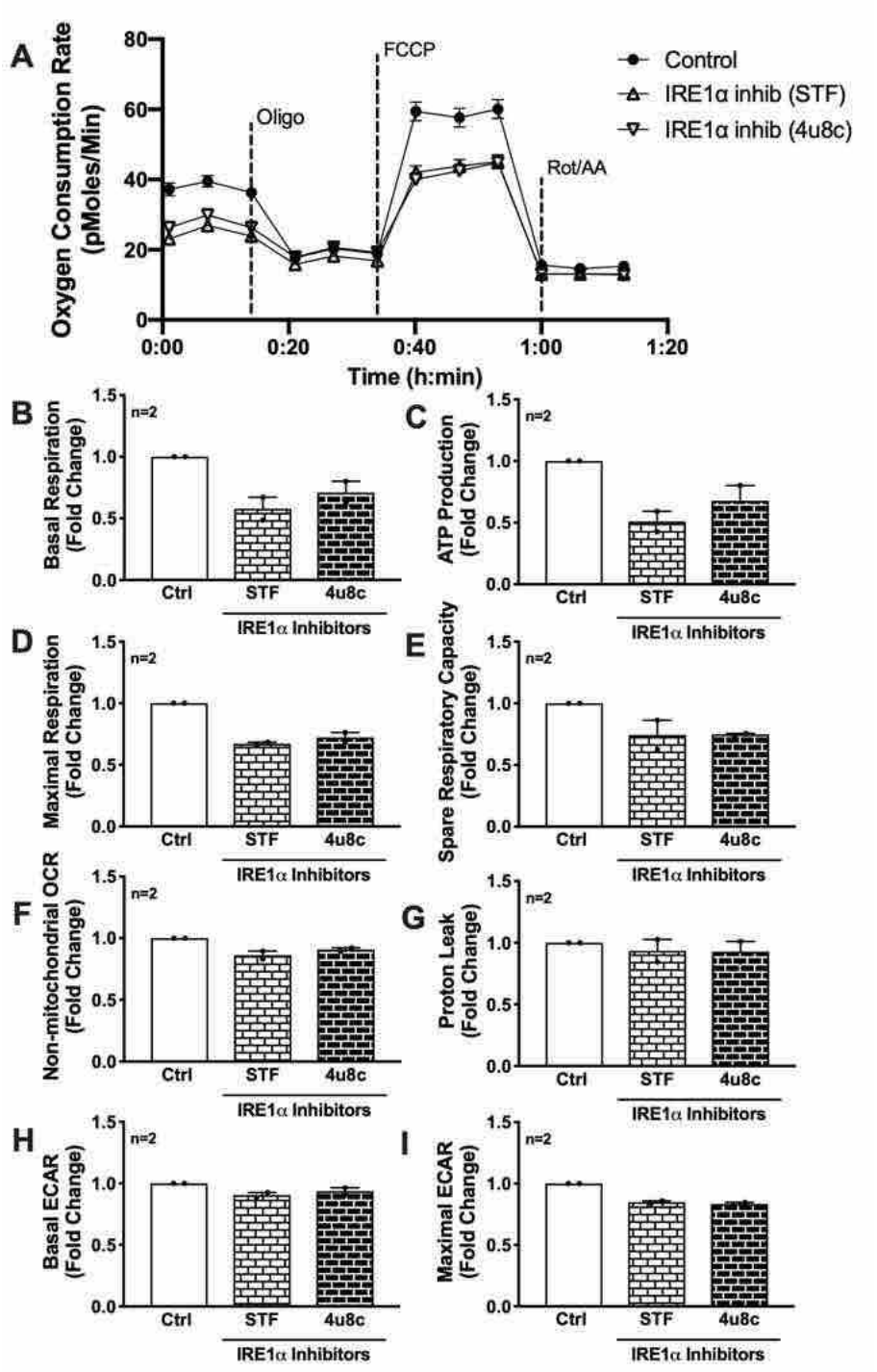

Supplementary Figure 3.3 Inhibition of IRE1α decreases astrocyte metabolic activity. (A-I) Astrocytes were treated with pharmacological inhibitors for IRE1α (STF-083010, 60 μM; 4μ8c, 50 μM) for 3 h prior to Seahorse Mito Stress Test. (A) Representative metabolic OCR profile

tracing from a single astrocyte donor. Compiled data from two separate biological donors quantifying fold changes in (B) basal respiration, (C) ATP production, (D) maximal respiration, (E) spare respiratory capacity, (F) non-mitochondrial OCR (G) proton leak (H) basal ECAR, and (I) maximal ECAR were graphed.

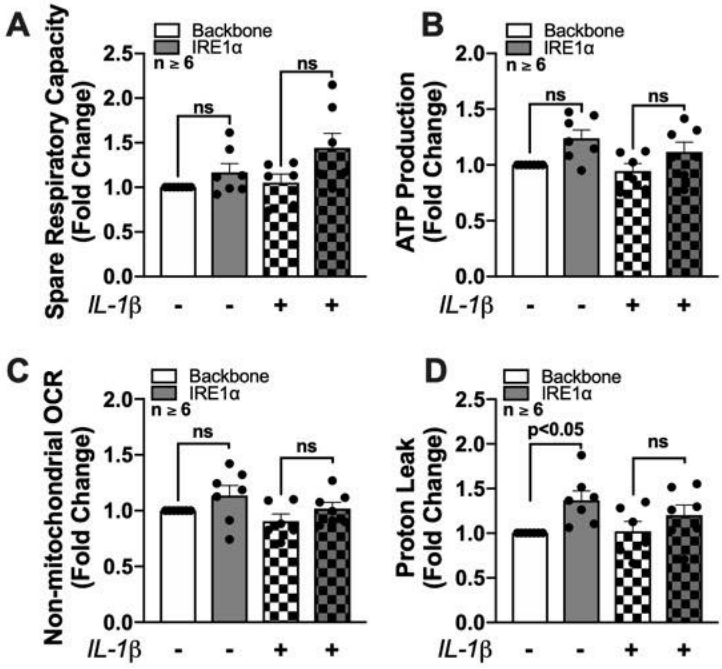

Supplementary Figure 3.4 IRE1α overexpression increases astrocyte metabolic activity. (A-D) Astrocytes were transfected with an IRE1α overexpression vector (gray bars) or backbone (white bars) and then treated with IL-1β for 24 h (checkered bars) prior to Seahorse Mito Stress Test assay. Compiled data from at least five separate biological donors quantifying fold changes in (A) spare respiratory capacity, (B) ATP production, (C) non-mitochondrial OCR, and (D) proton leak were graphed for statistical comparisons. Each dot on graphs represents a separate biological astrocyte donor. Significance was determined by one-way ANOVA and Tukey's post-hoc for multiple comparisons.

Table 3.1 Astrocyte IRE1α regulates ER stress, mitochondrial respiration, glycolysis, inflammation, and glutamate clearance.

IRE1α	**Activity**		**Over-expression**	**Overexpression + IL-1β**
	Inhibition	**IL-1β**		
ER Stress (BiP)	N/A	↑	-	↑↑
Mitochondrial Function (OCR)	↓	-	↑	↑
Glycolytic Activity (ECAR)	↓	-	-	↑↑
Inflammation (CCL2 & CXCL8)	N/A	↑	-	↑↑
Glutamate Clearance	N/A	↓	↑	-

CHAPTER 4

HIV-1 AND METHAMPHEATMINE COMORBIDITY IN PRIMARY HUMAN ASTROCYTES: TAARGETING ER/UPR DYSFUNCTION

AUTHOR

J. PROULX, I-W. PARK, & K. BORGMANN

PORTION IN PREPARATION FOR PUBLICATION AS:

Proulx J., Park I-W, & Borgmann K. HIV-1 and methamphetamine comorbidity in primary human astrocytes: TAARgeting ER/UPR dysfunction. *Journal of Neuroimmune Pharmacology*, 2022.

4.1 Abstract

Early during infection, human immunodeficiency virus 1 (HIV-1) can invade the central nervous system (CNS) and persist in the CNS for life despite effective antiretroviral treatment. Infection and activation of residential glial cells lead to low viral replication and chronic inflammation, which damage neurons contributing to a spectrum of HIV-associated neurocognitive disorders (HAND). Unfortunately, substance use, including methamphetamine (METH) is disproportionately elevated among people living with HIV-1. Thus, the National Institutes on Drug Abuse (NIDA) have declared HIV-1 and substance use comorbidity as a high research priority. Astrocytes are the most numerous glial cells in the CNS and provide essential support to neurons. During a neuropathological challenge, such as HAND or METH use disorders, astrocytes can shift their neurotrophic functions to become neurotoxic. Mitochondrial dysfunction and endoplasmic reticulum (ER)-associated signaling pathways, such as calcium and the unfolded protein response (UPR), are key mechanisms underlying HAND pathology and arise as potential targets to combat astrocyte dysfunction. Indeed, contact sites between ER and mitochondria, known as mitochondria-associated ER membranes (MAMs), are implicated in a number of neuropathologies. To investigate HIV-1/METH comorbidity on astrocyte ER-mitochondrial homeostasis, primary human astrocytes were infected with a pseudotyped HIV-1 model and exposed to low-dose METH for seven days. Chronic METH exposure increased astrocyte HIV-1 infection. Moreover, HIV-1/METH suppressed astrocyte antioxidant and metabolic capacity while increasing mitochondrial calcium load and protein expression of UPR/MAM mediators. We then tested a novel METH-binding receptor, trace amine-associated receptor 1 (TAAR1) as a potential upstream regulator to METH-induced UPR/MAM mediator expression as HIV-1 can increase TAAR1 expression, thus, could be a critical regulator of HIV-1/METH comorbidity in astrocytes.

Indeed, selective antagonism of TAAR1 significantly inhibited UPR/MAM protein expression. Altogether, our findings demonstrate HIV-1/METH-induced ER-mitochondrial dysfunction in astrocytes, whereas TAAR1 may be an upstream regulator for HIV-1/METH-mediated astrocyte dysfunction.

4.2 Introduction

Despite effective antiretroviral therapy (ART), approximately 50% of people living with HIV-1 (PLWH) develop some form of HIV-associated neurocognitive disorders (HAND) (Debalkie Animut et al. 2019; Nightingale et al. 2014; Simioni et al. 2010; Heaton et al. 2011; Zenebe et al. 2022). The primary pathology of HAND is mediated by persistent low levels of viral replication and chronic inflammation in the CNS leading to glial cell dysfunction and neuronal damage. The development and/or severity of HAND is further compounded by ART toxicity, socioeconomic factors, health comorbidities, and substance use disorders. Unfortunately, substance use, including methamphetamine (METH), is disproportionately elevated among PLWH. Thus, the National Institutes on Drug Abuse (NIDA) have declared HIV-1 and substance use comorbidity as a high research priority. The use of METH can induce neurotoxic and neurodegenerative consequences including increased blood brain barrier permeability, neuroinflammation, excitotoxicity, oxidative and endoplasmic reticulum (ER) stress, calcium dysregulation, and mitochondrial dysfunction (Salamanca et al. 2014; Krasnova and Cadet 2009; Cody and Vance 2016; MacDuffie et al. 2018; Soontornniyomkij et al. 2016), which can increase one's risk and severity of HAND.

Astrocytes are central mediators in both CNS homeostasis and neuroinflammation, implicating them in both HIV-1 and METH neuropathologies (Cisneros and Ghorpade 2012; Li et

al. 2019). In fact, astrocyte dysfunction is a hallmark of neurodegenerative pathologies (Wang and Ye 2021). By elucidating the intracellular mechanisms governing human astrocyte dysfunction during concomitant METH and HIV-1 exposure, better therapeutic targets can be identified to ameliorate astrocyte-associated neurotoxicity. It is well-established that the ER and mitochondria maintain constant communication, including direct contact sites termed mitochondria-associated ER membranes (MAMs) (Filadi, Theurey, and Pizzo 2017; Bravo et al. 2012). Prior studies of ER/mitochondrial cooperation have emphasized the ER as a regulator of mitochondrial function *via* calcium signaling and the unfolded protein response (UPR), especially under stress (Bravo et al. 2012; Lebeau et al. 2018; Rainbolt, Saunders, and Wiseman 2014; Vannuvel et al. 2013; Balsa et al. 2019; Proulx, Park, and Borgmann 2021; Proulx et al. 2022). Indeed, HIV-1 relevant stimuli or METH exposure can induce ER stress in astrocytes (Nooka and Ghorpade 2017; Fan and He 2016; Shah and Kumar 2016; Shah et al. 2016) as well as alter mitochondrial function, health, and/or morphology (Borgmann and Ghorpade 2017; Nooka and Ghorpade 2018; Borgmann and Ghorpade 2015).

The current report is focused on effects of low-dose chronic METH exposure on astrocyte HIV-1 infection and how HIV-1/METH comorbidity impacts the function and physiology of astrocyte ER and mitochondrial homeostasis. We then explore trace amine associated receptor 1 (TAAR1), a METH-binding receptor in astrocytes that is upregulated by HIV-1, as a potential upstream regulator of METH-mediated astrocyte ER/UPR dysfunction (Cisneros and Ghorpade 2014; Cisneros, Ghorpade, and Borgmann 2020).

4.3 Materials and Methods

Primary human astrocyte cultures: Brain tissues from first or second trimester were kindly provided by a biorepository at the University of Washington and in full compliance with local, federal, and National Institutes of Health (NIH) ethical guidelines. Written informed consent was obtained from all donors. Isolation and characterization of primary human astrocyte cultures are previously described (Borgmann and Ghorpade 2017; Gardner et al. 2006; You et al. 2020). Fresh and cryopreserved astrocyte cultures were used experimentally between passages two and seven. A total of 21 human astrocytes donors were isolated and evaluated for the present investigations. The biological sex and age of donors are illustrated in **Table 4.1**. Approximately six males and thirteen females were tested with two donors of unknown sex. All experiments were replicated in three or more astrocyte cultures isolated from biologically distinct biospecimens. Astrocytes were plated in T25 or T75 flasks at 3.33 or 10 million cells, respectively, or in 6-well plates at 2 million cells per well and allowed to adhere overnight, prior to treatment. Chronically treated astrocytes were passaged and replated at day 5 post treatment (48 h prior experimental assessment) for subsequent studies.

METH and EPPTB treatment: Astrocytes were treated with METH (cat # M8750, Sigma-Aldrich, St. Louis, MO, USA) for chronic experiments (50 nM; 7 d) and acute protein expression (5 μM; 8 h) or calcium signaling (250 μM; 5 min). Dose and time kinetics were determined based on the prolonged METH ranges (60 – 600 nM) and physiological peak (6 μM – 2 mM) found *in vivo* and our previous investigations (Won et al. 2001; Rivière, Gentry, and Owens 2000; Cisneros and Ghorpade 2014, 2012; Borgmann and Ghorpade 2015; Shah and Kumar 2016; Borgmann and Ghorpade 2017; Proulx et al. 2022). To inhibit METH-binding receptor, TAAR1, astrocytes were treated with N-(3-Ethoxy-phenyl)-4-pyrrolidin-1-yl-23-trifluoromethyl-benzamide (EPPTB, 5

μM, cat# 4518 Tocris-BioTechne, Minneapolis, MN) for 1 h prior to acute METH treatment. EPPTB is a cell permeable selective antagonist for TAAR1 (Stalder, Hoener, and Norcross 2011; Cisneros, Ghorpade, and Borgmann 2020)

Pseudotyped HIV-1: A pseudotyped HIV-1 model capable of astrocyte infection independent of the conventional CD4 receptor required for HIV-1 entry was constructed and characterized as previous described (Proulx et al. 2022). Briefly, human embryonic kidney (HEK) 293 T cells were co-transfected with HIV-1 infectious molecular clone (pNL4-3; cat # ARP-114, NIH HIV Reagent Program, Manassas, VA, USA, contributed by Dr. M. Martin) and p-human elongation-factor (pHEF)-vesicular stomatitis virus glycoprotein (VSVg; plasmid # 22501, Addgene, Watertown, MA, USA, a gift from Dr. Sergey Kasparov) by calcium phosphate precipitation per CalPhos Mammalian Transfection kit instructions (Clontech Laboratories, Inc., Mountain View, CA, USA) (Canki et al. 2001; Ojeda et al. 2018; Edara, Ghorpade, and Borgmann 2020; Proulx et al. 2022). The cells were incubated overnight, washed three times with PBS, and fresh culture media was added. Supernatants were collected 48 h post-wash, and progeny pseudotyped HIV-1 was quantified by reverse transcriptase (RT) activity *via* radiometric RT assay (Edara, Ghorpade, and Borgmann 2020). After RT quantification, astrocytes were infected with pseudotyped HIV-1 (500 RT) and remained in culture for a total of 7 d prior to experimental analyses. On day one post-infection, cells were washed three times with PBS and fresh media was added for the remaining days in culture. Confirmation and characterization of infection in primary human astrocytes was previously described **(Chapter 3; Figure 3.1)** based on HIV-1 DNA integration, detectable levels of viral protein expression, and minimal cytotoxicity to best mimic chronic *in vivo* HIV-1 astrocyte infection.

Reverse transcriptase (RT) activity: Supernatants from primary human astrocyte cultures were collected 7 d post-infection from the same wells used for protein assessment. Triplicate aliquots of 10 µl per viral sample were lysed with equal volume of dissociation buffer (100 mM Tris-HCl [pH 7.9], 300 mM KCl, 10 mM dithiothreitol [DTT], 0.1% NP-40) in a round-bottom-well plate and incubated at 37°C and 5% CO2 for 15 min. The level of reverse transcriptase was measeured in an enzymatic assay by adding 25 µl reaction buffer [50 mM Tris-HCl (pH 7.9), 150 mM KCl, 5 mM DTT, 0.05% NP-40, 15 mM MgCl2, 5 µl of 1 mg/ml poly(A)·(dT)15 (Roche, Indianapolis, IN), and 1 µCi/ml of [3H]dTTP tetrasodium salt (PerkinElmer, Inc., Waltham, MA)] Reactions incubated for 18 to 24 h at 37°C and 5% CO2. The reverse-transcribed cDNA was precipitated with 50 µl of ice-cold 10% trichloroacetic acid (TCA) for fifteen minutes before harvesting each sample. Precipitated DNA was transferred to a filter plate (MultiScreen 96-well harvest plates, catalog no. MAHFB1H60; Millipore, Burlington, MA) using a FilterMate harvester (PerkinElmer, Inc.), washed three times with 5% TCA and dehydrated with 95% ethanol. A MicroBeta2 scintillation counter (PerkinElmer, Inc.) was used to detect the level of 3H incorporation to quantify reverse transcriptase activity as a measure of RT protein concentration.

HIV-1 DNA integration assay: Astrocytes plated in 6-well plates at 1 million cells per well were collected using 0.05% Trypsin-EDTA (cat # T3924; Sigma-Aldrich) 7 d post treatment with or without METH (50 nM) and/or pseudotyped HIV-1 (500 RT). Astrocytes were washed with PBS prior to DNA isolation using QIAamp DNA Micro Kit per manufacturer's instructions (Qiagen, Germany). Successful integration of HIV-1 was determined by a nested, two-step PCR integration assay as previously described (Edara, Ghorpade, and Borgmann 2020; Proulx et al. 2022). HIV-1 lymphadenopathy-associated virus-infected 8E5 cells (8E5, cat # ARP-95, NIH HIV Reagent Program, contributed by Dr. Thomas Folks) were used as a positive control.

Protein expression via Simple Wes: Astrocytes treated with or without METH (50 nM) and/or pseudotyped HIV-1 (500 RT) were plated in 6-well plates at 2 million cells per well. Lysates were collected 7 d post treatment and protein expression was determined using Simple Wes per manufacturer's instructions and as previously described (Chapter 3). Targets included: ATF6 (clone D4Z8V, cat # 65880, Cell Signaling Technology; 1:50, ~115 kDa), binding immunoglobulin protein (BiP; clone C50B12, cat # 3177, Cell Signaling Technology, Danvers, MA, USA; 1:250, ~71 kDa), Drp1 (clone 4E11B11, cat # 14647, Cell Signaling Technology; 1:50, ~85 kDa), grp75 (cat # sc-133137, Santa Cruz Biotechnology; 1:50, ~67 kDa), HIV-1 negative factor protein (Nef; cat # ARP-3689, HIV Reagent Program, contributed by Dr. James Hoxie; 1:25, ~30 kDa), HIV-1 capsid protein (p24; cat # ab43037, Abcam, Cambridge, UK; 1:25, ~32 kDa), IRE1α (clone 14C10, cat # 3294, Cell Signaling Technology; 1:50, ~130 kDa), PERK (clone D11A8, cat # 5683, Cell Signaling Technology; 1:50, 170 kDa), SOD1 (cat # AF3418, Novus Biologicals; 1:200, 20 kDa), Sig1R (cat # NBP1-82479, Novus Biologicals; 1:50, 29 kDa), and vinculin (clone E1E9V, cat # 13901, Cell Signaling Technology; 1:20,000, ~117 kDa) Note: Molecular weights can shift in Simple Wes compared to classical western blot.

Chemokine expression: Supernatants from primary human astrocyte cultures were collected 7 d post-infection from the same wells used for protein assessment. Colorimetric enzyme-linked immunosorbent assays (ELISA) were performed according to the manufacturer's instructions to quantify C-C motif chemokine ligand 2 (CCL2) and C-X-C motif chemokine ligand 8 (CXCL8) secretion levels in culture supernatants (CCL2, cat # DCP00; CXCL8, cat # D8000C, R&D Systems) Protocol was standardized for primary human astrocytes as previously described (Edara, Ghorpade, and Borgmann 2020; You et al. 2020).

Mitochondria bioenergetics: Metabolic profiles were performed using Seahorse XFe96 analyzer technology per Seahorse XF Cell Mito Stress Test Kit User Guide instructions and as previously described (cat # 103015-100, Agilent Technologies, Santa Clara, CA, USA) (Prah et al. 2019; Chaphalkar et al. 2020; Proulx et al. 2022). Briefly, astrocytes treated with or without METH (50 nM) and/or pseudotyped HIV-1 (500 RT) for a *total* of 7 d were plated 48 h prior to Mito Stress Test in Seahorse 96-well plates at 25,000 – 30,000 cells per well. There was a minimum of 6 wells per condition for each biological donor. On the day of experiment, astrocyte media was exchanged with assay media 1 h before testing. During assay, consecutive injections of oligomycin (Oligo; 2 μM), carbonyl cyanide-4 (trifluoromethoxy) phenylhydrazone (FCCP; 2 μM), and rotenone/antimycin A (Rot/AA; 0.5 μM) were used to modulate components of the electron transport chain allowing assessment of key parameters of mitochondrial function. Data were collected using Wave V2.6.1.56 software and exported with Seahorse XF Cell Mito Stress Test Report Generator.

Mitochondrial calcium signaling: A green fluorescent calcium-measuring organelle-entrapped protein indicator for the mitochondria (pCMV-CEPIA2mt, plasmid # 58218, Addgene) was a gift from Masamitsu Iino (Suzuki et al. 2014). Chronic HIV-1 infected and/or METH treated astrocytes were transfected using the Amaxa P3 primary cell 96-well kit, nucleofector and shuttle attachment (cat # V4SP-3960, Lonza, Walkersville, MD, USA) per manufacturer's instructions with modification as previously published (Nooka and Ghorpade 2017). Briefly, 500 ng of plasmid DNA was transfected per 1.6 million astrocytes in 20 μL of nucleofection reagent. Astrocytes were plated at 150,000 cells per well in tissue culture treated, six channel μ-slides (0.4 VI, cat # 80606, ibidi, Madison, WI, USA) and allowed to recover for 48 h before downstream assessments. Each condition was performed in duplicate wells for each biological donor with a minimum of 15 cells

imaged per donor. Changes in calcium flux were imaged with a 40x objective at excitation of 450 – 490 nm and emission of 593 – 668 nm, using time series confocal microscopy *via* Carl Zeiss LSM 510 (Jena, Germany) (Nooka and Ghorpade 2017). Time-lapse micrographs were acquired every 500 msec for 4 min (480 cycles). Astrocytes were treated with control media, METH (250 μg/ml), histamine (100 μM), or ionomycin (10 μM) at 25 s (50 cycles). Analysis was performed using Fiji ImageJ software (Version: 2.0.0-rc-69/1.52i; National Institutes of Health, Bethesda, MD, USA). Individual cells were outlined and the change in fluorescence was calculated by: $\Delta F=(F-Fmin)/(Fmax-Fmin)$, where F is the fluorescence intensity at any given time; Fmin is the minimum fluorescence intensity recorded, and Fmax is the maximum fluorescence recorded. Calcium flux line tracings illustrate the ΔF at any given time point. Area under the curve (AUC) was calculated by the sum of ΔF following acute treatment (cycles 50-420).

Cytosolic calcium signaling: A circularly permutated green fluorescent protein (GFP) with a calmodulin tag was constructed as an ultrasensitive calcium sensor (GCaMP6s) and gifted from Dr. Douglas Kim (pGP-CMV-GCaMP6s, plasmid # 40753, Addgene) (Chen et al. 2013). Astrocytes were transfected with GCaMP6s using same nucleofection method as above. Briefly, 250 ng of plasmid DNA was transfected per 1.6 million astrocytes in 20 μL of nucleofection reagent. Astrocytes were plated at 100,000 cells per well in tissue culture treated, six channel μ-slides (0.4 VI, cat # 80606, ibidi, Madison, WI, USA) and allowed to recover for 48 h before downstream assessments. Each condition was performed in duplicate wells for each biological donor with a minimum of 20 cells imaged per donor. Changes in calcium flux were imaged with a 20x objective at excitation of 450 – 490 nm and emission of 593 – 668 nm, using time series confocal microscopy *via* Carl Zeiss LSM 510 (Jena, Germany) (Nooka and Ghorpade 2017). Time-lapse micrographs were acquired every 500 msec for 5 min. Astrocytes were treated with control

media or METH (250 μg/ml) at 10 s (20 cycles) then ionomycin (10 μM) at 225 s (450 cycles). Analysis was performed using Fiji ImageJ software (Version: 2.0.0-rc-69/1.52i; National Institutes of Health, Bethesda, MD, USA). Individual cells were outlined and the change in fluorescence was calculated by: $\Delta F=(F-F0)/(Fmax-F0)$, where F is the fluorescence intensity at any given time; F0 is the baseline (1 – 20 cycles) fluorescence intensity, and Fmax is the maximum fluorescence intensity when exposed to ionomycin (450 – 600 cycles). Calcium flux line tracings illustrate the ΔF at any given time point. Area under the curve (AUC) was calculated by the sum of ΔF between METH/media and ionomycin treatment (cycles 20 – 450).

Data analysis and interpretation: All experiments were performed in at least three separate biological donors. Data in graphs were analyzed and presented using GraphPad Prism (version 8.1.1, GraphPad Software, San Diego, CA, USA) as mean +/- standard error of the mean with replicates from each donor compiled and represented as a single dot on graphs. Paired two-tailed t-tests were performed for HIV-1 infection data to compare HIV-1 alone versus HIV-1/METH **(Figure 4.1A-B)**. All other statistics were determined *via* one-way ANOVA followed by Fisher's LSD test for multiple comparisons to account for variability across different biological donors. Significance was determined when $p < 0.05$.

4.4 Results

Previous reports on HIV-1/METH comorbidity demonstrate METH exposure can impair immune function and therapy efficacy while also enhancing viral replication and infectivity (Salamanca et al. 2014; Toussi et al. 2009; Liang et al. 2008; Basova et al. 2018; Passaro et al. 2015; Ellis et al. 2003; Colfax et al. 2007). To determine the consequences of METH exposure on astrocyte HIV-1 infection and inflammation, we developed and characterized a pseudotyped HIV-

1 model (500 RT) to infect astrocytes independent of the conventional CD4 receptor required for HIV-1 entry and in a manner representative of *in vivo* HIV-1 astrocyte infection, as previously described (Proulx et al. 2022). Moreover, to recapitulate the intermittent low levels of METH in the CNS between binges of a regular user, astrocytes were exposed to low dose METH (50 nM) for seven days (horizontal lines). Pseudotyped HIV-1 infection alone (vertical lines) or in combination METH exposure for seven days (checkered lines), revealed METH-induce increases in HIV-1 DNA integration **(Figure 4.1A**; 4-fold; $p < 0.05$**)** and expression of HIV-1 proteins **(Figure 4.1B)**, including p24 (10%; not significant), nef (40%; not significant) and reverse transcriptase (25%; $p < 0.05$). There was no effect on astrocyte inflammatory mediators, CCL2 **(Figure 4.1C)** or CXCL8 **(Figure 4.1D)** in our model for chronic METH exposure and/or HIV-1 infection. However, protein expression of superoxide dismutase 1 (SOD1), a key antioxidant produced by astrocytes to detoxify oxidative radicals in the CNS, was significantly decreased following seven days of METH exposure or HIV-1 infection, whether alone ($p < 0.05$) or in combination ($p < 0.001$) **(Figure 4.1E)**. Notably, these treatments did not alter changes in astrocyte cell growth **(Figure 4.1F)**.

Optimal mitochondrial function is required for astrocytes to provide essential metabolic and antioxidant support to neurons. To evaluate how HIV-1 infection with or without chronic METH exposure impacts astrocyte mitochondrial function, astrocytes were infected with pseudotyped HIV-1 (500 RT) and/or treated with METH (50 nM) for seven days prior to assessment *via* Seahorse XF Cell Mito Stress Test Profile **(Figure 4.2)**. The Cell Mito Stress Test measures real-time oxygen consumption rate (OCR) in response to an injection sequence of three electron transport chain (ETC) modulators permitting quantification of key parameters for mitochondrial function in cells. From calculated OCR readouts, the assay determines basal

respiration, maximal respiration, spare respiratory capacity, ATP-linked respiration, proton leak, and non-mitochondrial respiration. A thorough description for parameter calculations and their biological significances are illustrated in the previous chapter (Chapter 3). An OCR line tracing from a representative astrocyte donor graphed over time demonstrating primary human astrocytes have an elevated OCR overall after exposure to METH (50 nM) and/or infection with psuedotyped HIV-1 for seven days compared to untreated controls **(Figure 4.2A)**. Analysis mitochondrial OCR demonstrated METH exposure and HIV-1 infection, alone, increased basal respiration **(Figure 4.2B**; $p < 0.05$**)**, maximal respiration **(Figure 4.2C**; $p < 0.05$**)**, spare respiratory capacity **(Figure 4.2D**; $p < 0.05$**)**, ATP-linked respiration **(Figure 4.2E**; $p < 0.05$**)**, proton leak **(Figure 4.2F**; $p < 0.001$**)**, and non-mitochondrial respiration **(Figure 4.2G**; $p < 0.05$**)** coinciding with our previous report in Proulx et al., 2022 **(**Chapter 3; Figure 3.2**)**. Importantly, the combination of METH exposure with HIV-1 infection dysregulated METH- and HIV-1- induced increases in astrocyte respiratory activities. While maximal respiration **(Figure 4.2C**; $p < 0.05$**)**, spare respiratory capacity **(Figure 4.2D**; $p < 0.05$**)**, and proton leak **(Figure 4.2F**; $p < 0.001$**)** were all still significantly elevated during HIV-1/METH combination paradigms compared to control levels, there was no significant changes in basal respiration, ATP production, or non-mitochondrial OCR. In fact, exposure with METH in combination with HIV-1 infection significantly decreased basal respiration **(Figure 4.2B**; $p < 0.05$**)**, maximal respiration **(Figure 4.2C**; $p < 0.05$**)**, spare respiratory capacity **(Figure 4.2D**; $p < 0.05$**)**, ATP-linked respiration **(Figure 4.2E**; $p < 0.05$**)**, and non-mitochondrial respiration **(Figure 4.2G**; $p < 0.01$**)** when compared to HIV-1 infection alone. These findings suggest chronic METH may suppress astrocyte respiratory capacity during HIV-1 infection.

Mitochondrial respiration is regulated by mitochondrial calcium uptake (Huntington and Srinivasan 2021). To measure changes in astrocyte mitochondrial calcium flux following chronic METH exposure and/or HIV-1 infection, we utilized a genetically encoded calcium-measuring organelle-entrapped protein indicator targeted to the mitochondria and tagged with GFP (CEPIA2mt). Time series confocal analysis permitted real time fluorescent visualization of a single cell's mitochondrial calcium flux following stimulation with either control media, histamine (100 μM), or ionomycin (10 μM) **(Figure 4.3A)**. Changes in fluorescence were graphed over time **(Figure 4.3B; Supp. Figure 4.1)**. To illustrate differences in astrocyte mitochonidrial calcium responses across acute treatments and chronic conditions, five individual cellular responses were graphed per condition from a representative donor **(Supp. Figure 4.1)**. The area under the curve (AUC), following stimulation with either media, histamine (100 μM), or ionomycin (10 μM), was then graphed for statistical comparisons **(Figure 4.3C-D)**. In control (no pretreatment) astrocytes, histamine (100 μM) stimulation induces mitochondrial calcium influx ($p < 0.01$) **(Figure 4.3C**; light grey bars**)**. However, astrocyte pretreated with 7 d METH and/or HIV-1 infection no longer significantly respond to histamine. In fact, chronic treatments significantly elevated basal mitochondrial calcium to levels equivalent to those induced by histamine-stimulation ($p < 0.01$). The inability of chronic HIV-1/METH in astrocytes to respond to histamine suggests a dysregulated mitochondrial phenotype, where they are no longer able to internalize calcium or are at max capacity. Interestingly, chronic HIV-1/METH treated astrocytes stimulated with ionomycin **(Figure 4.3D**; dark grey bars**)**, have a significant decrease in mitochondrial calcium load compared to their respective chronic control paradigms ($p < 0.05$; clear bars). Decreases in calcium flux were accompanied by an increased visualization of apoptotic bleb formation **(Figure 4.3E)**, suggesting a mitochondrial calcium-driven hypersensitivity to ionomycin-induced apoptosis. Quantification

of apoptotic bleb formation particularly trended with chronic METH paradigms; however, these findings were not statistically significant due to high donor variability **(Figure 4.3F)**.

Contact and communication between the ER and mitochondria are essential for regulating mitochondrial dynamics, bioenergetics, and apoptotic signaling (Zhang et al. 2021; Proulx, Park, and Borgmann 2021). Thus, we wanted to investigate changes in MAM-associated proteins in astrocytes following 7 d METH exposure and/or HIV-1 infection using Simple Wes **(Figure 4.4)**. Briefly, mitochondrial fission protein, Drp1, has been implicated as a potential target in HAND pathology **(Chapter 2)** (Proulx, Park, and Borgmann 2021); however, these investigations were geared towards neurons and had contradictory findings. MFN2 is a mitochondrial fusion protein and has been highlighted as a key regulator of MAM tethering through interaction with UPR protein PERK; however, whether MFN2 positively or negatively regulates MAM tethering remains controversial (Chapter 2)(Proulx, Park, and Borgmann 2021). Coinciding with a potential interplay in HAND, Drp1 levels were significantly upregulated following HIV-1 infection **(Figure 4.4A**; $p < 0.05$**)**. Interestingly, when in combination with METH exposure, Drp1 levels were significantly decreased ($p < 0.05$). MFN2 levels followed similar trends, although not significant **(Figure 4.4B)**. Next, we evaluated expression changes of key proteins involved in MAM-mediated calcium transfer Sig1R **(Figure 4.4C)** and grp75 **(***a.k.a.* mortalin; **Figure 4.4D)**, both of which have been implicated as potential therapeutic targets for METH- or HIV-1- induced astrocyte dysfunction, respectively (Zhang et al. 2015; Priyanka et al. 2020). HIV-1 infection alone and in combination with METH significantly upregulated Sig1R expression **(Figure 4.4C**; $p < 0.05$, $p < 0.01$, respectively**)**. Similarly, grp75 expression was significantly upregulated following METH exposure alone **(Figure 4.4D**; $p < 0.05$**)** and when in combination with HIV-1 infection ($p < 0.01$). Finally, the three UPR arms also arise as potential regulators of astrocyte-mediated neurotoxicity

(Nooka and Ghorpade 2017; Fan and He 2016; Natarajaseenivasan et al. 2018; Shah et al. 2016; Nooka and Ghorpade 2018) and are now increasingly considered integral mediators within the MAM proteome beyond their classical UPR/ER stress functions (van Vliet and Agostinis 2016, 2018; Saito and Imaizumi 2018; Malli and Graier 2019). Following 7 d HIV-1 infection combined with METH exposure, protein expression of the classical ER stress negative regulating binding partner, BiP, was significantly decreased **(Figure 4.4E**; $p < 0.05$**)**. Of the three UPR arms, ATF6 **(Figure 4.4F)**, IRE1α **(Figure 4.4G)**, and PERK **(Figure 4.4H)**, HIV-1/METH in combination significantly increased expression of IRE1α ($p < 0.01$) and PERK ($p < 0.05$). Altogether, these findings demonstrate a disruption in astrocyte mitochondrial dynamic proteins with an augmented UPR/MAM mediator expression following HIV-1/METH comorbidity.

The prospect of targeting ER stress and the three UPR arms to combat neurodegeneration has been widely explored (Ghemrawi and Khair 2020). Indeed, our previous studies highlighted UPR arm, IRE1α, as a potential therapeutic target to combat astrocyte dysfunction during METH exposure or HIV-1 infection (Proulx et al.). However, the multifunctional complexity of the distinct arms and their disparate induction may make them difficult targets for therapeutic application. It is important to note variation across different biological astrocyte donors, especially in changes in UPR expression, which rely heavily on temporal induction. Our previous studies highlighted disparate induction between acute versus chronic exposure (Proulx 2022). Here, we uncover a disparate and unique time-dependent induction of selected UPR/MAM proteins, including BiP, ATF6, IRE1a, PERK, and MFN2 following acute METH exposure across four different primary human astrocyte cultures **(Supp. Figure 4.2A-D)**. For example, while all donors demonstrated similar trends with concurrent peaks in the protein expression of ATF6, IRE1a, PERK, and MFN2, these peaks uniquely occurred at different timepoints, 1, 3, 8 or 24 h,

respectively. Thus, identifying an upstream regulator of UPR/MAM dysfunction could provide a favorable avenue for therapeutic intervention. Our lab previously delineated trace amine associated receptor 1 (TAAR1) as a novel METH-binding receptor in astrocytes and as an upstream regulator of astrocyte-mediated excitotoxicity during METH exposure (Cisneros and Ghorpade 2014; Cisneros, Ghorpade, and Borgmann 2020). Additionally, TAAR1 expression is significantly elevated by HIV-1 and inflammation implicating a fundamental role for TAAR1 during HAND/METH comorbidity (Cisneros and Ghorpade 2014; Cisneros, Ghorpade, and Borgmann 2020). Following the current model of pseudotyped HIV-1 infection in astrocytes, we confirmed a HIV-1 dose-dependent upregulation in TAAR1 mRNA expression **(Figure 4.5A)**. To examine TAAR1 regulation on acute METH-induced intracellular calcium flux and UPR/MAM induction, astrocytes were pretreated with the selective TAAR1 antagonist, EPPTB (5 μM; orange bars) for 1 hour prior to acute METH stimulation (horizontal lines) for cytosolic calcium signaling (250 μM; ~5 min) **(Figure 4.5B)** or protein assessment (5 μM; 8 h) **(Figure 4.5C-F)**. Changes in astrocyte intracellular calcium flux, was measured using a genetically modified GFP cytosolic calcium sensor (GCaMP6s) followed by time series confocal analysis **(Figure 4.5B)** (Chen et al. 2013; Nooka and Ghorpade 2017). Acute stimulation of naïve astrocytes with METH (250 μM; ~5 min) significantly increased intracellular calcium flux ($p < 0.001$). Importantly, METH-induced calcium flux was suppressed when astrocytes were pretreated with EPPTB ($p < 0.05$). Similarly, METH-induced protein expression of MFN2 **(Figure 4.5C**; $p < 0.05$**)**, ATF6 **(Figure 4.5D**; $p < 0.05$**)**, IRE1α **(Figure 4.5E**; $p < 0.001$**)**, and PERK **(Figure 4.5F**; $p < 0.01$**)** were also significantly suppressed by EPPTB pretreatment compared to METH treatment alone (5 μM; 8 h). Together these data implicate astrocyte TAAR1 as an upstream regulator and potential therapeutic target for METH-induced UPR/MAM stress responses.

4.5 Discussion

HIV-1 or METH can induce astrocyte activation, which has been characterized by an increased metabolic (Natarajaseenivasan et al. 2018; Swinton et al. ; Borgmann and Ghorpade 2017; Proulx et al. 2022) and/or inflammatory profile (Shah et al. 2012; Natarajaseenivasan et al. 2018). Chronic astrocyte activation during conditions like HAND and METH use disorders can lead to astrocyte dysfunction and contribute to neurotoxic consequences. For example, astrocytes decrease provision of essential neurotrophic factors, including metabolite and antioxidant support (Natarajaseenivasan et al. 2018), while also increasing release of neurotoxic factors including excessive ATP (Fatima et al. 2017; Priyanka et al. 2020), toxic radicals (Natarajaseenivasan et al. 2018; Priyanka et al. 2020), and inflammatory cytokines (Shah et al. 2012; Natarajaseenivasan et al. 2018).

The present report investigated the combined effects of HIV-1/METH comorbidity on astrocyte infection and physiology. These results are summarized in **Table 4.2**. Low-dose chronic METH exposure enhanced HIV-1 DNA integration and HIV-1 protein expression. HIV-1 infection with or without chronic METH exposure had no impact on astrocyte inflammatory profile; however, astrocyte antioxidant capacity was significantly impaired by METH and HIV-1 infection, alone and in combination **(Figure 4.1)**. Treated alone, chronic METH exposure or HIV-1 infection significantly increased astrocyte mitochondrial respiration **(Figure 3.2 & Figure 4.2)**. Astrocyte mitochondrial dysfunction may threaten the ability of astrocytes to provide essential metabolic and antioxidant support to neurons and could also contribute to the release of toxic reactive oxygen and nitrogen species (ROS/RNS) to propagate oxidative stress. Interestingly, chronic METH exposure in combination with HIV-1 infection deceptively appears to restore basal, maximal, and spare respiratory capacity compared to untreated control astrocytes **(Figure 4.2)**. Likewise, HIV-

1-induced expression of mitochondrial fission (Drp1) and fusion (MFN2) proteins were similarly suppressed following chronic METH exposure **(Figure 4.4)**. Decreased expression of mitochondrial Drp1 has previously coincided with increased HIV-associated neurocognitive decline in the cortex of HIV+ brain tissues and astrocyte-restricted HIV-1 gp120 transgenic mice (Fields et al. 2016). Interestingly, overexpressing Drp1 reversed gp120-meditated neuronal mitochondrial dysfunction reducing both neuroinflammation and neurodegeneration. Decreased Drp1 and MFN2 expression has also been evident in T cells following exposure to HIV-1 Vpr protein. These changes coincided with impaired ER-mitochondrial interaction and morphology and induced mitochondrial depolarization and deformation. Overexpressing MFN2 or Drp1 was able to prevent T cell mitochondrial depolarization and deformation (Huang et al. 2012).

It is important to note that changes in mitochondrial respiration and dynamics are not a fully inclusive reflection of astrocyte mitochondrial health. For instance, changes in mitochondrial respiration and dynamics may not translate to neuroprotective outcomes (*i.e.,* production and release of metabolites and antioxidants). Coupling the current data with decreased SOD1 levels **(Figure 4.1)**, suppressed ATP production with persistent proton leak **(Figure 4.2)**, and increased basal mitochondrial calcium load **(Figure 4.3)**, indicate astrocyte mitochondrial dysfunction during HIV-1/METH comorbidity. Whether manipulation of MFN2 or Drp1 can optimize astrocyte mitochondrial function to promote astrocyte neuroprotective phenotypes and combat astrocyte-associated neurotoxic consequences requires additional investigations. Another consideration is the potential interplay of astrocyte mitochondria in HIV-1 immunity. Mitochondria are essential regulators of innate immunity and inflammation during an intracellular infection, as previously reviewed (Jin et al. 2017; Bahat, MacVicar, and Langer 2021). For example, mitochondrial-derived DNA (mtDNA) and reactive oxygen species (mtROS) can

activate innate immune sensors to promote the production of proinflammatory cytokines, type I interferons, and inflammasome formation. Moreover, mitochondrial have their own innate immune sensors on the outer mitochondrial membrane termed the mitochondrial antiviral signaling (MAVS) protein, which is activated by cytoplasmic viral RNA. Indeed, viruses and bacteria often modulate mitochondrial function and dynamics as a mechanism to evade host defenses (Elesela and Lukacs 2021; Tiku, Tan, and Dikic 2020). While the mechanism remains unclear, METH exposure can modulate inflammation and immunity leading to increased susceptibility to infections and exacerbated inflammation-related pathogenesis (Papageorgiou et al. 2019; Salamanca et al. 2014). Here, chronic METH exposure increased HIV-1 DNA integration and protein expression **(Figure 4.1)**. Thus, METH-induced dysregulation on astrocyte mitochondrial respiration and dynamics could also be suppressing mitochondrial-mediated HIV-1 immunity in astrocytes.

Mitochondrial bioenergetics, dynamics, and integrity are regulated by the MAM interface. ER-associated messengers, including calcium and the UPR sensors, are highlighted as potential therapeutic targets to combat mitochondrial dysfunction (Proulx, Park, and Borgmann 2021; Proulx et al. 2022). Here, two key regulators of MAM-mediated calcium transfer, grp75 and Sig1R, were significantly upregulated following HIV-1/METH comorbidity in astrocytes. Briefly, the transfer of calcium from the ER to mitochondria is facilitated by inositol 1,4,5-triphosphate receptors (IP_3R) on the ER membrane, voltage-dependent anion-selective channel (VDAC) on the outer mitochondrial membrane, and cytosolic grp75, which stabilizes IP_3R and VDAC association within the MAM interface. On the ER membrane side of the interface, Sig1R promotes calcium transfer by associating with IP_3R (Hayashi and Su 2007). In previous works, overexpression of grp75 in astrocytes expressing HIV-1 Tat was able to prevent astrocyte mitochondrial dysfunction

and fragmentation and protect neurons from astrocyte-mediated neurotoxicity by reducing the release of excess ATP, inflammatory cytokines, and extracellular glutamate (Priyanka et al. 2020). Moreover, blocking ER-mitochondrial calcium transfer *via* VDAC (Fatima et al. 2017) or mitochondrial calcium uniporter on the inner mitochondrial membrane (Natarajaseenivasan et al. 2018) restores astrocyte neurotrophic phenotypes. These studies emphasize the therapeutic application of MAM-mediated calcium transfer to combat astrocyte-mediated neurotoxicity during HAND/METH.

Targeting Sig1R has also been proposed to combat both MAM dysfunction and neuroinflammation in neurological diseases (Hedskog et al. 2013; Al-Saif, Al-Mohanna, and Bohlega 2011; Bernard-Marissal et al. 2015; Weng, Tsai, and Su 2017; Bernard-Marissal et al. 2019; Rosen et al. 2019; Jia et al. 2018); however, these studies are predominately in neurons or whole brain tissues. Astrocyte Sig1R has primarily been explored in the context astrogliosis and the production of brain-derived neurotrophic factor (BDNF) (Jia et al. 2018). Notably, Sig1R is one of two identified METH-binding receptors in astrocytes and is implicated as a regulator of METH-mediated astrocyte activation (Zhang et al. 2015; Robson et al. 2014). Interestingly, Sig1R was recently identified as a key modulator in HIV-1/METH comorbidity in CD4+ T cell activation and infection (Prasad et al. 2019). Here, astrocyte Sig1R was upregulated during both HIV-1 infection alone and HIV-1/METH comorbidity. Thus, additional studies are needed to evaluate Sig1R as a METH-binding receptor for HIV-1/METH-mediated astrocyte dysfunction.

Our previous works in Chapter 3, explored the UPR arms as potential regulators of astrocyte mitochondrial respiration using pharmacological inhibition **(Figure 3.4)**. While inhibition of PERK significantly reduced spare respiratory capacity, IRE1α inhibitors significantly decreased basal respiration, ATP production, maximal respiration, spare respiratory capacity, and

non-mitochondrial OCR. Further exploration of IRE1α using an overexpression plasmid, revealed that IRE1α regulates multiple aspects of astrocyte function including ER stress, mitochondrial respiration, glycolysis, inflammation, and glutamate clearance. Interestingly, signaling *via* IRE1α and/or Sig1R has been emphasized as a potential therapeutic target for dysfunctional immune and inflammatory pathologies (Rosen et al. 2019). Here, HIV-1/METH co-exposure significantly increased astrocyte UPR protein expression of IRE1α and PERK. Notably, these protein levels were amplified above either METH or HIV-1 alone, demonstrating a synergistic UPR upregulation following HIV-1/METH in astrocytes. Beyond their classical UPR function, IRE1α has recently been implicated in ER-mitochondrial calcium transfer, mitochondrial respiration and redox homeostasis through associations with IP_3R (Son et al. 2014; Carreras-Sureda et al. 2019) and/or Sig1R (Mori et al. 2013). Meanwhile, PERK is proposed as a key regulator of MAM tethering through direct interaction with MFN2 and is also linked to regulating mitochondrial dynamics and bioenergetics (Verfaillie et al. 2012; van Vliet and Agostinis 2016; Lebeau et al. 2018; Rainbolt, Saunders, and Wiseman 2014; Balsa et al. 2019; Munoz et al. 2013). Notably, MFN2 is one of the most researched proteins involved in MAM tethering. However, whether MFN2 positively or negatively regulates MAM tethering remains controversial across differing conditions and cell types (de Brito and Scorrano 2008; Filadi et al. 2015; Janikiewicz et al. 2018; Moltedo, Remondelli, and Amodio 2019; Leal and Martins 2021).

As mentioned above, two METH-binding receptors have been identified in astrocytes, Sig1R and TAAR1. Notably, both astrocyte Sig1R and TAAR1 are upregulated by HIV-1 or inflammatory stimuli, indicating that astrocytes may be especially sensitive to HIV-1/METH comorbidity. TAAR1 regulates excitatory amino acid transporter 2 expression and glutamate uptake during HIV-1/METH comorbidity, highlighting TAAR1 as a novel regulator of astrocyte-

mediated excitotoxicity (Cisneros and Ghorpade 2014; Cisneros, Ghorpade, and Borgmann 2020). Therefore, we evaluated TAAR1 as a target for METH-mediated calcium dysregulation and UPR/MAM induction. Indeed, selective inhibition of TAAR1 significantly blocked acute METH-induced intracellular calcium flux and UPR/MAM protein expression **(Figure 4.5)**.

Altogether, these findings demonstrate HIV-1/METH-induced ER-mitochondrial dysfunction in astrocytes, and astrocyte TAAR1 may be an upstream regulator for HIV-1/METH-mediated UPR/MAM dysfunction. Additional studies are needed to evaluate the role of TAAR1 on astrocyte ER-mitochondrial function and physiology, including the interplay of mitochondrial dynamics (Drp1) and MAM-mediated calcium transfer (grp75 and Sig1R). The potential therapeutic targeting of TAAR1 to modulate ER-associated signaling pathways, including UPR and calcium, may provide a novel mechanism to combat astrocyte dysfunction during HIV-1/METH neuropathology.

4.6 Figures and Tables

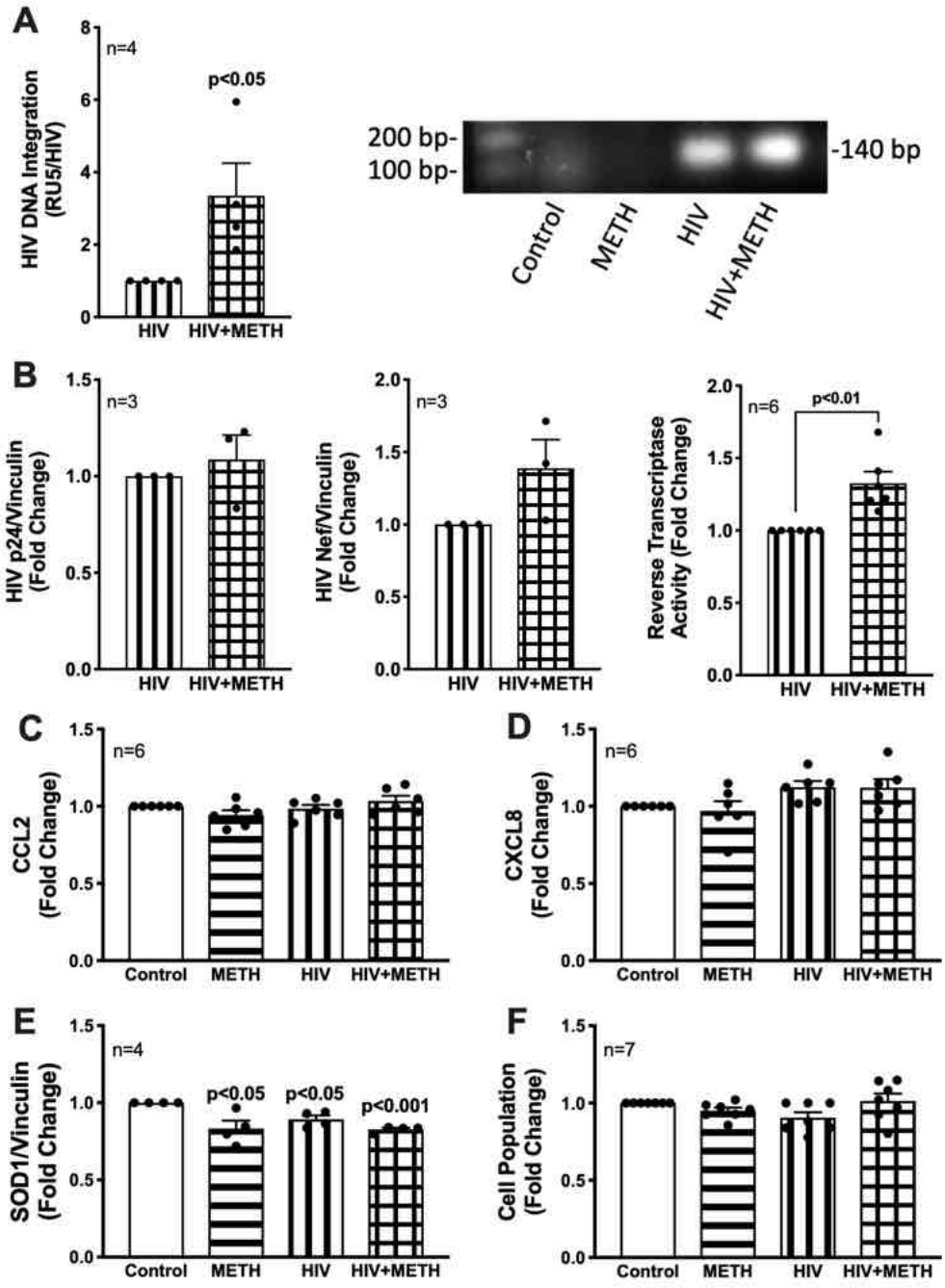

Figure 4.1 METH exposure increases astrocyte HIV-1 infection and HIV/METH impair astrocyte antioxidant support. Astrocytes were treated with METH (50 nM; horizontal lines), infected with pseudotyped HIV-1 (500 RT; vertical lines), or co-treated with METH and pseudotyped HIV-1 (checkered lines) for seven days. (A) HIV-1 DNA integration was detected

using a two-step Alu-Gag PCR assay. The amplified HIV-1 RU5 specific regions were quantified by RTPCR prior to agarose DNA gel electroporation. (B) Detection of HIV-1 proteins p24 or Nef in astrocyte lysates were measured using Simple Wes while expression of reverse transcriptase (RT) was measured *via* radiometric RT activity assay. Vinculin was used as an internal control for lysates. (C) CCL2 and (D) CXCL8 levels in supernatants were assessed by ELISA. (E) Protein expression of SOD1 was measured *via* Simple Wes. (F) Cell populations were counted at 5 d passages prior to plating for other assays. Fold changes for DNA integration and HIV-1 proteins were calculated to HIV-1 and statistical significance was determined *via* two-tailed paired t test. Fold changes for CCL2, CXCL8, SOD1 protein and cell number levels were calculated to control, and statistical significance was determined *via* one-way ANOVA followed by Fisher's LSD test for multiple comparisons. Experiments were performed in a minimum of three distinct human astrocyte cultures, each represented by a dot in bar graphs (n).

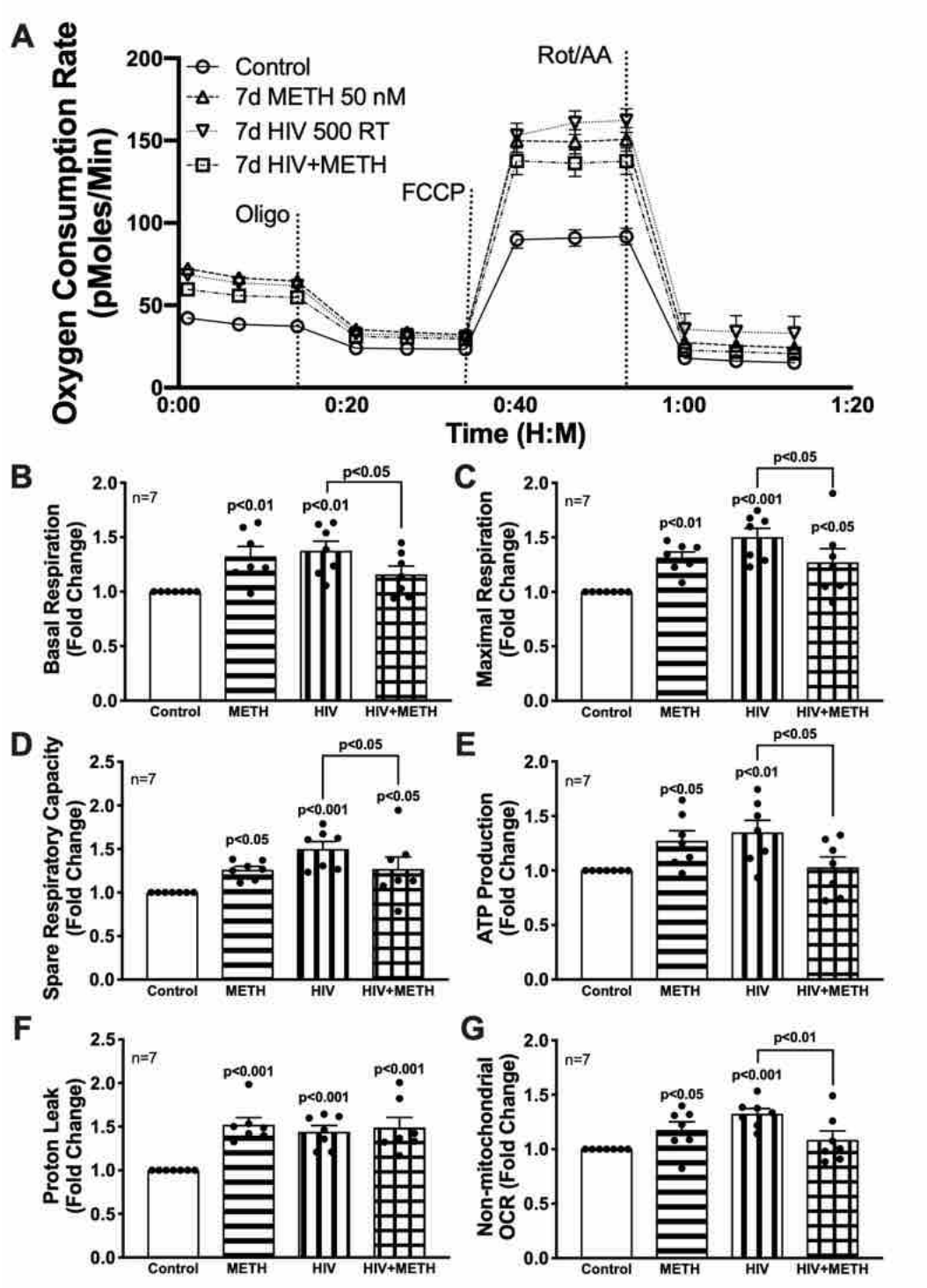

Figure 4.2 METH exposure and HIV-1 infection increase astrocyte respiration, which is dysregulated by HIV-1/METH comorbidity. Astrocytes were treated with or without METH (50 nM) and/or infected with pseudotyped HIV-1 (500 RT) for 7 d prior to Seahorse Mito Stress

Test for metabolic assessment. Representative (A) OCR profile tracings from a representative astrocyte donor were graphed over time. Compiled data from seven separate biological donors quantifying fold changes in (B) basal respiration, (C) maximal respiration, (D) spare respiratory capacity, (E) ATP production, (F) proton leak and (G) non-mitochondrial OCR were graphed for statistical comparisons. Statistical significance was determined *via* one-way ANOVA followed by Fisher's LSD test for multiple comparisons. Each dot on bar graphs represents the averaged data from a minimum of six replicates from a single biological astrocyte donor (n).

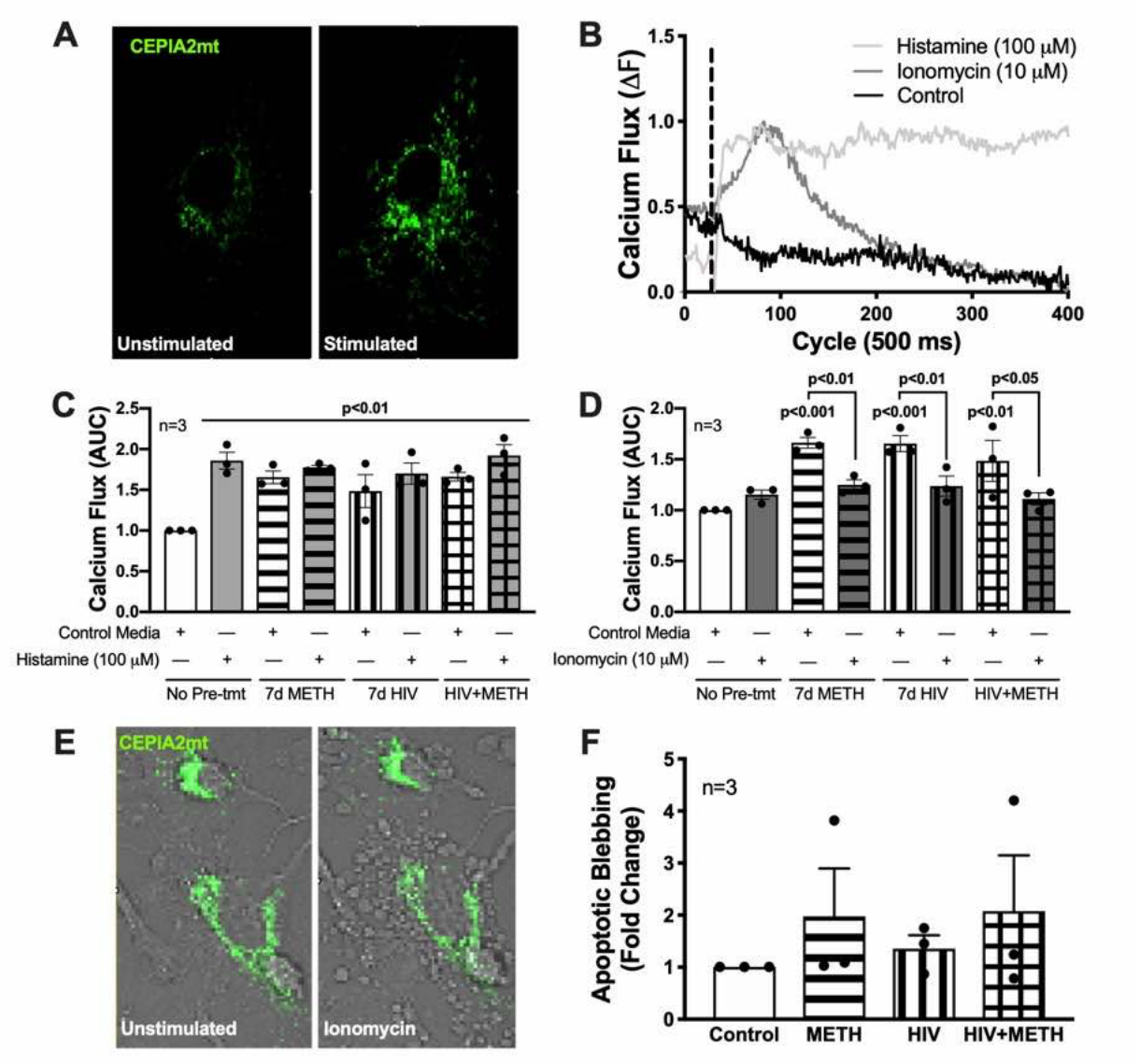

Figure 4.3 METH exposure and HIV-1 infection alone or in combination increase basal mitochondrial calcium flux. Astrocytes were treated with or without METH (50 nM) and/or infected with pseudotyped HIV-1 (500 RT) for 7 d prior to mitochondrial calcium imaging. Astrocytes were transfected with the calcium-measuring organelle-entrapped protein indicator targeted to the mitochondria and tagged with GFP (CEPIA2mt) reporter plasmid 48 h prior to calcium flux analysis. (A) Time series confocal imaging was used to measure changes in fluorescence following stimulation with media, histamine (100 μM), or ionomycin (10 μM). (B) Line tracings represents a single naïve astrocyte calcium flux response to acute media, histamine

(100 μM), or ionomycin (10 μM) at 50 cycles (25 sec). (C-D) Area under the curve (AUC) was calculated changes in fluorescence following treatment at 50 cycles (25 sec) up to cycle 420 and graphed as fold changes to control. (E) Representative astrocyte showing apoptotic blebbing following chronic HIV/METH and acute ionomycin treatment. (F) Compiled quantification of astrocyte blebbing for 7 d pre-treatment conditions following acute ionomycin treatment. Individual dots represent compiled data from a minimum of 15 cells per biological astrocyte donor (n) graphed as fold changes. One-way ANOVA was performed for statistical analysis followed by Fisher's LSD test for stand-alone comparisons to account for variation across different biological donors.

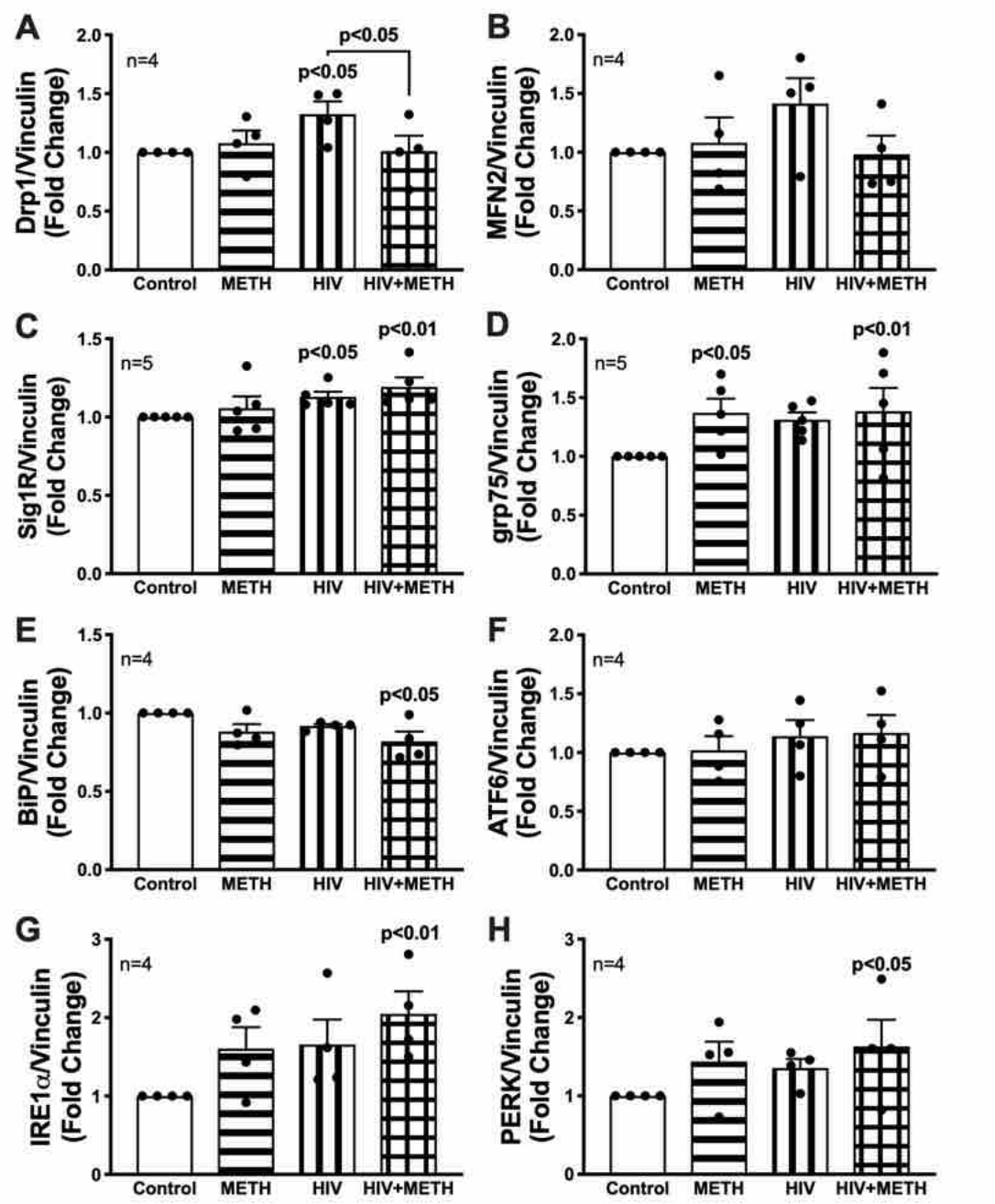

Figure 4.4 Chronic METH exposure and HIV-1 infection alone or in combination alter UPR/MAM-associated protein expression in astrocytes. Astrocytes were treated with or without METH (50 nM) and/or infected with pseudotyped HIV-1 (500 RT) for 7 d prior to lysate collection. Protein expression of (A) Drp1, (B) MFN2, (C) Sig1R, (D) grp75, (E) BiP, (F) ATF6, (G) IRE1α, and (H) PERK was measured *via* Simple Wes. Individual dots on bar graphs represent

fold changes to for separate biological donors (n) normalized to vinculin as an internal control. Statistical significance was determined *via* one-way ANOVA followed by Fisher's LSD test for multiple comparisons.

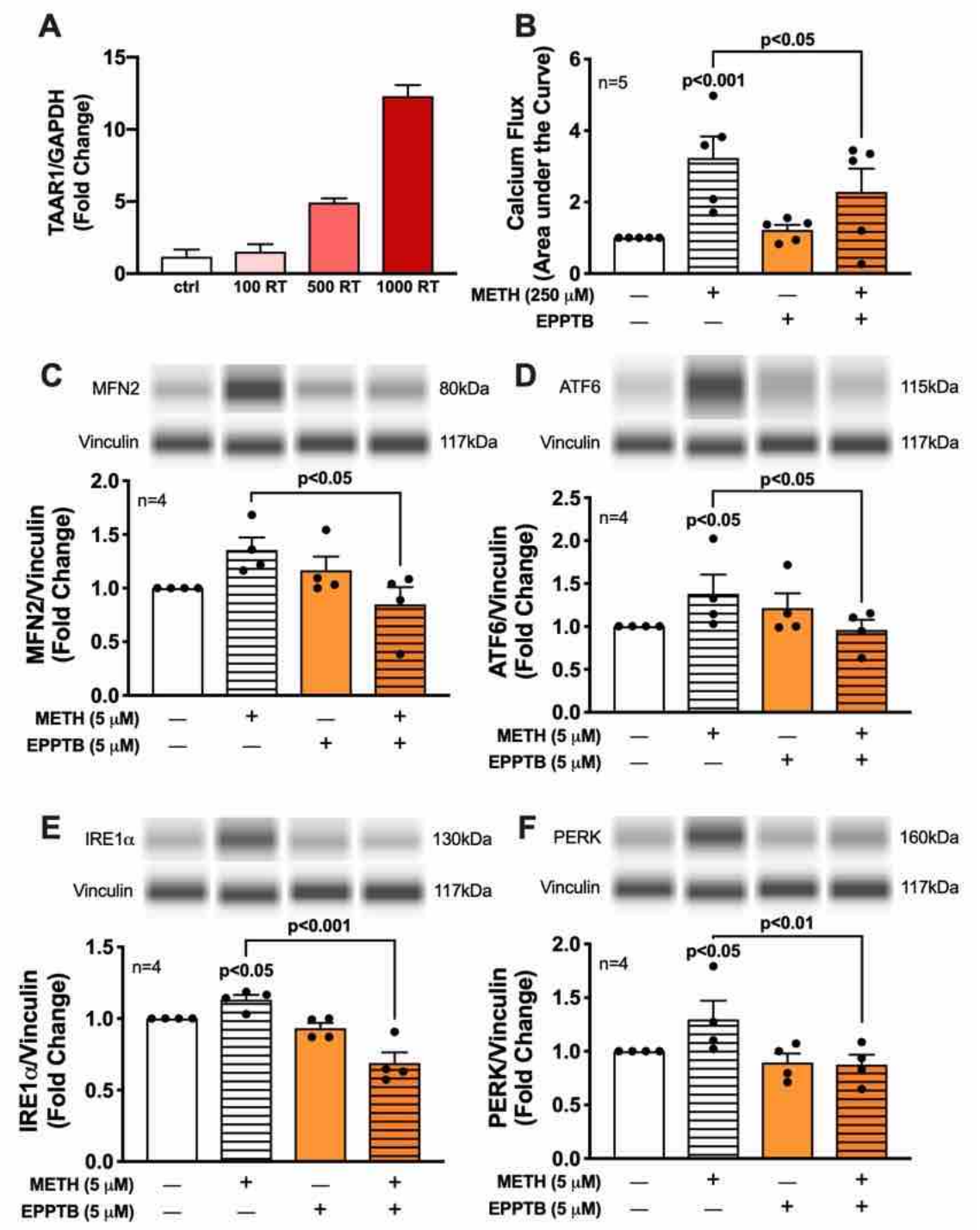

Figure 4.5 Astrocyte TAAR1 regulates METH-induced calcium flux and UPR/MAM mediator expression. (A) Astrocyte TAAR1 RNA expression was measured by RTPCR following infection with pseudotyped HIV-1 (100 – 1000 RT) for 7 d. GAPDH was used as an

internal control. Data from a representative donor is graphed. (B) For calcium flux analysis, naïve astrocytes were transfected with the cytosolic GFP-calmodulin calcium sensor (GCaMP6s) for 48 h prior to time series confocal imaging. Astrocyte cultures were exposed to EPPTB (5 μM), a TAAR1 selective antagonist, for 1 h prior to imaging. Area under the curve was calculated from changes in fluorescence following treatment with control media or METH (250 μM). Individual dots represent the average AUC from a minimum of 20 cells per biological donor and were graphed as fold changes. (C-F) Astrocyte TAAR1 was inhibited by pretreatment with EPPTB (5 μM) for 1 h followed by acute METH (5 μM) stimulation for 8 h. Protein expression of (C) MFN2, (D) ATF6, (E) IRE1α, and (F) PERK was measured *via* Simple Wes and normalized to vinculin as an internal control. Individual dots on graphs represent fold changes for separate biological donors (n). Statistical significance was determined *via* one-way ANOVA followed by Fisher's LSD test for stand-alone comparisons to account for variation across different biological donors.

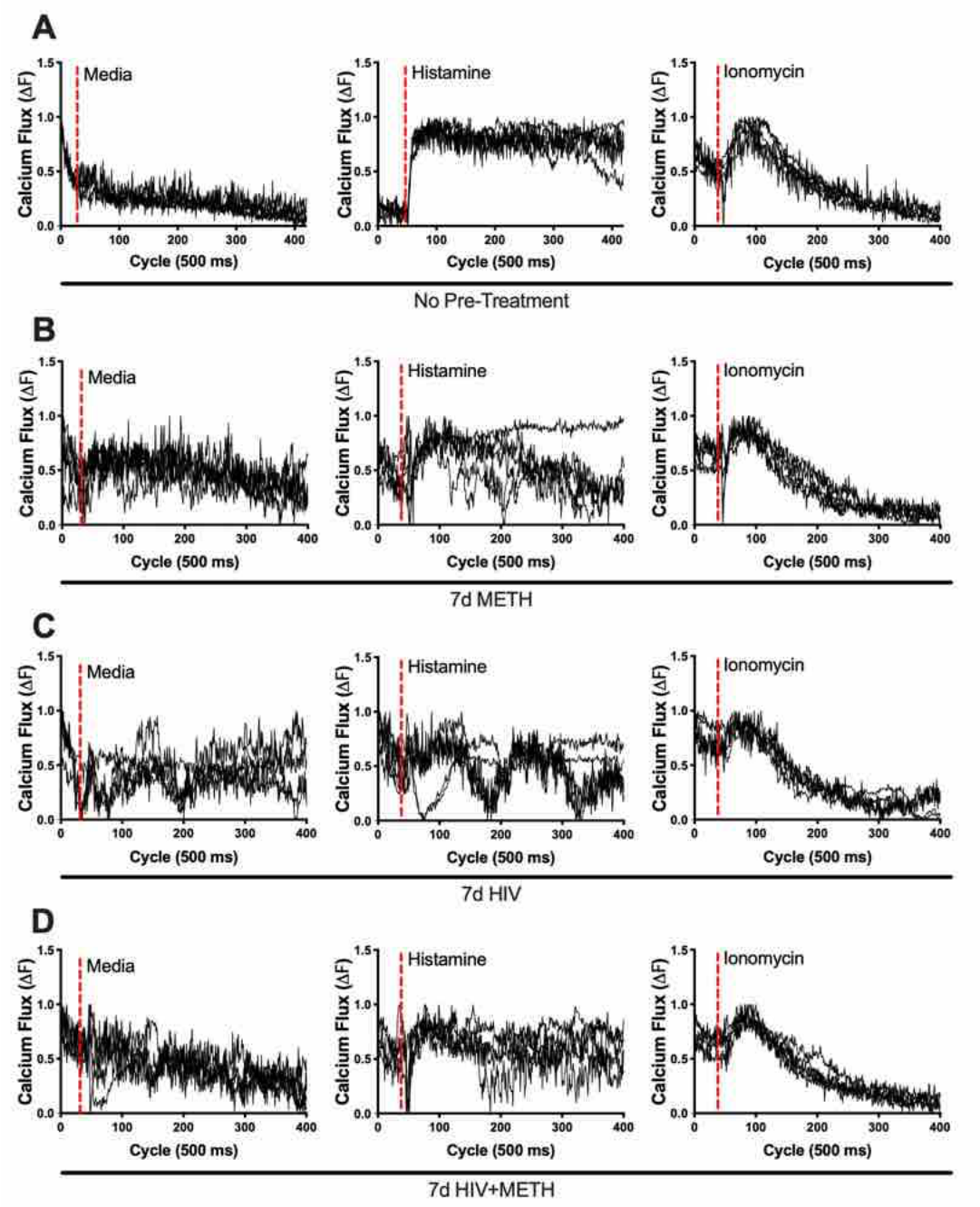

Supplementary Figure 4.1 Representative tracings of astrocyte mitochondrial calcium flux in response to acute histamine or ionomycin following 7 d METH exposure and/or HIV-1 infection. (A) Naïve astrocytes or astrocytes treated for 7 d with (B) METH (50 nM) (C) pseudotyped HIV-1 (500 RT) or (D) HIV/METH in combination were transfected with the calcium-measuring organelle-entrapped protein indicator targeted to the mitochondria and tagged

with GFP (CEPIA2mt) reporter plasmid 48 h prior to calcium imaging. Time series confocal imaging was used to measure changes in fluorescence following stimulation with media, histamine (100 μM), or ionomycin (10 μM) at 50 cycles (25 sec) up to cycle 420 (~ 4 min). Graphs illustrate line tracings from five representative astrocyte calcium flux responses. Calcium flux was calculated by: $\Delta F=(F-Fmin)/(Fmax-Fmin)$ and graphed over time, where F is the fluorescence intensity at any given time; Fmin is the minimum fluorescence intensity, and Fmax is the maximum fluorescence intensity.

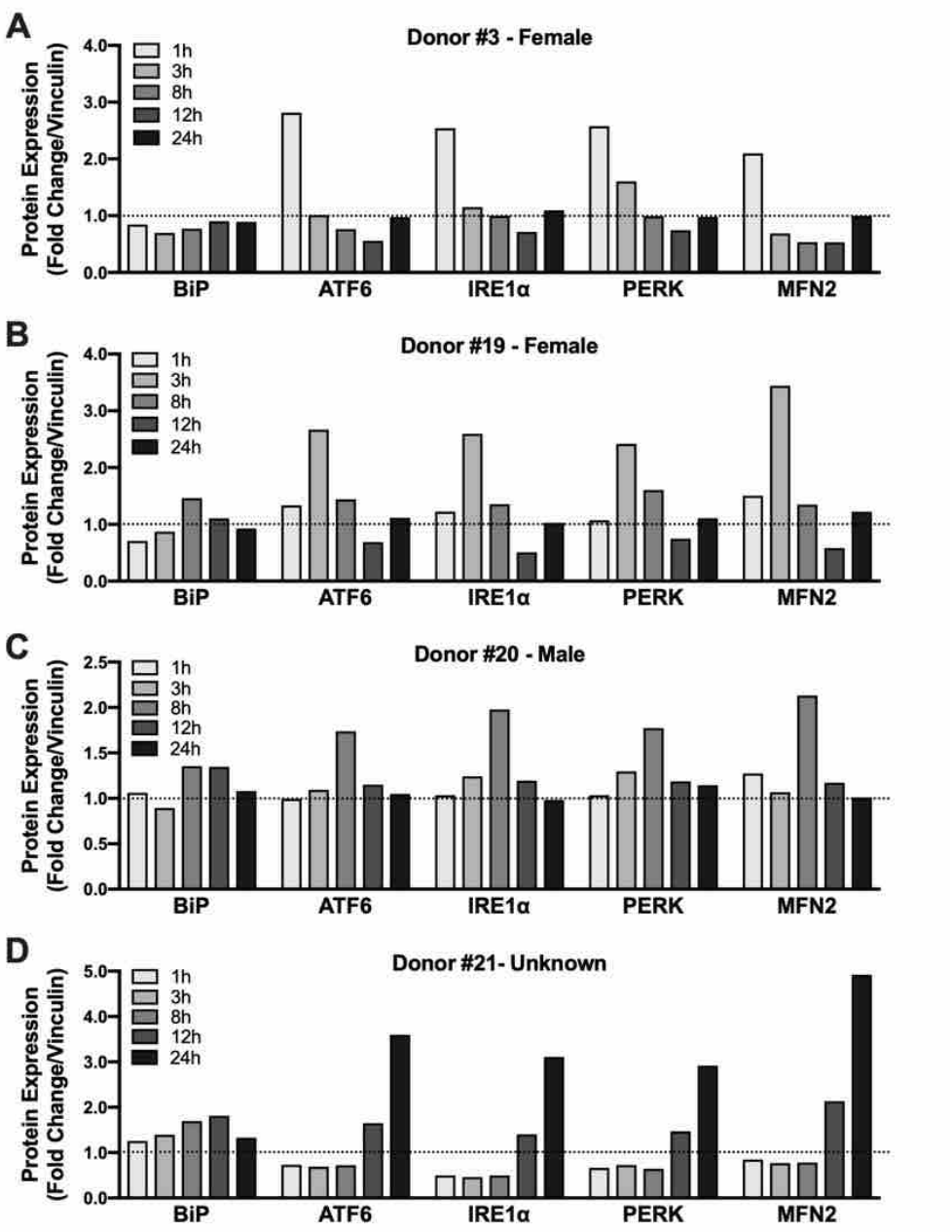

Supplementary Figure 4.2 Acute METH exposure induces unique UPR/MAM protein induction across different primary human astrocyte cultures. Astrocytes from four donor cultures (A-D) were treated with acute METH (5 μM) for 1, 3, 8, 12, and 24 h (shading darkens with time). Protein expression of BiP, ATF6, IRE1α, PERK, and MFN2 was measured *via* Simple Wes and graphed as fold change to untreated controls to illustrate trends across separate biological donors. Vinculin was used as an internal control.

Table 4.1 Demographic information of donor astrocytes used for HIV-1/METH comorbidity studies. (F = Female; M = Male; Unk = unknown)

Donor #	Sex	Gestational Age	Figure(s) Used
1	F	87 d	Figure 4.1, Figure 4.2 & Figure 4.3
2	F	108 d	Figure 4.1 Figure 4.2 & Figure 4.3
3	Unk	125 d	Figure 4.1, Figure 4.2, Figure 4.4, Figure 4.5 & Supp. Figure 4.2
4	F	89 d	Figure 4.1, Figure 4.3, Figure 4.4, & Supp. Figure 4.1
5	M	89 d	Figure 4.1, Figure 4.3 & Figure 4.5
6	F	108 d	Figure 4.1 & Figure 4.4
7	F	96 d	Figure 4.1 & Figure 4.4
8	F	90 d	Figure 4.1 & Figure 4.4
9	F	105 d	Figure 4.1 & Figure 4.5
10	M	120 d	Figure 4.2
11	M	89 d	Figure 4.2
12	M	113 d	Figure 4.2
13	F	74 d	Figure 4.2
14	F	125 d	Figure 4.2 & Figure 4.4
15	F	113 d	Figure 4.5
16	F	127 d	Figure 4.5
17	F	122 d	Figure 4.5
18	M	89 d	Figure 4.5
19	F	101 d	Figure 4.5 & Supp. Figure 4.2
20	M	125 d	Supp. Figure 4.2
21	Unk	127 d	Supp. Figure 4.2

Table 4.2 Summary of HIV-1/METH comorbidity on astrocyte HIV-1 infection and physiology.

(-- = N/A or not significant)

Experiment	**METH VS. Control**	**HIV-1 VS. Control**	**HIV-1/METH VS. Control**	**HIV-1/METH VS. HIV-1**
HIV-1 DNA integration	--	↑	↑ ↑	↑
HIV-1 protein expression	--	↑	↑ ↑	↑
Inflammation	--	--	--	--
Antioxidant expression	↓	↓	↓ ↓	--
Mitochondrial respiration	↑	↑ ↑	↑	↓
Mitochondrial calcium flux	↑	↑	↑	--
Mitochondrial dynamic protein expression	--	↑	--	↓
MAM calcium regulator expression	↑	↑	↑ ↑	--
UPR protein expression	↑	↑	↑ ↑	--

CHAPTER 5

DISCUSSION AND FUTURE DIRECTIONS

AUTHOR

J. PROULX

5.1 Summary

We interrogated the endoplasmic reticulum (ER)-mitochondrial interface for potential mediators and mechanisms that can regulate astrocyte metabolic, inflammatory, and tripartite synaptic profiles during HIV-1 infection and METH exposure. Mitochondrial-associated ER membranes (MAMs) are platforms for neuropathology, including Alzheimer's disease, Parkinson's disease, amyotrophic lateral sclerosis and potentially HAND, which had yet to be explored. Chapter 2 highlighted unfolded protein response (UPR)/ER stress, calcium dysregulation, and mitochondrial dysfunction as key MAM-mediated mechanisms underlying HAND pathology and potential therapeutic targets for astrocyte-mediated neurotoxicity. Thus, Chapters 3 and 4 focused on characterizing changes in astrocyte mitochondrial function, UPR/MAM protein expression, and intracellular calcium homeostasis following HIV-1 infection and/or acute and chronic METH exposure **(**summarized in **Figure 5.1)**.

We identified the UPR sensor inositol-requiring protein 1α (IRE1α) as a novel target for regulating astrocyte dysfunction through modulation of astrocyte mitochondrial respiration, glycolytic function, morphological activation, inflammation, and glutamate uptake (Chapter 3). Lastly, we examined the effects of chronic HIV-1/METH co-exposure in astrocyte to investigate key mediators and mechanisms which may be involved in HIV-1/METH comorbidity (Chapter 4). Notably, trace amine associated receptor 1 (TAAR1) was elevated by HIV-1 infection in astrocytes and served as an upstream regulator to METH-mediated calcium flux and UPR/MAM induction, including IRE1α. The multifunctional profile of astrocyte IRE1α highlights a key mediator that could manipulate astrocyte metabolic, inflammatory, and tripartite synaptic phenotypes. Indeed, as astrocyte dysfunction is a hallmark of neuropathology, targeting astrocyte IRE1α may be a therapeutically translatable mechanism to promote astrocyte-mediated neuroprotection against any

CNS disease or disorder. Moreover, targeting TAAR1 could not only modulate astrocyte IRE1α signaling but could also control other key ER/UPR/MAM messengers (PERK, ATF6, MFN2, and calcium). In the absence of a cure for HIV-1 and addiction, developing therapies to regulate astrocyte functional responses to chronic disease may ultimately preserve neuronal function and improve outcomes in various neurological disorders.

5.2 Discussion

The present investigations evaluated the etiology of HAND and METH use disorders in respect to key neurosupportive glial cells, astrocytes. Astrocytes are the most numerous glial cells in the CNS with multifunctional and heterogenetic profiles across distinct brain regions and conditions. The idea of specialized astrocyte subtypes was originally classified according to morphological differences, categorizing astrocytes as fibrous in white matter and protoplasmic in grey matter. Thanks to the advancement of innovative experimental tools, increasing studies can delve into astrocyte heterogeneity in both form and function across [and even within] different brain regions. The diversity of astrocyte phenotypes is engrained by the specific needs of the surrounding neuronal cells (Miller 2018; Batiuk et al. 2020). For example, astrocytes in the cortex are enriched with genes involved in neurotransmission (Batiuk et al. 2020) while astrocytes adjacent to the BBB are specialized to form tight envelopes around vessels for BBB integrity and protect neurons from circulating insults. Likewise, astrocyte metabolic profiles are increased in the hippocampus, striatum, cortex, and cerebellum regions and are lower in most subcortical regions (Oe et al. 2016). Recent studies suggest astrocyte heterogeneity may predict individual or brain region susceptibility to different CNS pathologies (Matias, Morgado, and Gomes 2019).

Thus, how an individual's astrocytes respond during HIV-1/METH-induced stress could influence one's sensitivity to HAND/METH pathology.

The clinically diverse manifestation of HAND is characterized by a variable distribution of brain atrophy in PLWH, including frontal, subcortical, temporal, parietal, occipital, and cerebellum (Ghosh, Sarkar, and Mitsuya 2017; Israel et al. 2019) (Debalkie Animut et al. 2019; Nightingale et al. 2014; Simioni et al. 2010; Heaton et al. 2011; Zenebe et al. 2022). Notably, the most consistent and conclusive findings correlate HAND pathology with the frontal lobe and basal ganglia. Interestingly, increased levels of ER stress (Lindl et al. 2007; Akay et al. 2012) and decreased expression of mitochondrial fission protein Drp1 (Fields et al. 2016) in the prefrontal cortex of postmortem HIV+ brain tissues, correlated with severity of cognitive decline. Importantly, astrocytes had higher expression of ER stress markers than neurons, supporting astrocyte ER stress as a key etiology in HAND pathology. Substance use disorders, including METH, are disproportionately elevated among PLWH and influence both the development and severity of HAND. The dopaminergic system in the brain is the primary physiological target for METH after consumption, achieving a 13:1 brain to plasma ratio. METH exposure can have widespread and long-lasting psychological and neurophysiological consequences, not unlike HIV-1. However, the combined HIV-1/METH pathophysiology strongly intersect at the frontal striatal circuitries connecting the frontal lobe with the basal ganglia (Soontornniyomkij et al. 2016).

There are a number of factors contributing to an individual's risk and severity to HAND, including sociodemographic and genetic influences, lifestyle choices, and health comorbidities. Sex differences are a notable trend in HIV-1/HAND pathogenesis. For example, women account for 54% of PLWH worldwide and are also more likely to experience greater neurocognitive impairment than men (Rubin et al. 2019; Rubin and Maki 2021). It is important to note that females

are widely underrepresented in most HIV-1 studies, despite their heightened prevalence of HIV-1 infection and severity of HIV-1 pathogenesis. Interestingly, men account for a greater incidence of new HIV-1 cases and in general have a greater prevalence of comorbid factors including substance use disorders, metabolic disorders, and cardiovascular diseases compared to women. However, women living with HIV-1 have higher rates for these same comorbidities compared to men living with HIV-1 (Pond, Collins, and Lahiri 2021; Addo and Altfeld 2014). In other words, women living with HIV-1 are more susceptible to developing non-AIDS comorbidities than men living with HIV-1. Potential influences for the sex-based differences in HIV-1 pathogenesis include sex chromosomes and hormones, sociobehavioral factors, and increased HIV-1-associated immune activation [in females].

All our experiments are performed in minimally three biologically distinct human astrocyte cultures to assess biological relevance. The current studies did not compare sex differences as a potential driver for donor variability on astrocyte ER-mitochondrial dysfunction. However, all cultures are subjected to an astrocyte characterization protocol prior to experimental use to assess astrocyte inflammatory and tripartite synaptic functions. These unpublished works do not illustrate any significant influences of gestational age or sex on our astrocyte cultures. An important limitation of our model is that each culture is isolated from premature brain tissues, thus region-specific phenotypes and influences of developmental sex hormones are unable to be accounted for. Other considerations for donor variations can include shipping conditions, collection/isolation techniques, passage number, or if the donor was cryopreserved prior to experiment use. Regardless, our studies support evidence of astrocyte heterogeneity and potential susceptibility during different challenges and conditions. Indeed, astrocyte variations across time, dosage, and/or amplitude of changes strongly support a unique genetic influence for astrocyte sensitivity to ER-

mitochondrial dysfunction. For example, induction of UPR/MAM mediator protein expression following acute METH across different astrocyte cultures varied in both temporal induction and amplitude of expression **(Supp. Figure 4.2)**. Importantly, those capable of resolving stress and establishing a new homeostasis, may be more resilient to HIV-1/METH neuropathological damage, and thus would be less likely to have poor outcomes.

Identifying a pivotal regulator of astrocyte functions may provide more insights into the mechanisms governing astrocyte diversity and/or vulnerability during both health and disease. Loss of cellular "identity" is a key mechanism underlying pathology. During a neuropathological challenge, such as HIV-1 infection of METH exposure, 'activation' of astrocytes can shift their primary functions and even alter cellular physiology. Acutely, these functional shifts optimize neuronal protection, such as a glial scar formation during a stroke. However, failure to restore homeostatic phenotypes, leads to prolonged states of astrocyte activation that can inadvertently lead to neuronal toxicity. For example, shifts in astrocyte mitochondrial function threaten the ability of astrocytes to provide essential metabolic and antioxidant support to neurons, while also contributing to the production of toxic reactive oxygen and nitrogen species (ROS/RNS) to propagate oxidative stress. The production of toxic radicals and/or inflammatory cytokines can perpetuate a vicious cycle of oxidative stress and neuroinflammation, respectively. Meanwhile, impaired tripartite synaptic maintenance or neurotrophic provision can be detrimental to proper neuronal function and health. Indeed, astrocyte-associated oxidative stress, neuroinflammation and glutamate excitotoxicity are key etiologies underlying neurodegenerative disorders.

In the present studies, HIV-1 infection and/or METH exposure increased astrocyte metabolic activities and decreased antioxidant production. The purpose of increased respiratory activity could be to prime astrocytes for activation or a compensatory mechanism for astrocytes to

protect neurons during a challenge. However, decreased antioxidant production does not coincide with neuroprotective properties. A previous report in the context of HIV-1 Tat and/or cocaine associated increased astrocyte mitochondrial respiration with an impaired metabolite provision and increase release of ROS and inflammatory cytokines leading to neurotoxic consequences (Natarajaseenivasan et al. 2018). Notably, these studies were under acute paradigms using vastly different models for HIV-1 and substance use. It is unknown in our model if increased astrocyte respiration associated wth metobolite capacity or ROS production. Given the resiliency of astrocytes facing chronic stress, the balance between neuroprective versus neutoxic functions may be able to undergo some level of restablization over time. Alternately, chronic stress could lead to some level of astrocyte exhaustion contributing to the impaired antioxidant protection. Regardless, chronic astrocyte activtion is well-known to be detrimental to neuronal health and function.

In addition to increased respiration and impaired antioxidant function, chronic HIV-1 infection and/or METH exposure significantly increased both astrocyte cytosolic and mitochondrial calcium flux – under both basal and challenged conditions. As calcium is a central second messenger in cell signaling, a dysregulated calcium homeostasis can have a multitude of ramifications on astrocyte health and function. For example, calcium can be an upstream regulator for ER stress, mitochondrial integrity, bioenergetic activity, autophagy, apoptosis, and inflammasome activation (van Vliet, Verfaillie, and Agostinis 2014). Thus, increased mitochondrial calcium uptake could be fueling the increased UPR induction, respiration and/or inflammatory functions. However, overload of mitochondrial calcium and subsequent impaired mitochondrial integrity could also make astrocytes more susceptible to apoptosis, which was evident when astrocytes were challenged with ionomycin **(Figure 4.3)**. The complete impact of increased basal cytosolic and mitochondrial calcium flux on astrocyte homeostasis and

intercellular communication are unknown. However, experimental manipulation of calcium signaling pathways, as discussed in chapter 2, supports calcium as a promising target to prevent astrocyte-mediated neurotoxicity in the context of HIV-1-relevant dysfunction. Teasing out the multitude of possible downstream effects of calcium dysregulation on astrocyte and neural cell function could provide insight into dominant pathways affecting neurological outcomes in HAND and METH use disorders.

Importantly, mitochondrial-associated ER membranes (MAMs) arise as pivotal platforms for astrocyte dysfunction. Despite obvious disruptions in ER and mitochondrial homeostasis in the context of HIV-1 or METH, the present investigations are the first to consider MAMs with respect to HAND or METH pathology. While some studies of HIV-1 in astrocytes have danced around the idea of ER-mitochondrial interplay through calcium signaling (Nooka and Ghorpade 2017; Ma et al. 2016 Khan, 2019 #18673), no research has considered MAMs as potential pathological platforms for HAND or METH pathogenesis. In fact, the only evidence of MAMs in HIV-1 biology was reported in T cells showing that HIV-1 Vpr localizes to both the ER and mitochondria, and MAMs serve as a possible route for intracellular trafficking of Vpr (Huang et al. 2012). Moreover, MAMs have rarely even been considered in astrocyte biology. There are only two previous investigations of MAMs in astrocytes, which were focused on astrocyte-mediated vascular remodeling (Gbel et al. 2020) and synaptic homeostasis (Serrat et al. 2021). Studies are needed to elucidate the roles of MAM mediators and mechanisms in astrocyte biology and HIV-1/METH pathogenesis, especially if MAM function and physiology are determinants for the multifunctional and heterogenetic profiles of astrocytes across distinct brain regions and conditions.

Our findings further implicate the ER-mitochondrial interface in astrocytes during HIV-1/METH comorbidity, highlighting IRE1α at the intersection of astrocyte dysfunction. Indeed, IRE1α maybe be a key regulator of the diverse astrocyte profiles through both canonical UPR and non-canonical MAM-mediated calcium signaling. Overexpression of IRE1α augmented mitochondrial respiration, glycolytic function, morphological activation, inflammation, and glutamate uptake. However, it remains unknown how to target IRE1α to promote astrocyte neuroprotective functions and prevent astrocyte-associated neurotoxic profiles. It is important to note that while all the UPR/MAM mediators we probed, including IRE1α, are located in MAMs, they are not restricted to these contact sites. Thus, functional changes in UPR/MAM mediator expression, calcium homeostasis and mitochondrial respiration and dynamics may indeed be MAM-independent. Regardless, the integrated stress responses and inter-organelle cooperation between the ER and mitochondria are the foundation for cellular health and function and, likewise, are not limited by ER and mitochondria contact.

Lastly, an important consideration for determining an optimal avenue for therapeutic intervention is how two distinct challenges (HIV-1 infection or METH) converge at the same intersection (IRE1α). With METH, we show TAAR-1 as an upstream regulator for METH-induced calcium flux and UPR/MAM induction. However, it is also possible for Sig-1R to be regulating some METH-induced astrocyte dysfunction. Moreover, it is well-known that METH can directly interact with and impair electron transport chain (ETC) components (Brown, Quinton, and Yamamoto 2005; Burrows, Nixdorf, and Yamamoto 2000; Feier et al. 2012; Burrows, Gudelsky, and Yamamoto 2000). Whether a direct or indirect mechanism, perturbation to the mitochondria could lead to permeability transitional pore (mPTP) opening or ROS production to then stimulate ER stress. The ER could then respond in attempt to rescue mitochondrial health and restore

homeostatic balance. This would again support increased oxygen consumption as a potential compensatory mechanism to overcome METH (and/or HIV-1)-induced mitochondrial dysfunction. Alternatively, mPTP opening and ROS production are also known mechanisms to regulate immune activation and inflammatory function (Abuaita et al. 2015; Abuaita, Schultz, and O'Riordan 2018; Dong et al. 2019; Abuaita et al. 2021). For HIV-1, there are several stages in the life cycle for potential triggering of ER and mitochondrial dysfunction. Intracellular HIV-1 RNA or DNA could activate innate immune sensors including mitochondrial-associated viral sensors (MAVS) on the mitochondrial membrane or stimulator of interferon genes (STING) on the ER membrane. Expression of HIV-1 proteins are known to cause ER stress, calcium dysregulation, and mitochondrial dysfunction, as discussed in chapter 2. However, transcriptome analysis comparing active versus restricted infection reveals a similar gene expression pattern infection, thus, harboring HIV-1 genome alone, profoundly alters astrocyte biology (Edara, Ghorpade, and Borgmann 2020). Both METH and HIV-1 have a multitude of avenues to initiate ER-mitochondrial integrated stress responses and eventually intersect at IRE1α. Whether the trigger begins at ER or the mitochondria, cooperation is a two-way street.

5.3 Future Directions & Therapeutic Translation

While our studies highlight IRE1α and/or TAAR1 as key targets to modulate astrocyte ER-mitochondrial dysfunction during HIV-1/METH neuropathology, additional studies will need to validate their potential to optimize the beneficial physiological coupling between astrocytes and neurons. As IRE1α and TAAR1 are not unique to astrocytes, potential off targeting effects in other cell types will need to be considered. Moreover, astrocyte specialization in different brain regions may further complicate therapeutic application.

The initial next steps to estimate the clinical implication and translational applicability could employ co-cultures or supernatant transfers between astrocytes and neurons to assess astrocyte neurotoxic versus neurosupportive factors. Moreover, while primary tissue cultures used here are an optimal *in vitro* model, *in vivo* translation is necessary for clinical application. To confirm *in vivo* translatability, healthy versus HIV+ brain tissues could be evaluated for expression changes in key UPR/MAM mediators and mitochondrial regulators. However, postmortem studies only grant a snapshot of the finite consequences of a pathology with limited insights into disease progression or key mechanisms that could be causing pathology. Live *in vivo* models are also limited since infection with HIV-1 is unique to humans. Common transgenic mice models to investigate HAND include astrocyte-restricted expression of HIV-1 proteins, such as Tat (Joshi et al. 2020) or gp120 (Fields et al. 2016). Additional models include seeding HIV+ human astroglia infected into mouse brains (Lutgen et al. 2020) or modifying human HIV-1 with a murine retrovirus envelope protein (Potash et al. 2005). Finally, primates are perhaps the most translatable *in vivo* model using a homologous HIV-1 variant, simian immunodeficiency virus (SIV). To accurately explore HIV-1/METH comorbidity, it will be important to establish a METH regimen representative of METH use disorders in PLWH. However, a key confounding factor for these studies will be the clinical intervention of antiretroviral therapy (ART), especially since some ART drugs have been shown to induce off-target toxicity, including ER stress in astrocytes (Nooka and Ghorpade 2018).

Finally, therapeutic targeting to the CNS brings about a whole new array of huddles and complexities. Indeed, poor penetration of ART into the CNS is the key limitation to current HAND intervention. To improve CNS therapeutics, our group has been optimizing polymeric nanoparticles for the delivery of antioxidants (Singhal et al. 2013; Reddy and Labhasetwar 2009;

Reddy et al. 2008), antiretroviral drugs (Rao, Ghorpade, and Labhasetwar 2009; Borgmann et al. 2011), as well as astrocyte-restricted gene therapy (Joshi et al. 2018; Proulx et al. 2020; Joshi et al. 2020)**.** Particularly, gene therapy allows for molecular intervention to regulate astrocyte function to restore a neuroprotective and/or reverse a neurotoxic phenotype. In fact, using astrocyte-restricted glial fibrillary acidic protein promoters would be able to circumvent any potential off-targeting effects in other cell types. Polymeric nanoparticles are advantageous for gene delivery due to their low immunogenicity, high biocompatibility, versatility, and protection against peripheral and intracellular degradation of the encapsulated cargo (Luten et al. 2008; Midoux et al. 2008; Jayant et al. 2016; Joshi, Labhasetwar, and Ghorpade 2017; Joshi et al. 2018; Proulx et al. 2020; Joshi et al. 2020). These studies identified several therapeutic targets that may help ameliorate HIV-1 and/or METH disease outcomes; however, they can only treat the pathophysiological mechanisms at play in the brain. Ultimately, HIV-1 is a lifelong, chronic disease that increases the risks for an array of comorbidities including neurological impairment and substance use.

5.4 Figures

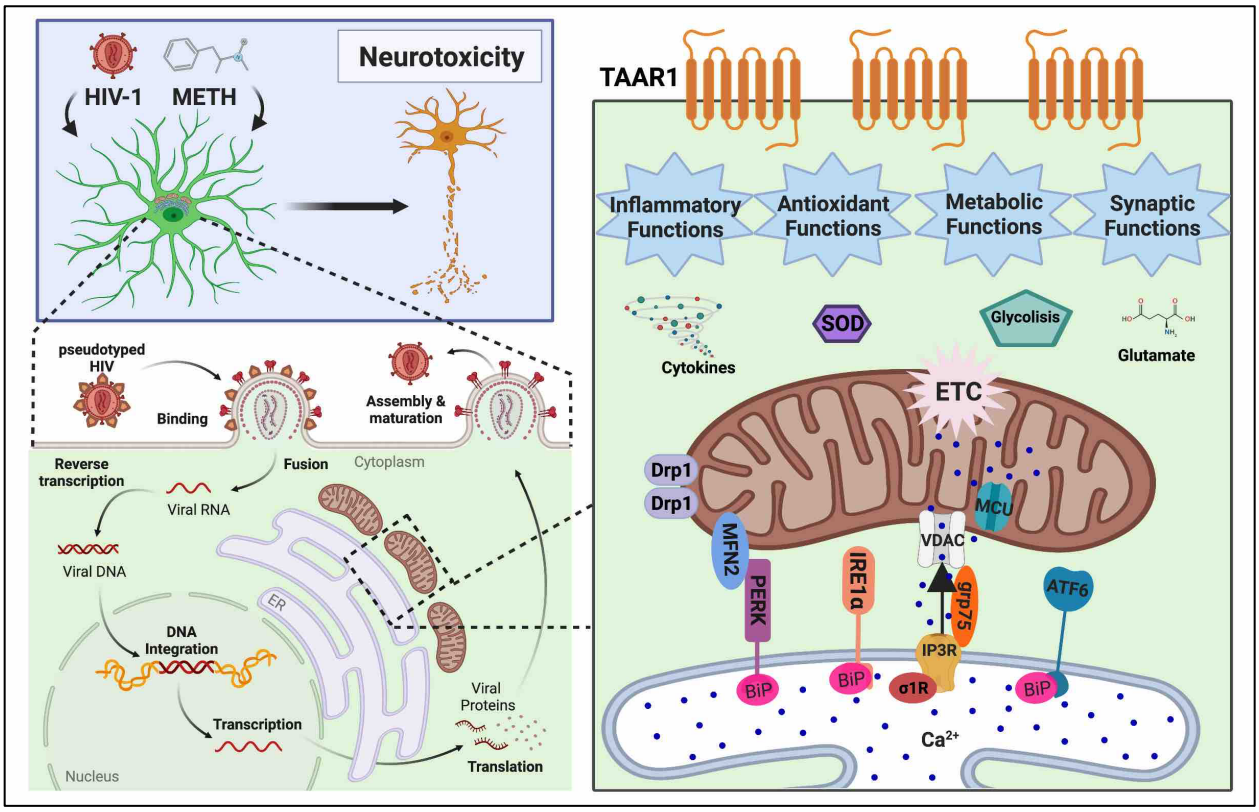

Figure 5.1 The ER-mitochondrial interface in astrocytes during METH exposure and HIV-1 infection. Following METH exposure and/or pseudotyped HIV-1 infection, astrocytes shift their physiology and function, which can impair astrocyte-mediated neuroprotection and increase neurotoxicity. The ER-mitochondrial interface arises as a key pathological platform for HIV-1/METH-mediated astrocyte dysfunction. Notably, astrocyte HIV-1 infection was increased by chronic METH exposure. The effects of HIV-1 infection and METH exposure, alone or in combination, dysregulate astrocyte calcium homeostasis, mitochondrial function and dynamics, and UPR/MAM protein expression. These changes in ER-mitochondrial function and physiology are important regulators for astrocyte inflammatory, antioxidant, metabolic, and synaptic functions. Image made with Biorender.

BIBLIOGRAPHY

Abuaita, B. H., K. M. Burkholder, B. R. Boles, and M. X. O'Riordan. 2015. 'The Endoplasmic Reticulum Stress Sensor Inositol-Requiring Enzyme 1alpha Augments Bacterial Killing through Sustained Oxidant Production', *MBio*, 6: e00705.

Abuaita, B. H., T. L. Schultz, and M. X. O'Riordan. 2018. 'Mitochondria-Derived Vesicles Deliver Antimicrobial Reactive Oxygen Species to Control Phagosome-Localized Staphylococcus aureus', *Cell Host Microbe*, 24: 625-36 e5.

Abuaita, B. H., G. J. Sule, T. L. Schultz, F. Gao, J. S. Knight, and M. X. O'Riordan. 2021. 'The IRE1alpha Stress Signaling Axis Is a Key Regulator of Neutrophil Antimicrobial Effector Function', *J Immunol*, 207: 210-20.

Addo, M. M., and M. Altfeld. 2014. 'Sex-based differences in HIV type 1 pathogenesis', *J Infect Dis*, 209 Suppl 3: S86-92.

Akay, C., K. A. Lindl, N. Shyam, B. Nabet, Y. Goenaga-Vazquez, J. Ruzbarsky, Y. Wang, D. L. Kolson, and K. L. Jordan-Sciutto. 2012. 'Activation status of integrated stress response pathways in neurones and astrocytes of HIV-associated neurocognitive disorders (HAND) cortex', *Neuropathol Appl Neurobiol*, 38: 175-200.

Al-Saif, A., F. Al-Mohanna, and S. Bohlega. 2011. 'A mutation in sigma-1 receptor causes juvenile amyotrophic lateral sclerosis', *Ann Neurol*, 70: 913-9.

Area-Gomez, E., A. J. de Groof, I. Boldogh, T. D. Bird, G. E. Gibson, C. M. Koehler, W. H. Yu, K. E. Duff, M. P. Yaffe, L. A. Pon, and E. A. Schon. 2009. 'Presenilins are enriched in endoplasmic reticulum membranes associated with mitochondria', *Am J Pathol*, 175: 1810-6.

Area-Gomez, E., M. Del Carmen Lara Castillo, M. D. Tambini, C. Guardia-Laguarta, A. J. de Groof, M. Madra, J. Ikenouchi, M. Umeda, T. D. Bird, S. L. Sturley, and E. A. Schon. 2012. 'Upregulated function of mitochondria-associated ER membranes in Alzheimer disease', *EMBO J*, 31: 4106-23.

Area-Gomez, E., and E. A. Schon. 2017. 'On the Pathogenesis of Alzheimer's Disease: The MAM Hypothesis', *FASEB J*, 31: 864-67.

Avdoshina, V., J. A. Fields, P. Castellano, S. Dedoni, G. Palchik, M. Trejo, A. Adame, E. Rockenstein, E. Eugenin, E. Masliah, and I. Mocchetti. 2016. 'The HIV Protein gp120 Alters Mitochondrial Dynamics in Neurons', *Neurotox Res*, 29: 583-93.

Bahat, A., T. MacVicar, and T. Langer. 2021. 'Metabolism and Innate Immunity Meet at the Mitochondria', *Front Cell Dev Biol*, 9: 720490.

Balsa, E., M. S. Soustek, A. Thomas, S. Cogliati, C. Garcia-Poyatos, E. Martin-Garcia, M. Jedrychowski, S. P. Gygi, J. A. Enriquez, and P. Puigserver. 2019. 'ER and Nutrient Stress Promote Assembly of Respiratory Chain Supercomplexes through the PERK-eIF2alpha Axis', *Mol Cell*, 74: 877-90 e6.

Bashir, S., M. Banday, O. Qadri, A. Bashir, N. Hilal, I. Fatima Nida, S. Rader, and K. M. Fazili. 2021. 'The molecular mechanism and functional diversity of UPR signaling sensor IRE1', *Life Sci*, 265: 118740.

Basova, L., J. A. Najera, N. Bortell, D. Wang, R. Moya, A. Lindsey, S. Semenova, R. J. Ellis, and M. C. G. Marcondes. 2018. 'Dopamine and its receptors play a role in the modulation of

CCR5 expression in innate immune cells following exposure to Methamphetamine: Implications to HIV infection', *PLoS One*, 13: e0199861.

Basso, V., E. Marchesan, and E. Ziviani. 2020. 'A trio has turned into a quartet: DJ-1 interacts with the IP3R-Grp75-VDAC complex to control ER-mitochondria interaction', *Cell Calcium*, 87: 102186.

Batiuk, M. Y., A. Martirosyan, J. Wahis, F. de Vin, C. Marneffe, C. Kusserow, J. Koeppen, J. F. Viana, J. F. Oliveira, T. Voet, C. P. Ponting, T. G. Belgard, and M. G. Holt. 2020. 'Identification of region-specific astrocyte subtypes at single cell resolution', *Nat Commun*, 11: 1220.

Bergami, M., and E. Motori. 2020. 'Reweaving the Fabric of Mitochondrial Contact Sites in Astrocytes', *Front Cell Dev Biol*, 8: 592651.

Bernard-Marissal, N., R. Chrast, and B. L. Schneider. 2018. 'Endoplasmic reticulum and mitochondria in diseases of motor and sensory neurons: a broken relationship?', *Cell Death Dis*, 9: 333.

Bernard-Marissal, N., J. J. Medard, H. Azzedine, and R. Chrast. 2015. 'Dysfunction in endoplasmic reticulum-mitochondria crosstalk underlies SIGMAR1 loss of function mediated motor neuron degeneration', *Brain*, 138: 875-90.

Bernard-Marissal, N., G. van Hameren, M. Juneja, C. Pellegrino, L. Louhivuori, L. Bartesaghi, C. Rochat, O. El Mansour, J. J. Medard, M. Croisier, C. Maclachlan, O. Poirot, P. Uhlen, V. Timmerman, N. Tricaud, B. L. Schneider, and R. Chrast. 2019. 'Altered interplay between endoplasmic reticulum and mitochondria in Charcot-Marie-Tooth type 2A neuropathy', *Proc Natl Acad Sci U S A*, 116: 2328-37.

Bettcher, B. M., K. E. Olson, N. E. Carlson, B. V. McConnell, T. Boyd, V. Adame, D. A. Solano, P. Anton, N. Markham, A. A. Thaker, A. M. Jensen, E. N. Dallmann, H. Potter, and C. Coughlan. 2021. 'Astrogliosis and episodic memory in late life: higher GFAP is related to worse memory and white matter microstructure in healthy aging and Alzheimer's disease', *Neurobiol Aging*, 103: 68-77.

Blackard, J. T., and K. E. Sherman. 2021. 'Drugs of Abuse and Their Impact on Viral Pathogenesis', *Viruses*, 13.

Bommiasamy, H., S. H. Back, P. Fagone, K. Lee, S. Meshinchi, E. Vink, R. Sriburi, M. Frank, S. Jackowski, R. J. Kaufman, and J. W. Brewer. 2009. 'ATF6alpha induces XBP1-independent expansion of the endoplasmic reticulum', *J Cell Sci*, 122: 1626-36.

Borgmann, K., and A. Ghorpade. 2015. 'HIV-1, methamphetamine and astrocytes at neuroinflammatory Crossroads', *Front Microbiol*, 6: 1143.

———. 2017. 'Methamphetamine Augments Concurrent Astrocyte Mitochondrial Stress, Oxidative Burden, and Antioxidant Capacity: Tipping the Balance in HIV-Associated Neurodegeneration', *Neurotox Res*.

Borgmann, K., K. S. Rao, V. Labhasetwar, and A. Ghorpade. 2011. 'Efficacy of Tat-Conjugated Ritonavir-Loaded Nanoparticles in Reducing HIV-1 Replication in Monocyte-Derived Macrophages and Cytocompatibility with Macrophages and Human Neurons', *AIDS research and human retroviruses*.

Borrajo, A., C. Spuch, M. A. Penedo, J. M. Olivares, and R. C. Agis-Balboa. 2021. 'Important role of microglia in HIV-1 associated neurocognitive disorders and the molecular pathways implicated in its pathogenesis', *Ann Med*, 53: 43-69.

Bortell, N., L. Basova, S. Semenova, H. S. Fox, T. Ravasi, and M. C. Marcondes. 2017. 'Astrocyte-specific overexpressed gene signatures in response to methamphetamine exposure in vitro', *J Neuroinflammation*, 14: 49.

Brand, M. D., A. L. Orr, I. V. Perevoshchikova, and C. L. Quinlan. 2013. 'The role of mitochondrial function and cellular bioenergetics in ageing and disease', *Br J Dermatol*, 169 Suppl 2: 1-8.

Bravo, R., T. Gutierrez, F. Paredes, D. Gatica, A. E. Rodriguez, Z. Pedrozo, M. Chiong, V. Parra, A. F. Quest, B. A. Rothermel, and S. Lavandero. 2012. 'Endoplasmic reticulum: ER stress regulates mitochondrial bioenergetics', *Int J Biochem Cell Biol*, 44: 16-20.

Bravo, R., J. M. Vicencio, V. Parra, R. Troncoso, J. P. Munoz, M. Bui, C. Quiroga, A. E. Rodriguez, H. E. Verdejo, J. Ferreira, M. Iglewski, M. Chiong, T. Simmen, A. Zorzano, J. A. Hill, B. A. Rothermel, G. Szabadkai, and S. Lavandero. 2011. 'Increased ER-mitochondrial coupling promotes mitochondrial respiration and bioenergetics during early phases of ER stress', *J Cell Sci*, 124: 2143-52.

Bravo-Sagua, R., C. Lopez-Crisosto, V. Parra, M. Rodriguez-Pena, B. A. Rothermel, A. F. Quest, and S. Lavandero. 2016. 'mTORC1 inhibitor rapamycin and ER stressor tunicamycin induce differential patterns of ER-mitochondria coupling', *Sci Rep*, 6: 36394.

Bronner, D. N., B. H. Abuaita, X. Chen, K. A. Fitzgerald, G. Nunez, Y. He, X. M. Yin, and M. X. O'Riordan. 2015. 'Endoplasmic Reticulum Stress Activates the Inflammasome via NLRP3- and Caspase-2-Driven Mitochondrial Damage', *Immunity*, 43: 451-62.

Brown, J. M., M. S. Quinton, and B. K. Yamamoto. 2005. 'Methamphetamine-induced inhibition of mitochondrial complex II: roles of glutamate and peroxynitrite', *J Neurochem*, 95: 429-36.

Brown, L. A., J. Scarola, A. J. Smith, P. R. Sanberg, J. Tan, and B. Giunta. 2014. 'The role of tau protein in HIV-associated neurocognitive disorders', *Mol Neurodegener*, 9: 40.

Brown, M. K., and N. Naidoo. 2012. 'The endoplasmic reticulum stress response in aging and age-related diseases', *Front Physiol*, 3: 263.

Burkewitz, K., G. Feng, S. Dutta, C. A. Kelley, M. Steinbaugh, E. J. Cram, and W. B. Mair. 2020. 'Atf-6 Regulates Lifespan through ER-Mitochondrial Calcium Homeostasis', *Cell Rep*, 32: 108125.

Burrows, K. B., G. Gudelsky, and B. K. Yamamoto. 2000. 'Rapid and transient inhibition of mitochondrial function following methamphetamine or 3,4-methylenedioxymethamphetamine administration', *Eur J Pharmacol*, 398: 11-8.

Burrows, K. B., W. L. Nixdorf, and B. K. Yamamoto. 2000. 'Central administration of methamphetamine synergizes with metabolic inhibition to deplete striatal monoamines', *J Pharmacol Exp Ther*, 292: 853-60.

Cali, T., D. Ottolini, A. Negro, and M. Brini. 2012. 'alpha-Synuclein controls mitochondrial calcium homeostasis by enhancing endoplasmic reticulum-mitochondria interactions', *J Biol Chem*, 287: 17914-29.

———. 2013. 'Enhanced parkin levels favor ER-mitochondria crosstalk and guarantee Ca(2+) transfer to sustain cell bioenergetics', *Biochim Biophys Acta*, 1832: 495-508.

Campestrini, J., D. B. Silveira, and A. R. Pinto. 2018. 'HIV-1 Tat-induced bystander apoptosis in Jurkat cells involves unfolded protein responses', *Cell Biochem Funct*, 36: 377-86.

Canki, M., J. N. Thai, W. Chao, A. Ghorpade, M. J. Potash, and D. J. Volsky. 2001. 'Highly productive infection with pseudotyped human immunodeficiency virus type 1 (hiv-1) indicates no intracellular restrictions to hiv-1 replication in primary human astrocytes', *J Virol*, 75: 7925-33.

Carreras-Sureda, A., F. Jana, H. Urra, S. Durand, D. E. Mortenson, A. Sagredo, G. Bustos, Y. Hazari, E. Ramos-Fernandez, M. L. Sassano, P. Pihan, A. R. van Vliet, M. Gonzalez-Quiroz, A. K. Torres, C. Tapia-Rojas, M. Kerkhofs, R. Vicente, R. J. Kaufman, N. C. Inestrosa, C. Gonzalez-Billault, R. L. Wiseman, P. Agostinis, G. Bultynck, F. A. Court, G. Kroemer, J. C. Cardenas, and C. Hetz. 2019. 'Non-canonical function of IRE1alpha determines mitochondria-associated endoplasmic reticulum composition to control calcium transfer and bioenergetics', *Nat Cell Biol*, 21: 755-67.

Chaphalkar, R. M., D. L. Stankowska, S. He, B. Kodati, N. Phillips, J. Prah, S. Yang, and R. R. Krishnamoorthy. 2020. 'Endothelin-1 Mediated Decrease in Mitochondrial Gene Expression and Bioenergetics Contribute to Neurodegeneration of Retinal Ganglion Cells', *Sci Rep*, 10: 3571.

Chen, T. W., T. J. Wardill, Y. Sun, S. R. Pulver, S. L. Renninger, A. Baohan, E. R. Schreiter, R. A. Kerr, M. B. Orger, V. Jayaraman, L. L. Looger, K. Svoboda, and D. S. Kim. 2013. 'Ultrasensitive fluorescent proteins for imaging neuronal activity', *Nature*, 499: 295-300.

Chen, Y., C. Qin, J. Huang, X. Tang, C. Liu, K. Huang, J. Xu, G. Guo, A. Tong, and L. Zhou. 2020. 'The role of astrocytes in oxidative stress of central nervous system: A mixed blessing', *Cell Prolif*, 53: e12781.

Cieri, D., M. Vicario, F. Vallese, B. D'Orsi, P. Berto, A. Grinzato, C. Catoni, D. De Stefani, R. Rizzuto, M. Brini, and T. Cali. 2018. 'Tau localises within mitochondrial sub-compartments and its caspase cleavage affects ER-mitochondria interactions and cellular Ca(2+) handling', *Biochim Biophys Acta Mol Basis Dis*, 1864: 3247-56.

Ciron, C., L. Zheng, W. Bobela, G. W. Knott, T. C. Leone, D. P. Kelly, and B. L. Schneider. 2015. 'PGC-1alpha activity in nigral dopamine neurons determines vulnerability to alpha-synuclein', *Acta Neuropathol Commun*, 3: 16.

Cisneros, I. E., and A. Ghorpade. 2012. 'HIV-1, methamphetamine and astrocyte glutamate regulation: combined excitotoxic implications for neuro-AIDS', *Curr HIV Res*, 10: 392-406.

———. 2014. 'Methamphetamine and HIV-1-induced neurotoxicity: role of trace amine associated receptor 1 cAMP signaling in astrocytes', *Neuropharmacology*, 85: 499-507.

Cisneros, I. E., A. Ghorpade, and K. Borgmann. 2020. 'Methamphetamine Activates Trace Amine Associated Receptor 1 to Regulate Astrocyte Excitatory Amino Acid Transporter-2 via Differential CREB Phosphorylation During HIV-Associated Neurocognitive Disorders', *Front Neurol*, 11: 593146.

Cody, S. L., and D. E. Vance. 2016. 'The neurobiology of HIV and its impact on cognitive reserve: A review of cognitive interventions for an aging population', *Neurobiol Dis*, 92: 144-56.

Colfax, G. N., E. Vittinghoff, R. Grant, P. Lum, G. Spotts, and F. M. Hecht. 2007. 'Frequent methamphetamine use is associated with primary non-nucleoside reverse transcriptase inhibitor resistance', *Aids*, 21: 239-41.

Cowan, K., O. Anichtchik, and S. Luo. 2019. 'Mitochondrial integrity in neurodegeneration', *CNS Neurosci Ther*, 25: 825-36.

Darbinian, N., A. Darbinyan, N. Merabova, M. E. Selzer, and S. Amini. 2020. 'HIV-1 and HIV-1-Tat Induce Mitochondrial DNA Damage in Human Neurons', *J HIV AIDS*, 6.

de Brito, O. M., and L. Scorrano. 2008. 'Mitofusin 2 tethers endoplasmic reticulum to mitochondria', *Nature*, 456: 605-10.

De Vos, K. J., G. M. Morotz, R. Stoica, E. L. Tudor, K. F. Lau, S. Ackerley, A. Warley, C. E. Shaw, and C. C. Miller. 2012. 'VAPB interacts with the mitochondrial protein PTPIP51 to regulate calcium homeostasis', *Hum Mol Genet*, 21: 1299-311.

Debalkie Animut, M., M. B. Sorrie, Y. W. Birhanu, and M. Y. Teshale. 2019. 'High prevalence of neurocognitive disorders observed among adult people living with HIV/AIDS in Southern Ethiopia: A cross-sectional study', *PLoS One*, 14: e0204636.

Desire, N., A. Dehee, V. Schneider, C. Jacomet, C. Goujon, P. M. Girard, W. Rozenbaum, and J. C. Nicolas. 2001. 'Quantification of human immunodeficiency virus type 1 proviral load by a TaqMan real-time PCR assay', *J Clin Microbiol*, 39: 1303-10.

Dong, H., N. M. Adams, Y. Xu, J. Cao, D. S. J. Allan, J. R. Carlyle, X. Chen, J. C. Sun, and L. H. Glimcher. 2019. 'The IRE1 endoplasmic reticulum stress sensor activates natural killer cell immunity in part by regulating c-Myc', *Nat Immunol*, 20: 865-78.

Edara, V. V., A. Ghorpade, and K. Borgmann. 2020. 'Insights into the Gene Expression Profiles of Active and Restricted Red/Green-HIV(+) Human Astrocytes: Implications for Shock or Lock Therapies in the Brain', *J Virol*, 94.

Edara, V. V., S. Nooka, J. Proulx, S. Stacy, A. Ghorpade, and K. Borgmann. 2020. 'beta-Catenin Regulates Wound Healing and IL-6 Expression in Activated Human Astrocytes', *Biomedicines*, 8.

Elesela, S., and N. W. Lukacs. 2021. 'Role of Mitochondria in Viral Infections', *Life (Basel)*, 11.

Ellis, R. J., M. E. Childers, M. Cherner, D. Lazzaretto, S. Letendre, and I. Grant. 2003. 'Increased human immunodeficiency virus loads in active methamphetamine users are explained by reduced effectiveness of antiretroviral therapy', *J Infect Dis*, 188: 1820-6.

Eng, L. F., and R. S. Ghirnikar. 1994. 'GFAP and astrogliosis', *Brain pathology*, 4: 229-37.

Erpapazoglou, Z., F. Mouton-Liger, and O. Corti. 2017. 'From dysfunctional endoplasmic reticulum-mitochondria coupling to neurodegeneration', *Neurochem Int*, 109: 171-83.

Fan, Y., and J. J. He. 2016. 'HIV-1 Tat Induces Unfolded Protein Response and Endoplasmic Reticulum Stress in Astrocytes and Causes Neurotoxicity through Glial Fibrillary Acidic Protein (GFAP) Activation and Aggregation', *J Biol Chem*, 291: 22819-29.

Fatima, M., B. Prajapati, K. Saleem, R. Kumari, C. Mohindar Singh Singal, and P. Seth. 2017. 'Novel insights into role of miR-320a-VDAC1 axis in astrocyte-mediated neuronal damage in neuroAIDS', *Glia*, 65: 250-63.

Fattakhov, N., S. Torices, M. Stangis, M. Park, and M. Toborek. 2021. 'Synergistic Impairment of the Neurovascular Unit by HIV-1 Infection and Methamphetamine Use: Implications for HIV-1-Associated Neurocognitive Disorders', *Viruses*, 13.

Feier, G., S. S. Valvassori, J. Lopes-Borges, R. B. Varela, D. V. Bavaresco, G. Scaini, M. O. Morais, M. L. Andersen, E. L. Streck, and J. Quevedo. 2012. 'Behavioral changes and brain energy metabolism dysfunction in rats treated with methamphetamine or dextroamphetamine', *Neurosci Lett*, 530: 75-9.

Fields, J. A., and R. J. Ellis. 2019. 'HIV in the cART era and the mitochondrial: immune interface in the CNS', *Int Rev Neurobiol*, 145: 29-65.

Fields, J. A., E. Serger, S. Campos, A. S. Divakaruni, C. Kim, K. Smith, M. Trejo, A. Adame, B. Spencer, E. Rockenstein, A. N. Murphy, R. J. Ellis, S. Letendre, I. Grant, and E. Masliah. 2016. 'HIV alters neuronal mitochondrial fission/fusion in the brain during HIV-associated neurocognitive disorders', *Neurobiol Dis*, 86: 154-69.

Filadi, R., E. Greotti, G. Turacchio, A. Luini, T. Pozzan, and P. Pizzo. 2015. 'Mitofusin 2 ablation increases endoplasmic reticulum-mitochondria coupling', *Proc Natl Acad Sci U S A*, 112: E2174-81.

———. 2016. 'Presenilin 2 Modulates Endoplasmic Reticulum-Mitochondria Coupling by Tuning the Antagonistic Effect of Mitofusin 2', *Cell Rep*, 15: 2226-38.

Filadi, R., P. Theurey, and P. Pizzo. 2017. 'The endoplasmic reticulum-mitochondria coupling in health and disease: Molecules, functions and significance', *Cell Calcium*, 62: 1-15.

Friedman, J. R., L. L. Lackner, M. West, J. R. DiBenedetto, J. Nunnari, and G. K. Voeltz. 2011. 'ER tubules mark sites of mitochondrial division', *Science*, 334: 358-62.

Friedman, J. R., and J. Nunnari. 2014. 'Mitochondrial form and function', *Nature*, 505: 335-43.

Friend, D. M., and K. A. Keefe. 2013. 'Glial reactivity in resistance to methamphetamine-induced neurotoxicity', *J Neurochem*, 125: 566-74.

Gabuzda, D., B. D. Jamieson, R. G. Collman, M. M. Lederman, T. H. Burdo, S. G. Deeks, D. P. Dittmer, H. S. Fox, N. T. Funderburg, S. G. Pahwa, I. Pandrea, C. C. Wilson, and P. W. Hunt. 2020. 'Pathogenesis of Aging and Age-related Comorbidities in People with HIV: Highlights from the HIV ACTION Workshop', *Pathog Immun*, 5: 143-74.

Galla, L., N. Redolfi, T. Pozzan, P. Pizzo, and E. Greotti. 2020. 'Intracellular Calcium Dysregulation by the Alzheimer's Disease-Linked Protein Presenilin 2', *Int J Mol Sci*, 21.

Gardner, J., K. Borgmann, M. S. Deshpande, A. Dhar, L. Wu, R. Persidsky, and A. Ghorpade. 2006. 'Potential mechanisms for astrocyte-TIMP-1 downregulation in chronic inflammatory diseases', *Journal of Neuroscience Research*, 83: 1281-92.

Garrido-Maraver, J., S. H. Y. Loh, and L. M. Martins. 2020. 'Forcing contacts between mitochondria and the endoplasmic reticulum extends lifespan in a Drosophila model of Alzheimer's disease', *Biol Open*, 9.

Gautier, C. A., Z. Erpapazoglou, F. Mouton-Liger, M. P. Muriel, F. Cormier, S. Bigou, S. Duffaure, M. Girard, B. Foret, A. Iannielli, V. Broccoli, C. Dalle, D. Bohl, P. P. Michel, J. C. Corvol, A. Brice, and O. Corti. 2016. 'The endoplasmic reticulum-mitochondria interface is perturbed in PARK2 knockout mice and patients with PARK2 mutations', *Hum Mol Genet*, 25: 2972-84.

Gbel, J., E. Engelhardt, P. Pelzer, V. Sakthivelu, H. M. Jahn, M. Jevtic, K. Folz-Donahue, C. Kukat, A. Schauss, C. K. Frese, P. Giavalisco, A. Ghanem, K. K. Conzelmann, E. Motori, and M. Bergami. 2020. 'Mitochondria-Endoplasmic Reticulum Contacts in Reactive Astrocytes Promote Vascular Remodeling', *Cell Metab*, 31: 791-808 e8.

Gelmetti, V., P. De Rosa, L. Torosantucci, E. S. Marini, A. Romagnoli, M. Di Rienzo, G. Arena, D. Vignone, G. M. Fimia, and E. M. Valente. 2017. 'PINK1 and BECN1 relocalize at mitochondria-associated membranes during mitophagy and promote ER-mitochondria tethering and autophagosome formation', *Autophagy*, 13: 654-69.

Ghemrawi, R., and M. Khair. 2020. 'Endoplasmic Reticulum Stress and Unfolded Protein Response in Neurodegenerative Diseases', *Int J Mol Sci*, 21.

Ghosh, A. K., A. Sarkar, and H. Mitsuya. 2017. 'HIV-Associated Neurocognitive Disorder (HAND) and the Prospect of Brain-Penetrating Protease Inhibitors for Antiretroviral Treatment', *Med Res Arch*, 5.

Giorgi, C., S. Marchi, and P. Pinton. 2018. 'The machineries, regulation and cellular functions of mitochondrial calcium', *Nat Rev Mol Cell Biol*, 19: 713-30.

Gkogkas, C., S. Middleton, A. M. Kremer, C. Wardrope, M. Hannah, T. H. Gillingwater, and P. Skehel. 2008. 'VAPB interacts with and modulates the activity of ATF6', *Hum Mol Genet*, 17: 1517-26.

Gomez-Suaga, P., J. M. Bravo-San Pedro, R. A. Gonzalez-Polo, J. M. Fuentes, and M. Niso-Santano. 2018. 'ER-mitochondria signaling in Parkinson's disease', *Cell Death Dis*, 9: 337.

Gomez-Suaga, P., S. Paillusson, R. Stoica, W. Noble, D. P. Hanger, and C. C. J. Miller. 2017. 'The ER-Mitochondria Tethering Complex VAPB-PTPIP51 Regulates Autophagy', *Curr Biol*, 27: 371-85.

Gomez-Suaga, P., B. G. Perez-Nievas, E. B. Glennon, D. H. W. Lau, S. Paillusson, G. M. Morotz, T. Cali, P. Pizzo, W. Noble, and C. C. J. Miller. 2019. 'The VAPB-PTPIP51 endoplasmic reticulum-mitochondria tethering proteins are present in neuronal synapses and regulate synaptic activity', *Acta Neuropathol Commun*, 7: 35.

Grimm, A., and A. Eckert. 2017. 'Brain aging and neurodegeneration: from a mitochondrial point of view', *J Neurochem*, 143: 418-31.

Guardia-Laguarta, C., E. Area-Gomez, C. Rub, Y. Liu, J. Magrane, D. Becker, W. Voos, E. A. Schon, and S. Przedborski. 2014. 'alpha-Synuclein is localized to mitochondria-associated ER membranes', *J Neurosci*, 34: 249-59.

Halliday, M., and G. R. Mallucci. 2014. 'Targeting the unfolded protein response in neurodegeneration: A new approach to therapy', *Neuropharmacology*, 76 Pt A: 169-74.

Hategan, A., E. Masliah, and A. Nath. 2019. 'HIV and Alzheimer's disease: complex interactions of HIV-Tat with amyloid beta peptide and Tau protein', *J Neurovirol*, 25: 648-60.

Haughey, N. J., and M. P. Mattson. 2002. 'Calcium dysregulation and neuronal apoptosis by the HIV-1 proteins Tat and gp120', *J Acquir Immune Defic Syndr*, 31 Suppl 2: S55-61.

Hayashi, T., and T. P. Su. 2007. 'Sigma-1 receptor chaperones at the ER-mitochondrion interface regulate Ca(2+) signaling and cell survival', *Cell*, 131: 596-610.

He, X., W. Yang, Z. Zeng, Y. Wei, J. Gao, B. Zhang, L. Li, L. Liu, Y. Wan, Q. Zeng, Z. Gong, L. Liu, H. Zhang, Y. Li, S. Yang, T. Hu, L. Wu, E. Masliah, S. Huang, and H. Cao. 2020. 'NLRP3-dependent pyroptosis is required for HIV-1 gp120-induced neuropathology', *Cell Mol Immunol*, 17: 283-99.

Heaton, R. K., D. R. Franklin, R. J. Ellis, J. A. McCutchan, S. L. Letendre, S. Leblanc, S. H. Corkran, N. A. Duarte, D. B. Clifford, S. P. Woods, A. C. Collier, C. M. Marra, S. Morgello, M. R. Mindt, M. J. Taylor, T. D. Marcotte, J. H. Atkinson, T. Wolfson, B. B. Gelman, J. C. McArthur, D. M. Simpson, I. Abramson, A. Gamst, C. Fennema-Notestine, T. L. Jernigan, J. Wong, and I. Grant. 2011. 'HIV-associated neurocognitive disorders before and during the era of combination antiretroviral therapy: differences in rates, nature, and predictors', *Journal of neurovirology*, 17: 3-16.

Hedskog, L., C. M. Pinho, R. Filadi, A. Ronnback, L. Hertwig, B. Wiehager, P. Larssen, S. Gellhaar, A. Sandebring, M. Westerlund, C. Graff, B. Winblad, D. Galter, H. Behbahani, P. Pizzo, E. Glaser, and M. Ankarcrona. 2013. 'Modulation of the endoplasmic reticulum-

mitochondria interface in Alzheimer's disease and related models', *Proc Natl Acad Sci U S A*, 110: 7916-21.

Herrera-Cruz, M. S., and T. Simmen. 2017. 'Over Six Decades of Discovery and Characterization of the Architecture at Mitochondria-Associated Membranes (MAMs)', *Advances in experimental medicine and biology*, 997: 13-31.

Hoefer, M. M., A. B. Sanchez, R. Maung, C. M. de Rozieres, I. C. Catalan, C. C. Dowling, V. E. Thaney, J. Pina-Crespo, D. Zhang, A. J. Roberts, and M. Kaul. 2015. 'Combination of methamphetamine and HIV-1 gp120 causes distinct long-term alterations of behavior, gene expression, and injury in the central nervous system', *Experimental neurology*, 263: 221-34.

Honrath, B., I. Metz, N. Bendridi, J. Rieusset, C. Culmsee, and A. M. Dolga. 2017. 'Glucose-regulated protein 75 determines ER-mitochondrial coupling and sensitivity to oxidative stress in neuronal cells', *Cell Death Discov*, 3: 17076.

Hu, X. T. 2016. 'HIV-1 Tat-Mediated Calcium Dysregulation and Neuronal Dysfunction in Vulnerable Brain Regions', *Curr Drug Targets*, 17: 4-14.

Huang, C. Y., S. F. Chiang, T. Y. Lin, S. H. Chiou, and K. C. Chow. 2012. 'HIV-1 Vpr triggers mitochondrial destruction by impairing Mfn2-mediated ER-mitochondria interaction', *PLoS One*, 7: e33657.

Huntington, T. E., and R. Srinivasan. 2021. 'Astrocytic mitochondria in adult mouse brain slices show spontaneous calcium influx events with unique properties', *Cell Calcium*, 96: 102383.

Israel, S. M., S. Hassanzadeh-Behbahani, P. E. Turkeltaub, D. J. Moore, R. J. Ellis, and X. Jiang. 2019. 'Different roles of frontal versus striatal atrophy in HIV-associated neurocognitive disorders', *Hum Brain Mapp*, 40: 3010-26.

Iwasawa, R., A. L. Mahul-Mellier, C. Datler, E. Pazarentzos, and S. Grimm. 2011. 'Fis1 and Bap31 bridge the mitochondria-ER interface to establish a platform for apoptosis induction', *EMBO J*, 30: 556-68.

Jablonski, S. A., M. T. Williams, and C. V. Vorhees. 2016. 'Mechanisms involved in the neurotoxic and cognitive effects of developmental methamphetamine exposure', *Birth Defects Res C Embryo Today*, 108: 131-41.

Janikiewicz, J., J. Szymanski, D. Malinska, P. Patalas-Krawczyk, B. Michalska, J. Duszynski, C. Giorgi, M. Bonora, A. Dobrzyn, and M. R. Wieckowski. 2018. 'Mitochondria-associated membranes in aging and senescence: structure, function, and dynamics', *Cell Death Dis*, 9: 332.

Jayant, R. D., D. Sosa, A. Kaushik, V. Atluri, A. Vashist, A. Tomitaka, and M. Nair. 2016. 'Current status of non-viral gene therapy for CNS disorders', *Expert Opin Drug Deliv*, 13: 1433-45.

Jia, J., J. Cheng, C. Wang, and X. Zhen. 2018. 'Sigma-1 Receptor-Modulated Neuroinflammation in Neurological Diseases', *Front Cell Neurosci*, 12: 314.

Jiang, X., Y. Wei, T. Zhang, Z. Zhang, S. Qiu, X. Zhou, and S. Zhang. 2017. 'Effects of GSK2606414 on cell proliferation and endoplasmic reticulum stressassociated gene expression in retinal pigment epithelial cells', *Mol Med Rep*, 15: 3105-10.

Jin, H. S., H. W. Suh, S. J. Kim, and E. K. Jo. 2017. 'Mitochondrial Control of Innate Immunity and Inflammation', *Immune Netw*, 17: 77-88.

Jones, G. J., N. L. Barsby, E. A. Cohen, J. Holden, K. Harris, P. Dickie, J. Jhamandas, and C. Power. 2007. 'HIV-1 Vpr causes neuronal apoptosis and in vivo neurodegeneration', *J Neurosci*, 27: 3703-11.

Joshi, C. R., V. Labhasetwar, and A. Ghorpade. 2017. 'Destination Brain: the Past, Present, and Future of Therapeutic Gene Delivery', *J Neuroimmune Pharmacol*, 12: 51-83.

Joshi, C. R., V. Raghavan, S. Vijayaraghavalu, Y. Gao, M. Saraswathy, V. Labhasetwar, and A. Ghorpade. 2018. 'Reaching for the Stars in the Brain: Polymer-Mediated Gene Delivery to Human Astrocytes', *Mol Ther Nucleic Acids*, 12: 645-57.

Joshi, C. R., S. Stacy, N. Sumien, A. Ghorpade, and K. Borgmann. 2020. 'Astrocyte HIV-1 Tat Differentially Modulates Behavior and Brain MMP/TIMP Balance During Short and Prolonged Induction in Transgenic Mice', *Front Neurol*, 11: 593188.

Kesby, J. P., R. K. Heaton, J. W. Young, A. Umlauf, S. P. Woods, S. L. Letendre, A. Markou, I. Grant, and S. Semenova. 2015. 'Methamphetamine Exposure Combined with HIV-1 Disease or gp120 Expression: Comparison of Learning and Executive Functions in Humans and Mice', *Neuropsychopharmacology*, 40: 1899-909.

Khan, N., N. J. Haughey, A. Nath, and J. D. Geiger. 2019. 'Involvement of organelles and inter-organellar signaling in the pathogenesis of HIV-1 associated neurocognitive disorder and Alzheimer's disease', *Brain Res*, 1722: 146389.

Kim, J., J. H. Yoon, and Y. S. Kim. 2013. 'HIV-1 Tat interacts with and regulates the localization and processing of amyloid precursor protein', *PLoS One*, 8: e77972.

Kou, W., S. Banerjee, J. Eudy, L. M. Smith, R. Persidsky, K. Borgmann, L. Wu, N. Sakhuja, M. S. Deshpande, T. F. Walseth, and A. Ghorpade. 2009. 'CD38 regulation in activated astrocytes: implications for neuroinflammation and HIV-1 brain infection', *J Neurosci Res*, 87: 2326-39.

Krasnova, I. N., and J. L. Cadet. 2009. 'Methamphetamine toxicity and messengers of death', *Brain Res Rev*, 60: 379-407.

Kruman, II, A. Nath, and M. P. Mattson. 1998. 'HIV-1 protein Tat induces apoptosis of hippocampal neurons by a mechanism involving caspase activation, calcium overload, and oxidative stress', *Experimental neurology*, 154: 276-88.

Lara-Reyna, S., T. Scambler, J. Holbrook, C. Wong, H. H. Jarosz-Griffiths, F. Martinon, S. Savic, D. Peckham, and M. F. McDermott. 2019. 'Metabolic Reprograming of Cystic Fibrosis Macrophages via the IRE1alpha Arm of the Unfolded Protein Response Results in Exacerbated Inflammation', *Front Immunol*, 10: 1789.

Lau, D. H. W., N. Hartopp, N. J. Welsh, S. Mueller, E. B. Glennon, G. M. Morotz, A. Annibali, P. Gomez-Suaga, R. Stoica, S. Paillusson, and C. C. J. Miller. 2018. 'Disruption of ER-mitochondria signalling in fronto-temporal dementia and related amyotrophic lateral sclerosis', *Cell Death Dis*, 9: 327.

Lau, D. H. W., S. Paillusson, N. Hartopp, H. Rupawala, G. M. Morotz, P. Gomez-Suaga, J. Greig, C. Troakes, W. Noble, and C. C. J. Miller. 2020. 'Disruption of endoplasmic reticulum-mitochondria tethering proteins in post-mortem Alzheimer's disease brain', *Neurobiol Dis*, 143: 105020.

Leal, N. S., G. Dentoni, B. Schreiner, O. P. Kamarainen, N. Partanen, S. K. Herukka, A. M. Koivisto, M. Hiltunen, T. Rauramaa, V. Leinonen, and M. Ankarcrona. 2018. 'Alterations

in mitochondria-endoplasmic reticulum connectivity in human brain biopsies from idiopathic normal pressure hydrocephalus patients', *Acta Neuropathol Commun*, 6: 102.
Leal, N. S., G. Dentoni, B. Schreiner, L. Naia, A. Piras, C. Graff, A. Cattaneo, G. Meli, M. Hamasaki, P. Nilsson, and M. Ankarcrona. 2020. 'Amyloid Beta-Peptide Increases Mitochondria-Endoplasmic Reticulum Contact Altering Mitochondrial Function and Autophagosome Formation in Alzheimer's Disease-Related Models', *Cells*, 9.
Leal, N. S., and L. M. Martins. 2021. 'Mind the Gap: Mitochondria and the Endoplasmic Reticulum in Neurodegenerative Diseases', *Biomedicines*, 9.
Leal, N. S., B. Schreiner, C. M. Pinho, R. Filadi, B. Wiehager, H. Karlstrom, P. Pizzo, and M. Ankarcrona. 2016. 'Mitofusin-2 knockdown increases ER-mitochondria contact and decreases amyloid beta-peptide production', *J Cell Mol Med*, 20: 1686-95.
Lebeau, J., J. M. Saunders, V. W. R. Moraes, A. Madhavan, N. Madrazo, M. C. Anthony, and R. L. Wiseman. 2018. 'The PERK Arm of the Unfolded Protein Response Regulates Mitochondrial Morphology during Acute Endoplasmic Reticulum Stress', *Cell Rep*, 22: 2827-36.
Li, G. H., D. Maric, E. O. Major, and A. Nath. 2020. 'Productive HIV infection in astrocytes can be established via a nonclassical mechanism', *Aids*, 34: 963-78.
Li, K., J. Li, J. Zheng, and S. Qin. 2019. 'Reactive Astrocytes in Neurodegenerative Diseases', *Aging Dis*, 10: 664-75.
Liang, H., X. Wang, H. Chen, L. Song, L. Ye, S. H. Wang, Y. J. Wang, L. Zhou, and W. Z. Ho. 2008. 'Methamphetamine enhances HIV infection of macrophages', *Am J Pathol*, 172: 1617-24.
Liao, Y., Y. Dong, and J. Cheng. 2017. 'The Function of the Mitochondrial Calcium Uniporter in Neurodegenerative Disorders', *Int J Mol Sci*, 18.
———. 2020. 'The Molecular Determinants of Mitochondrial Membrane Contact With ER, Lysosomes and Peroxisomes in Neuronal Physiology and Pathology', *Front Cell Neurosci*, 14: 194.
Lindl, K. A., C. Akay, Y. Wang, M. G. White, and K. L. Jordan-Sciutto. 2007. 'Expression of the endoplasmic reticulum stress response marker, BiP, in the central nervous system of HIV-positive individuals', *Neuropathol Appl Neurobiol*, 33: 658-69.
Liu, L., X. Qi, Z. Chen, L. Shaw, J. Cai, L. H. Smith, M. B. Grant, and M. E. Boulton. 2013. 'Targeting the IRE1alpha/XBP1 and ATF6 arms of the unfolded protein response enhances VEGF blockade to prevent retinal and choroidal neovascularization', *Am J Pathol*, 182: 1412-24.
Liu, L., L. Xu, S. Zhang, D. Wang, G. Dong, H. Chen, X. Li, C. Shu, and R. Wang. 2018. 'STF-083010, an inhibitor of XBP1 splicing, attenuates acute renal failure in rats by suppressing endoplasmic reticulum stress-induced apoptosis and inflammation', *Exp Anim*, 67: 373-82.
Liu, Y., X. Ma, H. Fujioka, J. Liu, S. Chen, and X. Zhu. 2019. 'DJ-1 regulates the integrity and function of ER-mitochondria association through interaction with IP3R3-Grp75-VDAC1', *Proc Natl Acad Sci U S A*, 116: 25322-28.
Luo, X., and J. J. He. 2015. 'Cell-cell contact viral transfer contributes to HIV infection and persistence in astrocytes', *J Neurovirol*, 21: 66-80.

Luten, J., C. F. van Nostrum, S. C. De Smedt, and W. E. Hennink. 2008. 'Biodegradable polymers as non-viral carriers for plasmid DNA delivery', *J Control Release*, 126: 97-110.

Lutgen, V., S. D. Narasipura, H. J. Barbian, M. Richards, J. Wallace, R. Razmpour, T. Buzhdygan, S. H. Ramirez, L. Prevedel, E. A. Eugenin, and L. Al-Harthi. 2020. 'HIV infects astrocytes in vivo and egresses from the brain to the periphery', *PLoS Pathog*, 16: e1008381.

Ma, R., L. Yang, F. Niu, and S. Buch. 2016. 'HIV Tat-Mediated Induction of Human Brain Microvascular Endothelial Cell Apoptosis Involves Endoplasmic Reticulum Stress and Mitochondrial Dysfunction', *Mol Neurobiol*, 53: 132-42.

MacDuffie, K. E., G. G. Brown, B. S. McKenna, T. T. Liu, M. J. Meloy, B. Tawa, S. Archibald, C. Fennema-Notestine, J. H. Atkinson, Jr., R. J. Ellis, S. L. Letendre, J. R. Hesselink, M. Cherner, I. Grant, and Tmarc Group. 2018. 'Effects of HIV Infection, methamphetamine dependence and age on cortical thickness, area and volume', *Neuroimage Clin*, 20: 1044-52.

Mackiewicz, M. M., C. Overk, C. L. Achim, and E. Masliah. 2019. 'Pathogenesis of age-related HIV neurodegeneration', *J Neurovirol*, 25: 622-33.

Malli, R., and W. F. Graier. 2019. 'IRE1alpha modulates ER and mitochondria crosstalk', *Nat Cell Biol*, 21: 667-68.

Mamik, M. K., S. Banerjee, T. F. Walseth, R. Hirte, L. Tang, K. Borgmann, and A. Ghorpade. 2011. 'HIV-1 and IL-1beta regulate astrocytic CD38 through mitogen-activated protein kinases and nuclear factor-kappaB signaling mechanisms', *J Neuroinflammation*, 8: 145.

Manfredi, G., and H. Kawamata. 2016. 'Mitochondria and endoplasmic reticulum crosstalk in amyotrophic lateral sclerosis', *Neurobiol Dis*, 90: 35-42.

Manninen, A., and K. Saksela. 2002. 'HIV-1 Nef interacts with inositol trisphosphate receptor to activate calcium signaling in T cells', *J Exp Med*, 195: 1023-32.

Marchi, S., M. Bittremieux, S. Missiroli, C. Morganti, S. Patergnani, L. Sbano, A. Rimessi, M. Kerkhofs, J. B. Parys, G. Bultynck, C. Giorgi, and P. Pinton. 2017. 'Endoplasmic Reticulum-Mitochondria Communication Through Ca(2+) Signaling: The Importance of Mitochondria-Associated Membranes (MAMs)', *Advances in experimental medicine and biology*, 997: 49-67.

Martinez, A., N. Lopez, C. Gonzalez, and C. Hetz. 2019. 'Targeting of the unfolded protein response (UPR) as therapy for Parkinson's disease', *Biol Cell*, 111: 161-68.

Mathe, G., C. Morette, M. Hallard, and D. Blanquet. 1997. 'Combinations of three or four HIV virostatics applied in short sequences which differ from each other by drug rotation. Preliminary results of the viral loads and CD4 numbers', *Biomed Pharmacother*, 51: 417-26.

Matias, I., J. Morgado, and F. C. A. Gomes. 2019. 'Astrocyte Heterogeneity: Impact to Brain Aging and Disease', *Front Aging Neurosci*, 11: 59.

Meeker, R. B., W. Poulton, G. Clary, M. Schriver, and F. M. Longo. 2016. 'Novel p75 neurotrophin receptor ligand stabilizes neuronal calcium, preserves mitochondrial movement and protects against HIV associated neuropathogenesis', *Experimental neurology*, 275 Pt 1: 182-98.

Midoux, Patrick, Gilles Breuzard, Jean P Gomez, and Chantal Pichon. 2008. 'Polymer-based gene delivery: a current review on the uptake and intracellular trafficking of polyplexes', *Current gene therapy*, 8: 335-52.

Miller, S. J. 2018. 'Astrocyte Heterogeneity in the Adult Central Nervous System', *Front Cell Neurosci*, 12: 401.

Misko, A., S. Jiang, I. Wegorzewska, J. Milbrandt, and R. H. Baloh. 2010. 'Mitofusin 2 is necessary for transport of axonal mitochondria and interacts with the Miro/Milton complex', *J Neurosci*, 30: 4232-40.

Misko, A. L., Y. Sasaki, E. Tuck, J. Milbrandt, and R. H. Baloh. 2012. 'Mitofusin2 mutations disrupt axonal mitochondrial positioning and promote axon degeneration', *J Neurosci*, 32: 4145-55.

Modi, S., G. Lopez-Domenech, E. F. Halff, C. Covill-Cooke, D. Ivankovic, D. Melandri, I. L. Arancibia-Carcamo, J. J. Burden, A. R. Lowe, and J. T. Kittler. 2019. 'Miro clusters regulate ER-mitochondria contact sites and link cristae organization to the mitochondrial transport machinery', *Nat Commun*, 10: 4399.

Moltedo, O., P. Remondelli, and G. Amodio. 2019. 'The Mitochondria-Endoplasmic Reticulum Contacts and Their Critical Role in Aging and Age-Associated Diseases', *Front Cell Dev Biol*, 7: 172.

Monaco, A., and A. Fraldi. 2020. 'Protein Aggregation and Dysfunction of Autophagy-Lysosomal Pathway: A Vicious Cycle in Lysosomal Storage Diseases', *Front Mol Neurosci*, 13: 37.

Mori, T., T. Hayashi, E. Hayashi, and T. P. Su. 2013. 'Sigma-1 receptor chaperone at the ER-mitochondrion interface mediates the mitochondrion-ER-nucleus signaling for cellular survival', *PLoS One*, 8: e76941.

Muller, M., U. Ahumada-Castro, M. Sanhueza, C. Gonzalez-Billault, F. A. Court, and C. Cardenas. 2018. 'Mitochondria and Calcium Regulation as Basis of Neurodegeneration Associated With Aging', *Front Neurosci*, 12: 470.

Munoz, J. P., S. Ivanova, J. Sanchez-Wandelmer, P. Martinez-Cristobal, E. Noguera, A. Sancho, A. Diaz-Ramos, M. I. Hernandez-Alvarez, D. Sebastian, C. Mauvezin, M. Palacin, and A. Zorzano. 2013. 'Mfn2 modulates the UPR and mitochondrial function via repression of PERK', *EMBO J*, 32: 2348-61.

Narita, M., M. Suzuki, N. Kuzumaki, M. Miyatake, and T. Suzuki. 2008. 'Implication of activated astrocytes in the development of drug dependence: differences between methamphetamine and morphine', *Ann N Y Acad Sci*, 1141: 96-104.

Natarajaseenivasan, K., B. Cotto, S. Shanmughapriya, A. A. Lombardi, P. K. Datta, M. Madesh, J. W. Elrod, K. Khalili, and D. Langford. 2018. 'Astrocytic metabolic switch is a novel etiology for Cocaine and HIV-1 Tat-mediated neurotoxicity', *Cell Death Dis*, 9: 415.

Nightingale, S., A. Winston, S. Letendre, B. D. Michael, J. C. McArthur, S. Khoo, and T. Solomon. 2014. 'Controversies in HIV-associated neurocognitive disorders', *Lancet Neurol*, 13: 1139-51.

Nishimura, A. L., M. Mitne-Neto, H. C. Silva, A. Richieri-Costa, S. Middleton, D. Cascio, F. Kok, J. R. Oliveira, T. Gillingwater, J. Webb, P. Skehel, and M. Zatz. 2004. 'A mutation in the vesicle-trafficking protein VAPB causes late-onset spinal muscular atrophy and amyotrophic lateral sclerosis', *Am J Hum Genet*, 75: 822-31.

Nooka, S., and A. Ghorpade. 2017. 'HIV-1-associated inflammation and antiretroviral therapy regulate astrocyte endoplasmic reticulum stress responses', *Cell Death Discov*, 3: 17061.

———. 2018. 'Organellar stress intersects the astrocyte endoplasmic reticulum, mitochondria and nucleolus in HIV associated neurodegeneration', *Cell Death Dis*, 9: 317.

Norman, J. P., S. W. Perry, H. M. Reynolds, M. Kiebala, K. L. De Mesy Bentley, M. Trejo, D. J. Volsky, S. B. Maggirwar, S. Dewhurst, E. Masliah, and H. A. Gelbard. 2008. 'HIV-1 Tat activates neuronal ryanodine receptors with rapid induction of the unfolded protein response and mitochondrial hyperpolarization', *PLoS One*, 3: e3731.

Oe, Y., O. Baba, H. Ashida, K. C. Nakamura, and H. Hirase. 2016. 'Glycogen distribution in the microwave-fixed mouse brain reveals heterogeneous astrocytic patterns', *Glia*, 64: 1532-45.

Ojeda, D. S., D. Grasso, J. Urquiza, A. Till, M. I. Vaccaro, and J. Quarleri. 2018. 'Cell Death Is Counteracted by Mitophagy in HIV-Productively Infected Astrocytes but Is Promoted by Inflammasome Activation Among Non-productively Infected Cells', *Front Immunol*, 9: 2633.

Ottolini, D., T. Cali, A. Negro, and M. Brini. 2013. 'The Parkinson disease-related protein DJ-1 counteracts mitochondrial impairment induced by the tumour suppressor protein p53 by enhancing endoplasmic reticulum-mitochondria tethering', *Hum Mol Genet*, 22: 2152-68.

Paillusson, S., P. Gomez-Suaga, R. Stoica, D. Little, P. Gissen, M. J. Devine, W. Noble, D. P. Hanger, and C. C. J. Miller. 2017. 'alpha-Synuclein binds to the ER-mitochondria tethering protein VAPB to disrupt Ca(2+) homeostasis and mitochondrial ATP production', *Acta Neuropathol*, 134: 129-49.

Paillusson, S., R. Stoica, P. Gomez-Suaga, D. H. W. Lau, S. Mueller, T. Miller, and C. C. J. Miller. 2016. 'There's Something Wrong with my MAM; the ER-Mitochondria Axis and Neurodegenerative Diseases', *Trends in neurosciences*, 39: 146-57.

Papageorgiou, M., A. Raza, S. Fraser, K. Nurgali, and V. Apostolopoulos. 2019. 'Methamphetamine and its immune-modulating effects', *Maturitas*, 121: 13-21.

Parikh, N., M. R. Nonnemacher, V. Pirrone, T. Block, A. Mehta, and B. Wigdahl. 2012. 'Substance abuse, HIV-1 and hepatitis', *Curr HIV Res*, 10: 557-71.

Passaro, R. C., J. Pandhare, H. Z. Qian, and C. Dash. 2015. 'The Complex Interaction Between Methamphetamine Abuse and HIV-1 Pathogenesis', *J Neuroimmune Pharmacol*, 10: 477-86.

Perreault, S., O. Bousquet, M. Lauzon, J. Paiement, and N. Leclerc. 2009. 'Increased association between rough endoplasmic reticulum membranes and mitochondria in transgenic mice that express P301L tau', *J Neuropathol Exp Neurol*, 68: 503-14.

Picca, A., R. Calvani, H. J. Coelho-Junior, F. Landi, R. Bernabei, and E. Marzetti. 2020. 'Inter-Organelle Membrane Contact Sites and Mitochondrial Quality Control during Aging: A Geroscience View', *Cells*, 9.

Pinton, P. 2018. 'Mitochondria-associated membranes (MAMs) and pathologies', *Cell Death Dis*, 9: 413.

Pond, R. A., L. F. Collins, and C. D. Lahiri. 2021. 'Sex Differences in Non-AIDS Comorbidities Among People With Human Immunodeficiency Virus', *Open Forum Infect Dis*, 8: ofab558.

Popov, L. D. 2020. 'Mitochondrial biogenesis: An update', *J Cell Mol Med*, 24: 4892-99.

Potash, M. J., W. Chao, G. Bentsman, N. Paris, M. Saini, J. Nitkiewicz, P. Belem, L. Sharer, A. I. Brooks, and D. J. Volsky. 2005. 'A mouse model for study of systemic HIV-1 infection,

antiviral immune responses, and neuroinvasiveness', *Proc Natl Acad Sci U S A*, 102: 3760-5.

Prah, J., A. Winters, K. Chaudhari, J. Hersh, R. Liu, and S. H. Yang. 2019. 'A novel serum free primary astrocyte culture method that mimic quiescent astrocyte phenotype', *J Neurosci Methods*, 320: 50-63.

Prasad, A., R. Kulkarni, A. Shrivastava, S. Jiang, K. Lawson, and J. E. Groopman. 2019. 'Methamphetamine functions as a novel CD4(+) T-cell activator via the sigma-1 receptor to enhance HIV-1 infection', *Sci Rep*, 9: 958.

Priyanka, R. Wadhwa, R. Chaudhuri, T. C. Nag, and P. Seth. 2020. 'Novel role of mortalin in attenuating HIV-1 Tat-mediated astrogliosis', *J Neuroinflammation*, 17: 276.

Proulx, J., C. Joshi, S. Vijayaraghavalu, M. Saraswathy, V. Labhasetwar, A. Ghorpade, and K. Borgmann. 2020. 'Arginine-Modified Polymers Facilitate Poly (Lactide-Co-Glycolide)-Based Nanoparticle Gene Delivery to Primary Human Astrocytes', *Int J Nanomedicine*, 15: 3639-47.

Proulx, J., I. W. Park, and K. Borgmann. 2021. 'Cal'MAM'ity at the Endoplasmic Reticulum-Mitochondrial Interface: A Potential Therapeutic Target for Neurodegeneration and Human Immunodeficiency Virus-Associated Neurocognitive Disorders', *Front Neurosci*, 15: 715945.

Proulx, J., S. Stacy, I. W. Park, and K. Borgmann. 2022. 'A Non-Canonical Role for IRE1alpha Links ER and Mitochondria as Key Regulators of Astrocyte Dysfunction: Implications in Methamphetamine use and HIV-Associated Neurocognitive Disorders', *Front Neurosci*, 16: 906651.

Raeisossadati, R., and M. F. R. Ferrari. 2020. 'Mitochondria-ER Tethering in Neurodegenerative Diseases', *Cellular and molecular neurobiology*.

Rainbolt, T. K., J. M. Saunders, and R. L. Wiseman. 2014. 'Stress-responsive regulation of mitochondria through the ER unfolded protein response', *Trends Endocrinol Metab*, 25: 528-37.

Rao, K. S., A. Ghorpade, and V. Labhasetwar. 2009. 'Targeting anti-HIV drugs to the CNS', *Expert Opin Drug Deliv*, 6: 771-84.

Rawat, P., C. Teodorof-Diedrich, and S. A. Spector. 2019. 'Human immunodeficiency virus Type-1 single-stranded RNA activates the NLRP3 inflammasome and impairs autophagic clearance of damaged mitochondria in human microglia', *Glia*, 67: 802-24.

Reddy, M. K., and V. Labhasetwar. 2009. 'Nanoparticle-mediated delivery of superoxide dismutase to the brain: an effective strategy to reduce ischemia-reperfusion injury', *FASEB J*, 23: 1384-95.

Reddy, M. K., L. Wu, W. Kou, A. Ghorpade, and V. Labhasetwar. 2008. 'Superoxide dismutase-loaded PLGA nanoparticles protect cultured human neurons under oxidative stress', *Appl Biochem Biotechnol*, 151: 565-77.

Remondelli, P., and M. Renna. 2017. 'The Endoplasmic Reticulum Unfolded Protein Response in Neurodegenerative Disorders and Its Potential Therapeutic Significance', *Front Mol Neurosci*, 10: 187.

Riaz, T. A., R. P. Junjappa, M. Handigund, J. Ferdous, H. R. Kim, and H. J. Chae. 2020. 'Role of Endoplasmic Reticulum Stress Sensor IRE1alpha in Cellular Physiology, Calcium, ROS Signaling, and Metaflammation', *Cells*, 9.

Ricci, G., L. Volpi, L. Pasquali, L. Petrozzi, and G. Siciliano. 2009. 'Astrocyte-neuron interactions in neurological disorders', *J Biol Phys*, 35: 317-36.
Rippeth, J. D., R. K. Heaton, C. L. Carey, T. D. Marcotte, D. J. Moore, R. Gonzalez, T. Wolfson, and I. Grant. 2004. 'Methamphetamine dependence increases risk of neuropsychological impairment in HIV infected persons', *J Int Neuropsychol Soc*, 10: 1-14.
Rivière, Gilles J, W Brooks Gentry, and S Michael Owens. 2000. 'Disposition of methamphetamine and its metabolite amphetamine in brain and other tissues in rats after intravenous administration', *Journal of Pharmacology and Experimental Therapeutics*, 292: 1042-47.
Rizzuto, R., D. De Stefani, A. Raffaello, and C. Mammucari. 2012. 'Mitochondria as sensors and regulators of calcium signalling', *Nat Rev Mol Cell Biol*, 13: 566-78.
Robertson, K. R., M. Smurzynski, T. D. Parsons, K. Wu, R. J. Bosch, J. Wu, J. C. McArthur, A. C. Collier, S. R. Evans, and R. J. Ellis. 2007. 'The prevalence and incidence of neurocognitive impairment in the HAART era', *Aids*, 21: 1915-21.
Robson, M. J., R. C. Turner, Z. J. Naser, C. R. McCurdy, J. P. O'Callaghan, J. D. Huber, and R. R. Matsumoto. 2014. 'SN79, a sigma receptor antagonist, attenuates methamphetamine-induced astrogliosis through a blockade of OSMR/gp130 signaling and STAT3 phosphorylation', *Experimental neurology*, 254: 180-9.
Rodriguez-Arribas, M., S. M. S. Yakhine-Diop, J. M. B. Pedro, P. Gomez-Suaga, R. Gomez-Sanchez, G. Martinez-Chacon, J. M. Fuentes, R. A. Gonzalez-Polo, and M. Niso-Santano. 2017. 'Mitochondria-Associated Membranes (MAMs): Overview and Its Role in Parkinson's Disease', *Mol Neurobiol*, 54: 6287-303.
Rosen, D. A., S. M. Seki, A. Fernandez-Castaneda, R. M. Beiter, J. D. Eccles, J. A. Woodfolk, and A. Gaultier. 2019. 'Modulation of the sigma-1 receptor-IRE1 pathway is beneficial in preclinical models of inflammation and sepsis', *Sci Transl Med*, 11.
Roux-Lombard, P., C. Modoux, A. Cruchaud, and J. M. Dayer. 1989. 'Purified blood monocytes from HIV 1-infected patients produce high levels of TNF alpha and IL-1', *Clinical immunology and immunopathology*, 50: 374-84.
Rozzi, S. J., V. Avdoshina, J. A. Fields, and I. Mocchetti. 2018. 'Human immunodeficiency virus Tat impairs mitochondrial fission in neurons', *Cell Death Discov*, 4: 8.
Rozzi, S. J., V. Avdoshina, J. A. Fields, M. Trejo, H. T. Ton, G. P. Ahern, and I. Mocchetti. 2017. 'Human Immunodeficiency Virus Promotes Mitochondrial Toxicity', *Neurotox Res*.
Rubin, L. H., and P. M. Maki. 2021. 'Neurocognitive Complications of HIV Infection in Women: Insights from the WIHS Cohort', *Curr Top Behav Neurosci*, 50: 175-91.
Rubin, L. H., G. N. Neigh, E. E. Sundermann, Y. Xu, E. P. Scully, and P. M. Maki. 2019. 'Sex Differences in Neurocognitive Function in Adults with HIV: Patterns, Predictors, and Mechanisms', *Curr Psychiatry Rep*, 21: 94.
Saito, A., and K. Imaizumi. 2018. 'Unfolded Protein Response-Dependent Communication and Contact among Endoplasmic Reticulum, Mitochondria, and Plasma Membrane', *Int J Mol Sci*, 19.
Salamanca, S. A., E. E. Sorrentino, J. D. Nosanchuk, and L. R. Martinez. 2014. 'Impact of methamphetamine on infection and immunity', *Front Neurosci*, 8: 445.
Schank, M., J. Zhao, J. P. Moorman, and Z. Q. Yao. 2021. 'The Impact of HIV- and ART-Induced Mitochondrial Dysfunction in Cellular Senescence and Aging', *Cells*, 10.

Schousboe, A., S. Scafidi, L. K. Bak, H. S. Waagepetersen, and M. C. McKenna. 2014. 'Glutamate metabolism in the brain focusing on astrocytes', *Adv Neurobiol*, 11: 13-30.

Schouten, J., F. W. Wit, I. G. Stolte, N. A. Kootstra, M. van der Valk, S. E. Geerlings, M. Prins, P. Reiss, and A. GEhIV Cohort Study Group. 2014. 'Cross-sectional comparison of the prevalence of age-associated comorbidities and their risk factors between HIV-infected and uninfected individuals: the AGEhIV cohort study', *Clinical infectious diseases : an official publication of the Infectious Diseases Society of America*, 59: 1787-97.

Schreiner, B., L. Hedskog, B. Wiehager, and M. Ankarcrona. 2015. 'Amyloid-beta peptides are generated in mitochondria-associated endoplasmic reticulum membranes', *J Alzheimers Dis*, 43: 369-74.

Serrat, R., A. Covelo, V. Kouskoff, S. Delcasso, A. Ruiz-Calvo, N. Chenouard, C. Stella, C. Blancard, B. Salin, F. Julio-Kalajzic, A. Cannich, F. Massa, M. Varilh, S. Deforges, L. M. Robin, D. De Stefani, A. Busquets-Garcia, F. Gambino, A. Beyeler, S. Pouvreau, and G. Marsicano. 2021. 'Astroglial ER-mitochondria calcium transfer mediates endocannabinoid-dependent synaptic integration', *Cell Rep*, 37: 110133.

Shah, A., and A. Kumar. 2016. 'Methamphetamine-mediated endoplasmic reticulum (ER) stress induces type-1 programmed cell death in astrocytes via ATF6, IRE1alpha and PERK pathways', *Oncotarget*.

Shah, A., S. Kumar, S. D. Simon, D. P. Singh, and A. Kumar. 2013. 'HIV gp120- and methamphetamine-mediated oxidative stress induces astrocyte apoptosis via cytochrome P450 2E1', *Cell Death Dis*, 4: e850.

Shah, A., P. S. Silverstein, D. P. Singh, and A. Kumar. 2012. 'Involvement of metabotropic glutamate receptor 5, AKT/PI3K signaling and NF-kappaB pathway in methamphetamine-mediated increase in IL-6 and IL-8 expression in astrocytes', *J Neuroinflammation*, 9: 52.

Shah, A., N. K. Vaidya, H. K. Bhat, and A. Kumar. 2016. 'HIV-1 gp120 induces type-1 programmed cell death through ER stress employing IRE1alpha, JNK and AP-1 pathway', *Sci Rep*, 6: 18929.

Shelton, M. N., M. B. Huang, S. A. Ali, M. D. Powell, and V. C. Bond. 2012. 'Secretion modification region-derived peptide disrupts HIV-1 Nef's interaction with mortalin and blocks virus and Nef exosome release', *J Virol*, 86: 406-19.

Shim, J., T. Umemura, E. Nothstein, and C. Rongo. 2004. 'The unfolded protein response regulates glutamate receptor export from the endoplasmic reticulum', *Molecular biology of the cell*, 15: 4818-28.

Shirokova, O. M., P. V. Pchelin, and I. V. Mukhina. 2020. 'MERCs. The Novel Assistant to Neurotransmission?', *Front Neurosci*, 14: 589319.

Silva, J. G., N. P. Martins, R. Henriques, and H. Soares. 2016. 'HIV-1 Nef Impairs the Formation of Calcium Membrane Territories Controlling the Signaling Nanoarchitecture at the Immunological Synapse', *J Immunol*, 197: 4042-52.

Simioni, S., M. Cavassini, J. M. Annoni, A. Rimbault Abraham, I. Bourquin, V. Schiffer, A. Calmy, J. P. Chave, E. Giacobini, B. Hirschel, and R. A. Du Pasquier. 2010. 'Cognitive dysfunction in HIV patients despite long-standing suppression of viremia', *Aids*, 24: 1243-50.

Simmen, T., J. E. Aslan, A. D. Blagoveshchenskaya, L. Thomas, L. Wan, Y. Xiang, S. F. Feliciangeli, C. H. Hung, C. M. Crump, and G. Thomas. 2005. 'PACS-2 controls endoplasmic reticulum-mitochondria communication and Bid-mediated apoptosis', *EMBO J*, 24: 717-29.

Singhal, A., V. B. Morris, V. Labhasetwar, and A. Ghorpade. 2013. 'Nanoparticle-mediated catalase delivery protects human neurons from oxidative stress', *Cell Death Dis*, 4: e903.

Skowronska, M., M. McDonald, M. Velichkovska, A. R. Leda, M. Park, and M. Toborek. 2018. 'Methamphetamine increases HIV infectivity in neural progenitor cells', *J Biol Chem*, 293: 296-311.

Son, J., S. Mogre, F. E. Chalmers, J. Ibinson, S. Worrell, and A. B. Glick. 2021. 'The Endoplasmic Reticulum Stress Sensor IRE1alpha Regulates the UV DNA Repair Response through the Control of Intracellular Calcium Homeostasis', *J Invest Dermatol*.

Son, S. M., J. Byun, S. E. Roh, S. J. Kim, and I. Mook-Jung. 2014. 'Reduced IRE1alpha mediates apoptotic cell death by disrupting calcium homeostasis via the InsP3 receptor', *Cell Death Dis*, 5: e1188.

Soontornniyomkij, V., J. P. Kesby, E. E. Morgan, A. Bischoff-Grethe, A. Minassian, G. G. Brown, I. Grant, and Aids Research Center Group Translational Methamphetamine. 2016. 'Effects of HIV and Methamphetamine on Brain and Behavior: Evidence from Human Studies and Animal Models', *J Neuroimmune Pharmacol*, 11: 495-510.

Spudich, S., K. R. Robertson, R. J. Bosch, R. T. Gandhi, J. C. Cyktor, H. Mar, B. J. Macatangay, C. M. Lalama, C. Rinaldo, A. C. Collier, C. Godfrey, J. J. Eron, D. McMahon, J. L. Jacobs, D. Koontz, E. Hogg, A. Vecchio, and J. W. Mellors. 2019. 'Persistent HIV-infected cells in cerebrospinal fluid are associated with poorer neurocognitive performance', *J Clin Invest*, 129: 3339-46.

Stalder, H., M. C. Hoener, and R. D. Norcross. 2011. 'Selective antagonists of mouse trace amine-associated receptor 1 (mTAAR1): discovery of EPPTB (RO5212773)', *Bioorg Med Chem Lett*, 21: 1227-31.

Stoica, R., K. J. De Vos, S. Paillusson, S. Mueller, R. M. Sancho, K. F. Lau, G. Vizcay-Barrena, W. L. Lin, Y. F. Xu, J. Lewis, D. W. Dickson, L. Petrucelli, J. C. Mitchell, C. E. Shaw, and C. C. Miller. 2014. 'ER-mitochondria associations are regulated by the VAPB-PTPIP51 interaction and are disrupted by ALS/FTD-associated TDP-43', *Nat Commun*, 5: 3996.

Stoica, R., S. Paillusson, P. Gomez-Suaga, J. C. Mitchell, D. H. Lau, E. H. Gray, R. M. Sancho, G. Vizcay-Barrena, K. J. De Vos, C. E. Shaw, D. P. Hanger, W. Noble, and C. C. Miller. 2016. 'ALS/FTD-associated FUS activates GSK-3beta to disrupt the VAPB-PTPIP51 interaction and ER-mitochondria associations', *EMBO Rep*, 17: 1326-42.

Suzuki, J., K. Kanemaru, K. Ishii, M. Ohkura, Y. Okubo, and M. Iino. 2014. 'Imaging intraorganellar Ca2+ at subcellular resolution using CEPIA', *Nat Commun*, 5: 4153.

Sweeney, P., H. Park, M. Baumann, J. Dunlop, J. Frydman, R. Kopito, A. McCampbell, G. Leblanc, A. Venkateswaran, A. Nurmi, and R. Hodgson. 2017. 'Protein misfolding in neurodegenerative diseases: implications and strategies', *Transl Neurodegener*, 6: 6.

Swinton, M. K., A. Carson, F. Telese, A. B. Sanchez, B. Soontornniyomkij, L. Rad, I. Batki, B. Quintanilla, J. Perez-Santiago, C. L. Achim, S. Letendre, R. J. Ellis, I. Grant, A. N. Murphy, and J. A. Fields. 2019. 'Mitochondrial biogenesis is altered in HIV+ brains exposed to ART: Implications for therapeutic targeting of astroglia', *Neurobiol Dis*, 130: 104502.

Szabo, L., A. Eckert, and A. Grimm. 2020. 'Insights into Disease-Associated Tau Impact on Mitochondria', *Int J Mol Sci*, 21.

Tambini, M. D., M. Pera, E. Kanter, H. Yang, C. Guardia-Laguarta, D. Holtzman, D. Sulzer, E. Area-Gomez, and E. A. Schon. 2016. 'ApoE4 upregulates the activity of mitochondria-associated ER membranes', *EMBO Rep*, 17: 27-36.

Teodorof-Diedrich, C., and S. A. Spector. 2018. 'Human Immunodeficiency Virus Type 1 gp120 and Tat Induce Mitochondrial Fragmentation and Incomplete Mitophagy in Human Neurons', *J Virol*, 92.

Thangaraj, A., P. Periyasamy, K. Liao, V. S. Bendi, S. Callen, G. Pendyala, and S. Buch. 2018. 'HIV-1 TAT-mediated microglial activation: role of mitochondrial dysfunction and defective mitophagy', *Autophagy*, 14: 1596-619.

Tiku, V., M. W. Tan, and I. Dikic. 2020. 'Mitochondrial Functions in Infection and Immunity', *Trends Cell Biol*, 30: 263-75.

Ton, H., and H. Xiong. 2013. 'Astrocyte Dysfunctions and HIV-1 Neurotoxicity', *J AIDS Clin Res*, 4: 255.

Toussi, S. S., A. Joseph, J. H. Zheng, M. Dutta, L. Santambrogio, and H. Goldstein. 2009. 'Short communication: Methamphetamine treatment increases in vitro and in vivo HIV replication', *AIDS Res Hum Retroviruses*, 25: 1117-21.

Tsai, S. A., R. M. Bendriem, and C. D. Lee. 2019. 'The cellular basis of fetal endoplasmic reticulum stress and oxidative stress in drug-induced neurodevelopmental deficits', *Neurobiol Stress*, 10: 100145.

Urra, H., P. Pihan, and C. Hetz. 2020. 'The UPRosome - decoding novel biological outputs of IRE1alpha function', *J Cell Sci*, 133.

van Vliet, A. R., and P. Agostinis. 2016. 'When under pressure, get closer: PERKing up membrane contact sites during ER stress', *Biochemical Society transactions*, 44: 499-504.

———. 2018. 'Mitochondria-Associated Membranes and ER Stress', *Curr Top Microbiol Immunol*, 414: 73-102.

van Vliet, A. R., T. Verfaillie, and P. Agostinis. 2014. 'New functions of mitochondria associated membranes in cellular signaling', *Biochim Biophys Acta*, 1843: 2253-62.

Vannuvel, K., P. Renard, M. Raes, and T. Arnould. 2013. 'Functional and morphological impact of ER stress on mitochondria', *J Cell Physiol*, 228: 1802-18.

Verfaillie, T., N. Rubio, A. D. Garg, G. Bultynck, R. Rizzuto, J. P. Decuypere, J. Piette, C. Linehan, S. Gupta, A. Samali, and P. Agostinis. 2012. 'PERK is required at the ER-mitochondrial contact sites to convey apoptosis after ROS-based ER stress', *Cell Death Differ*, 19: 1880-91.

Vincenz-Donnelly, L., and M. S. Hipp. 2017. 'The endoplasmic reticulum: A hub of protein quality control in health and disease', *Free Radic Biol Med*, 108: 383-93.

Volkow, N. D., L. Chang, G. J. Wang, J. S. Fowler, D. Franceschi, M. Sedler, S. J. Gatley, E. Miller, R. Hitzemann, Y. S. Ding, and J. Logan. 2001. 'Loss of dopamine transporters in methamphetamine abusers recovers with protracted abstinence', *J Neurosci*, 21: 9414-8.

Wang, P., and Y. Ye. 2021. 'Astrocytes in Neurodegenerative Diseases: A Perspective from Tauopathy and alpha-Synucleinopathy', *Life (Basel)*, 11.

Wang, Y., M. Santerre, I. Tempera, K. Martin, R. Mukerjee, and B. E. Sawaya. 2017. 'HIV-1 Vpr disrupts mitochondria axonal transport and accelerates neuronal aging', *Neuropharmacology*, 117: 364-75.

Weng, T. Y., S. A. Tsai, and T. P. Su. 2017. 'Roles of sigma-1 receptors on mitochondrial functions relevant to neurodegenerative diseases', *J Biomed Sci*, 24: 74.

Wheeler, M. A., M. Jaronen, R. Covacu, S. E. J. Zandee, G. Scalisi, V. Rothhammer, E. C. Tjon, C. C. Chao, J. E. Kenison, M. Blain, V. T. S. Rao, P. Hewson, A. Barroso, C. Gutierrez-Vazquez, A. Prat, J. P. Antel, R. Hauser, and F. J. Quintana. 2019. 'Environmental Control of Astrocyte Pathogenic Activities in CNS Inflammation', *Cell*, 176: 581-96 e18.

Wilburn, K. M., H. C. Mwandumba, K. C. Jambo, S. Boliar, S. Solouki, D. G. Russell, and D. W. Gludish. 2016. 'Heterogeneous loss of HIV transcription and proviral DNA from 8E5/LAV lymphoblastic leukemia cells revealed by RNA FISH:FLOW analyses', *Retrovirology*, 13: 55.

Wilson, E. L., and E. Metzakopian. 2020. 'ER-mitochondria contact sites in neurodegeneration: genetic screening approaches to investigate novel disease mechanisms', *Cell Death Differ*.

Won, L., N. Bubula, H. McCoy, and A. Heller. 2001. 'Methamphetamine concentrations in fetal and maternal brain following prenatal exposure', *Neurotoxicol Teratol*, 23: 349-54.

Yang, M., C. Li, S. Yang, Y. Xiao, X. Xiong, W. Chen, H. Zhao, Q. Zhang, Y. Han, and L. Sun. 2020. 'Mitochondria-Associated ER Membranes - The Origin Site of Autophagy', *Front Cell Dev Biol*, 8: 595.

Yoboue, E. D., R. Sitia, and T. Simmen. 2018. 'Redox crosstalk at endoplasmic reticulum (ER) membrane contact sites (MCS) uses toxic waste to deliver messages', *Cell Death Dis*, 9: 331.

You, Y., K. Borgmann, V. V. Edara, S. Stacy, A. Ghorpade, and T. Ikezu. 2020. 'Activated human astrocyte-derived extracellular vesicles modulate neuronal uptake, differentiation and firing', *J Extracell Vesicles*, 9: 1706801.

Zampese, E., C. Fasolato, M. J. Kipanyula, M. Bortolozzi, T. Pozzan, and P. Pizzo. 2011. 'Presenilin 2 modulates endoplasmic reticulum (ER)-mitochondria interactions and Ca2+ cross-talk', *Proc Natl Acad Sci U S A*, 108: 2777-82.

Zenebe, Y., M. Necho, W. Yimam, and B. Akele. 2022. 'Worldwide Occurrence of HIV-Associated Neurocognitive Disorders and Its Associated Factors: A Systematic Review and Meta-Analysis', *Front Psychiatry*, 13: 814362.

Zhang, P., D. Konja, Y. Zhang, and Y. Wang. 2021. 'Communications between Mitochondria and Endoplasmic Reticulum in the Regulation of Metabolic Homeostasis', *Cells*, 10.

Zhang, Y., X. Lv, Y. Bai, X. Zhu, X. Wu, J. Chao, M. Duan, S. Buch, L. Chen, and H. Yao. 2015. 'Involvement of sigma-1 receptor in astrocyte activation induced by methamphetamine via up-regulation of its own expression', *J Neuroinflammation*, 12: 29.